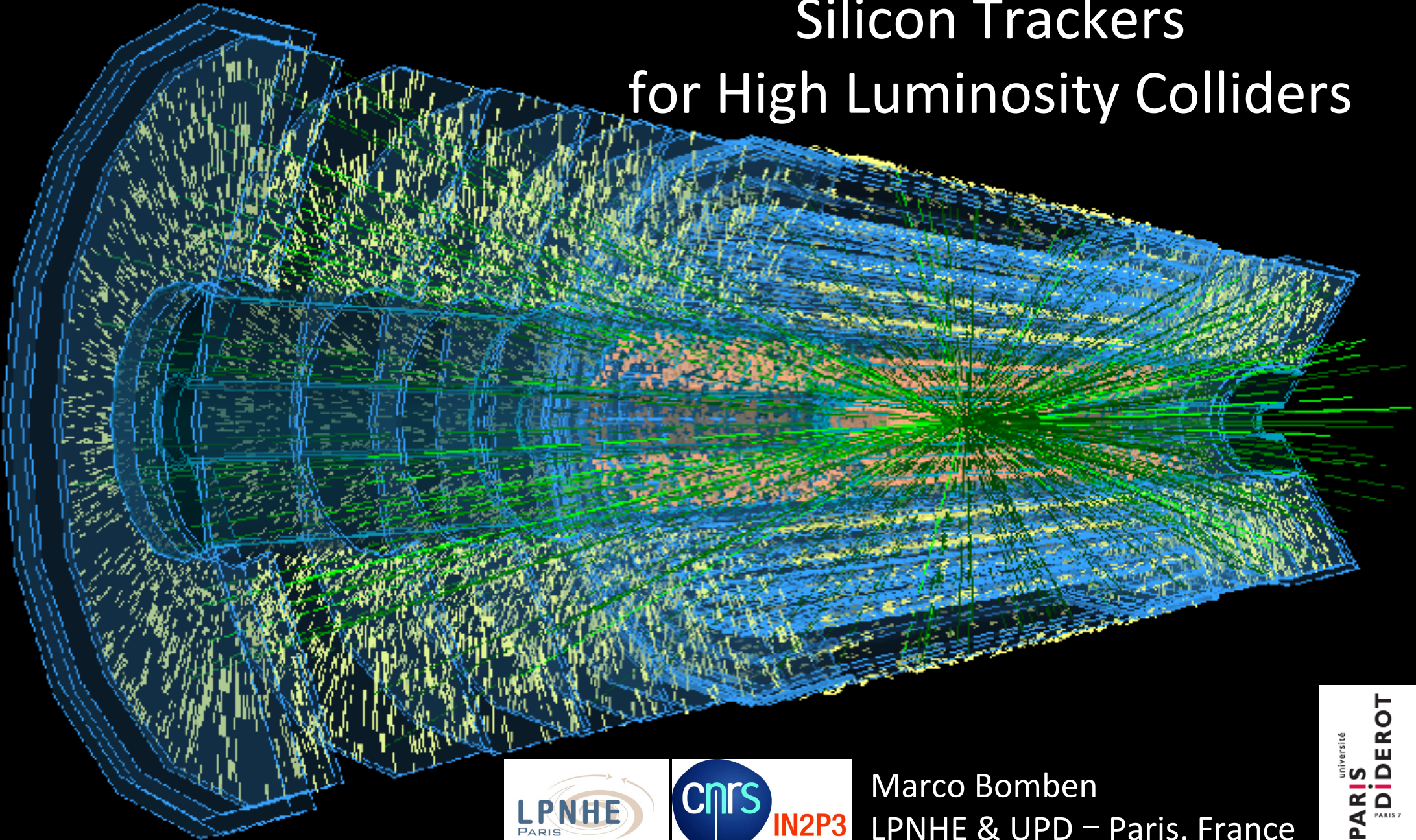


Habilitation à diriger des recherches

Silicon Trackers for High Luminosity Colliders



Marco Bomben
LPNHE & UPD – Paris, France



Outline

- Biography & Context
- Silicon detectors for high energy physics
- The Slim5 Project
- Radiation damage modelling for the ATLAS Pixel detector
- Pixel detectors for the new ATLAS Inner Tracker
- Perspectives
- Summary

Outline

- Biography & Context
- Silicon detectors for high energy physics
- The Slim5 Project
- Radiation damage modelling for the ATLAS Pixel detector
- Pixel detectors for the new ATLAS Inner Tracker
- Perspectives
- Summary

Disclaimer: in what follows

References to original contributions are in red

References to support material are in green

BIOGRAPHY

Education, research and teaching

Università di Trieste & INFN
Laurea, PhD & Post-doc

LPNHE – CNRS – UPD
Post-doc & Maître de Conférences

2003-2007



2007-2009



2010-now



Laurea (2003): semileptonic decays
of B mesons

Silicon sensors for high luminosity
e+e- colliders

Silicon trackers for the future high
luminosity hadronic colliders

PhD (2007): CP violation in
b → c decays
+ Silicon Tracker Operations

Radiation damage studies on the
ATLAS pixel detector

Advising students, from
undergraduates to PhD

Teaching, in Italy and France

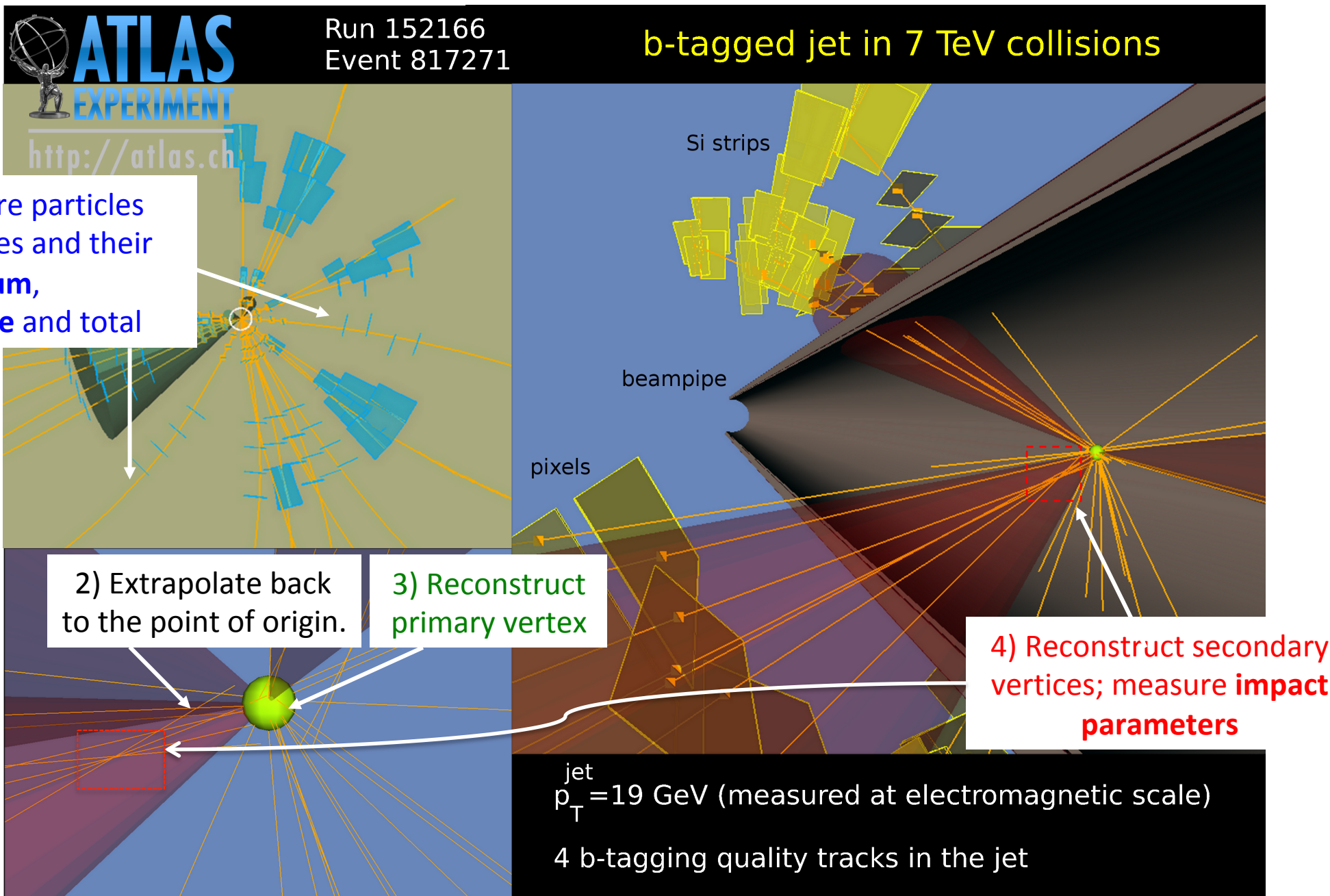
- Università degli Studi di Trieste, Faculty of Engineering, undergraduate program
- Université Paris Diderot, Natural Sc. And Phys. Dept., undergr. and master program

Students supervision

- Gonzague Le Mesre De Pas, stage d'école d'ingénieur, 2011
 - Characterisation and simulation of silicon diodes
- Qu An, M1 stage, 2012
 - Simulation of irradiated silicon sensors
- Audrey Ducourthial, M1 stage, 2014
 - Characterisation of pixel detectors for the ATLAS tracker upgrade
- Audrey Ducourthial, M2 stage, 2015
 - Analysis of testbeam data of pixel detectors for the ATLAS tracker upgrade
- Audrey Ducourthial, PhD Thesis, 2015-ongoing
 - ATLAS Tracking detector upgrade and its importance for H->bb analysis
- Kenji Nardone, stage d'école d'ingénieur, 2017-2018
 - Characterisation and simulation of silicon detectors
- Plus students working at testbeams (Louis D'Eramo, Ilaria Luise, etc.)

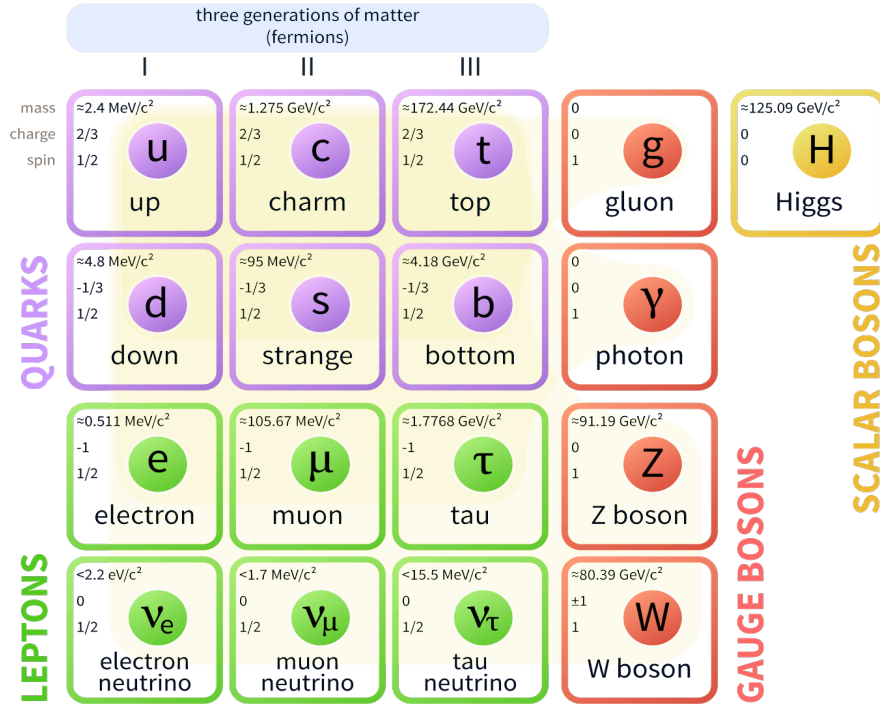
CONTEXT

Role of trackers in HEP experiments

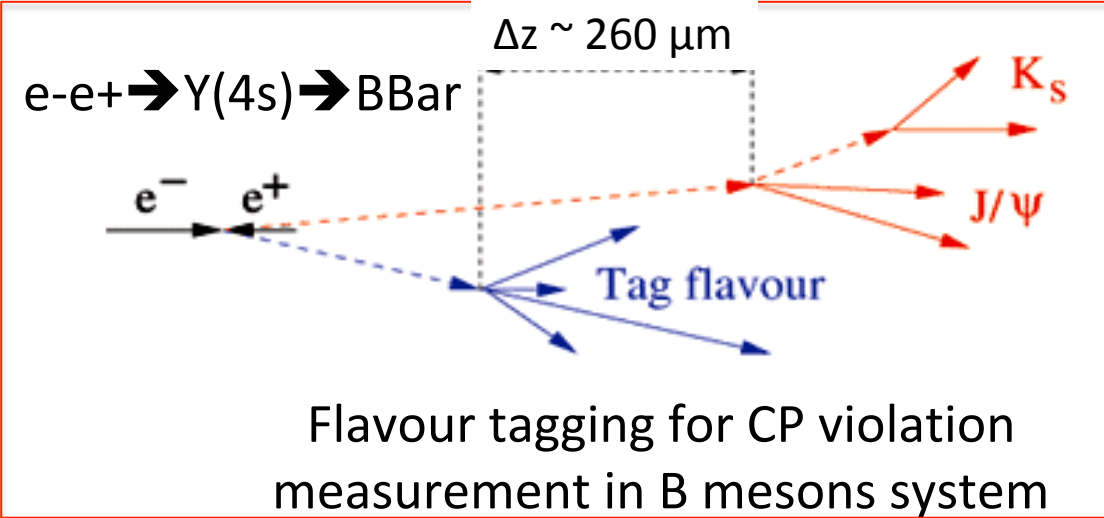


Elementary particles and flavour tagging

Standard Model of Elementary Particles



+ New Physics...

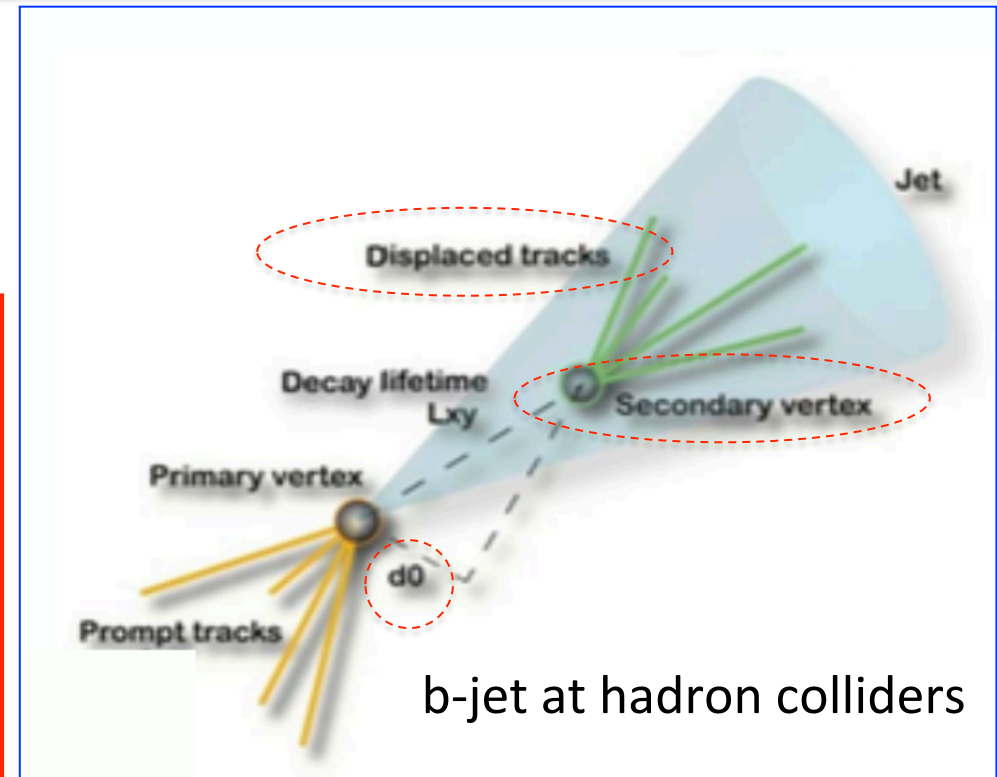


Lifetimes of tau leptons, charm and beauty hadrons: from 0.2 to 1.5 ps

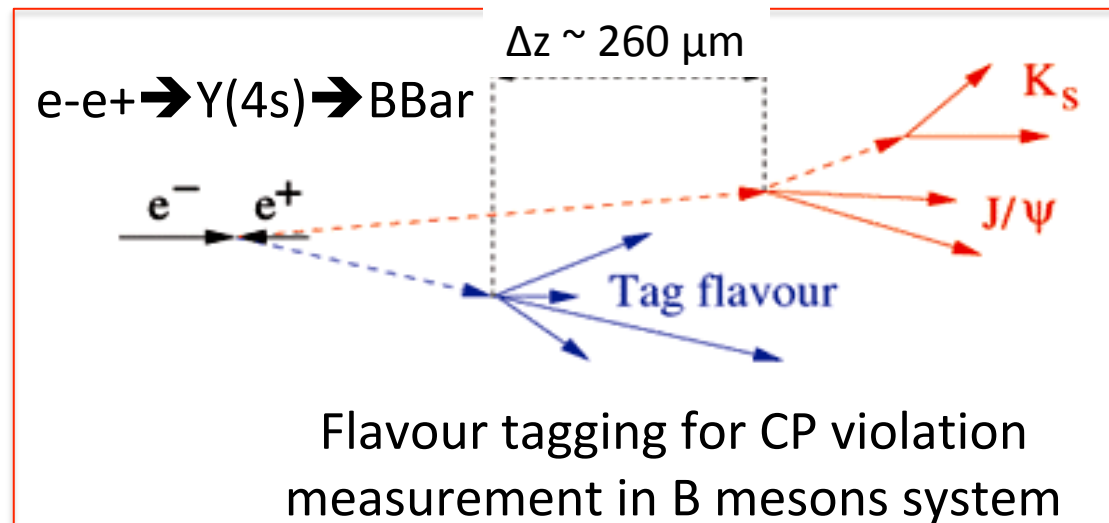


Typically the decay vertex is at a distance of single millimeters from the interaction vertex

→ **sub-millimeter precision needed!**



Flavour tagging at B-factories



In order to have a **better than 10% precision in measuring CP violation** the **vertices had to be reconstructed with a $80 \mu\text{m}$ resolution**, corresponding to about $1/3$ of the average vertices distance

In reality **fully reconstructed Bs had vertex precision of $50 \mu\text{m}$** , while for *tag side it was about $100-150 \mu\text{m}$*

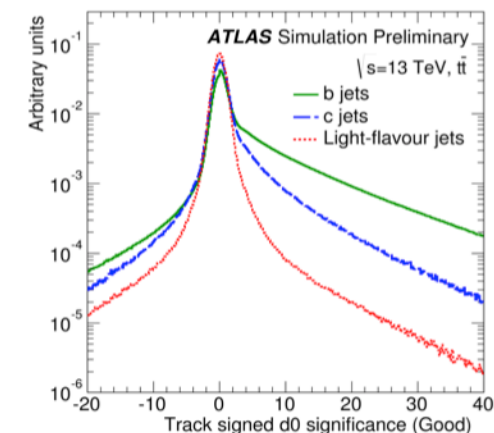
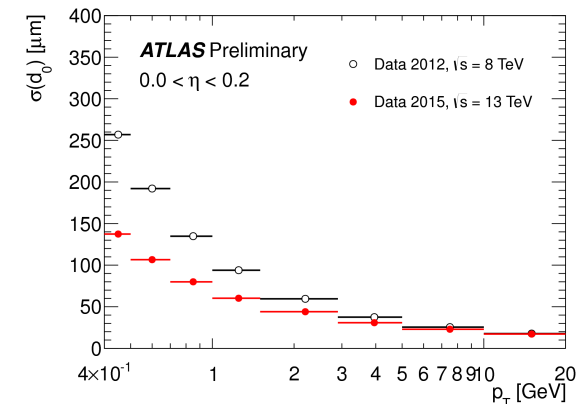
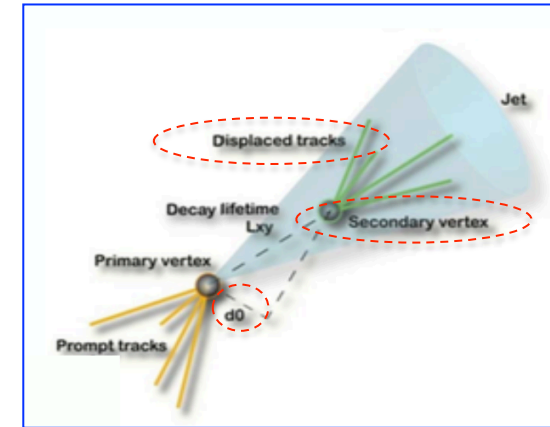
BaBar tracker performance allowed also to measure precisely τ_B too

Jet tagging at LHC

The ability to identify jets containing b-hadrons is important for the high- p_T physics program of a general-purpose experiment at the LHC such as ATLAS

Fundamental tool to

- select pure top samples
- search for (SUSY) Higgs coupling to heavy object
- veto large dominant $t\bar{t}$ background
- search for new physics: SUSY decay chains, heavy gauge bosons, etc



Transverse momentum resolution

Transverse momentum resolution: need strong B , long path length L , excellent space point resolution σ_{point} and keep material budget at minimum

$$\frac{\sigma_{p_T}}{p_T} = \left(\frac{p_T \sigma_{point}}{0.3|z| L^2 B} \sqrt{\frac{720}{N+4}} \right) \oplus \frac{0.054}{\beta B L} \sqrt{\frac{x/\sin\theta}{X_0}}$$

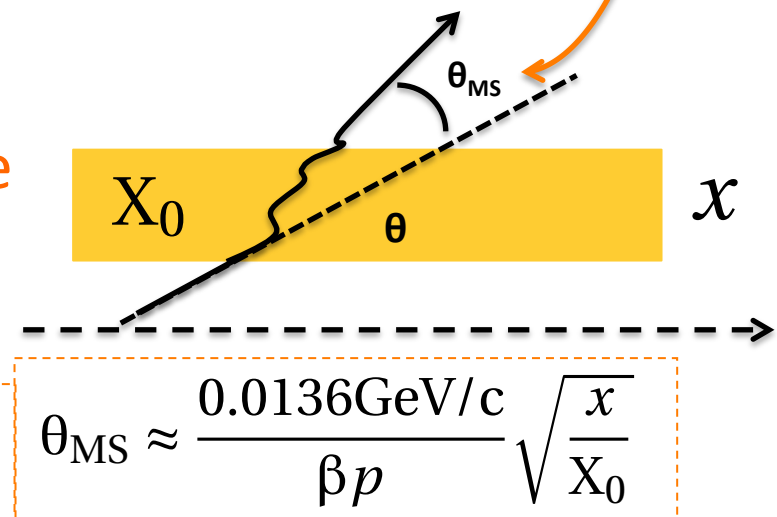
Multiple Scattering

e.g.: arXiv:1705.10150

N: number of equidistant measuring layers

Particle incident on a thin slab undergoes Multiple deflections due to Coulomb Scattering (MS)

θ_{MS} depends on material budget and momentum



Vertexing resolution

The **precision on vertexing** is linked to the **impact parameter resolution**

$$\sigma_{d0} \approx \frac{\sigma_{point}}{\sqrt{N}} \sqrt{1 + \frac{12(N-1)}{N+1} \left(\frac{r}{L}\right)^2} \oplus \theta_{MS} r_{pv} \sqrt{\frac{N(2N-1)}{6(N-1)^2}}$$

e.g.: arXiv:1705.10150

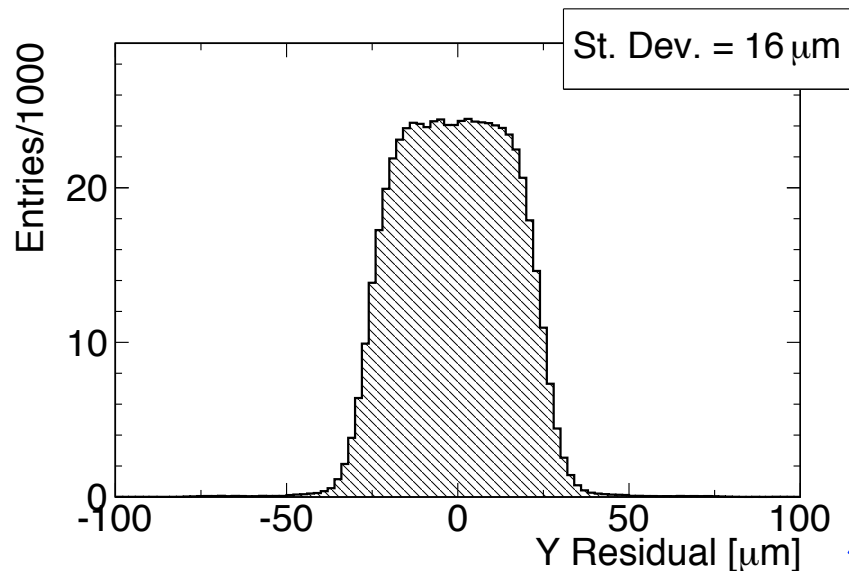
r_{pv} is the distance of the first layer from the primary vertex

- σ_{point} is the space point resolution
- N is the number of equidistant measuring layers
- r/L is the ratio of extrapolation distance over tracker length

(Limited gain for large N)

- Need for:
- **Excellent** space point resolution σ_{point}
 - A **plane** as **close** as possible **to** the **interaction point** (r)
 - **Long lever arm** L
 - **Minimize material** (x and X_0)

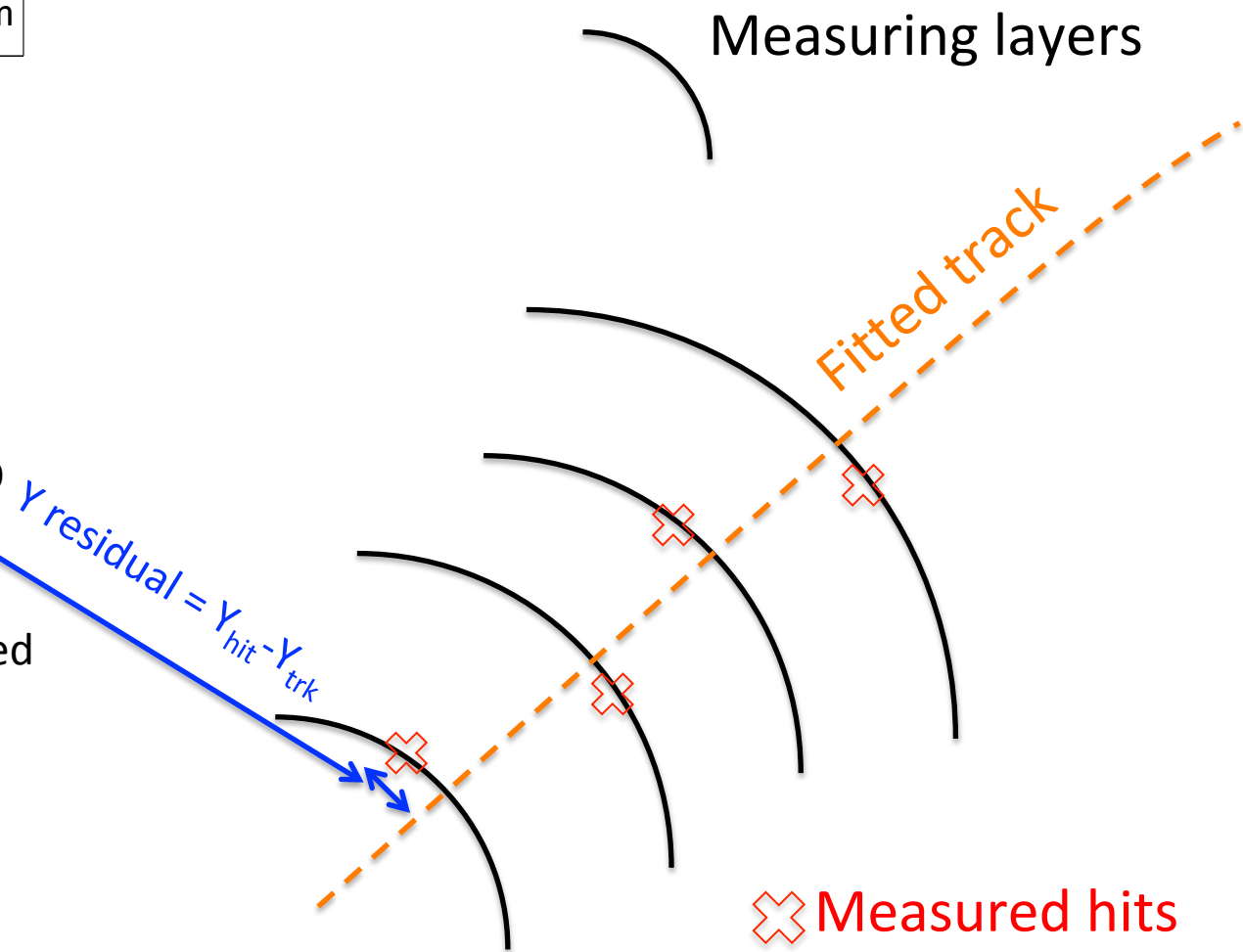
How to estimate σ_{point} ? Residuals



➤ From the RMS of the residuals distribution the space point resolution σ_{point} can be inferred

➤ Several effects enter involved:

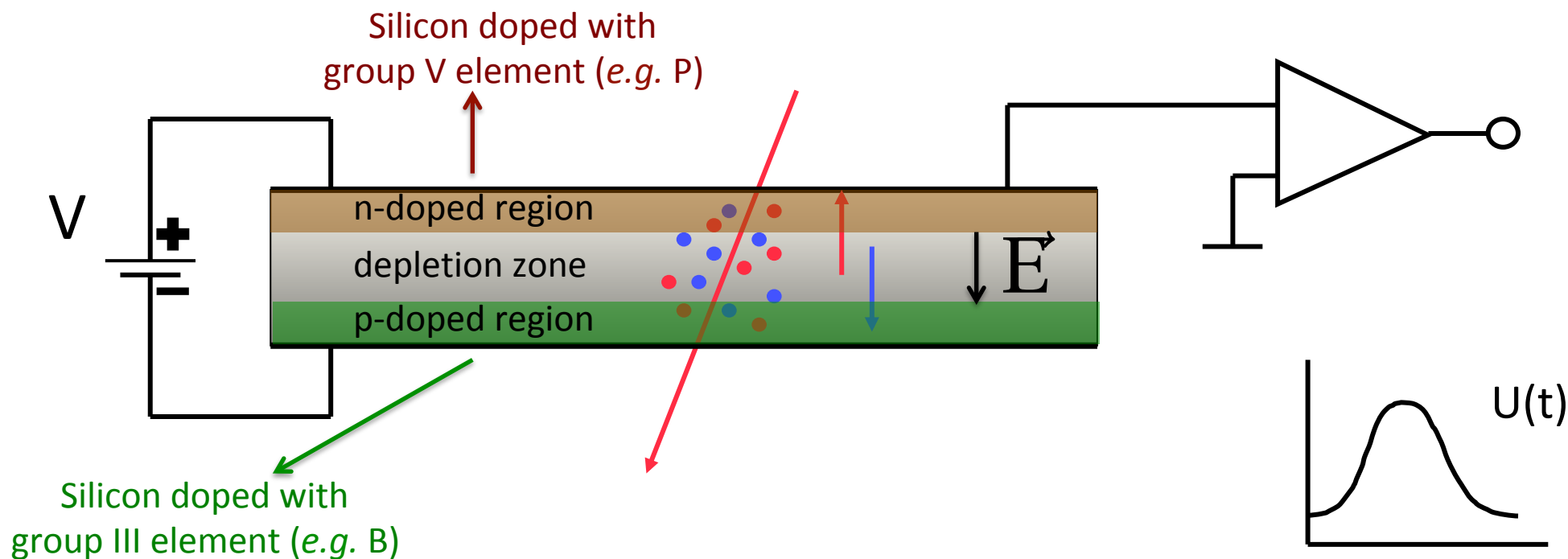
- Statistical fluctuations in energy loss
- Diffusion
- Lorentz Angle
- Sensor pitch
- Cluster size
- Analog/Binary r.o.
- S/N ratio
- Alignment
- ...



$$\sigma_{\text{res}} = \sigma_{\text{DUT}} \oplus \sigma_{\text{trk}}$$

SILICON DETECTORS FOR HIGH ENERGY PHYSICS

The basics: p-n junction in reverse bias

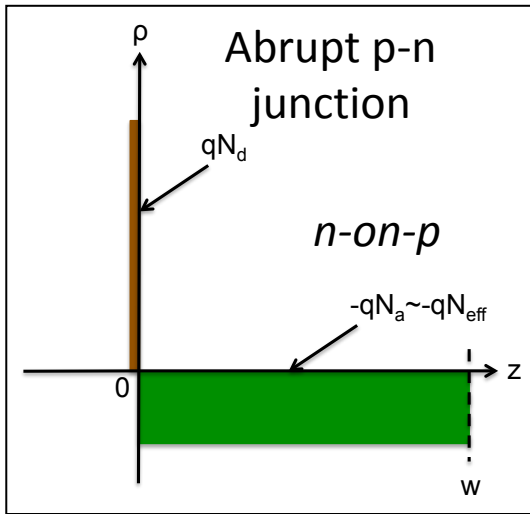


A solid state ionization chamber

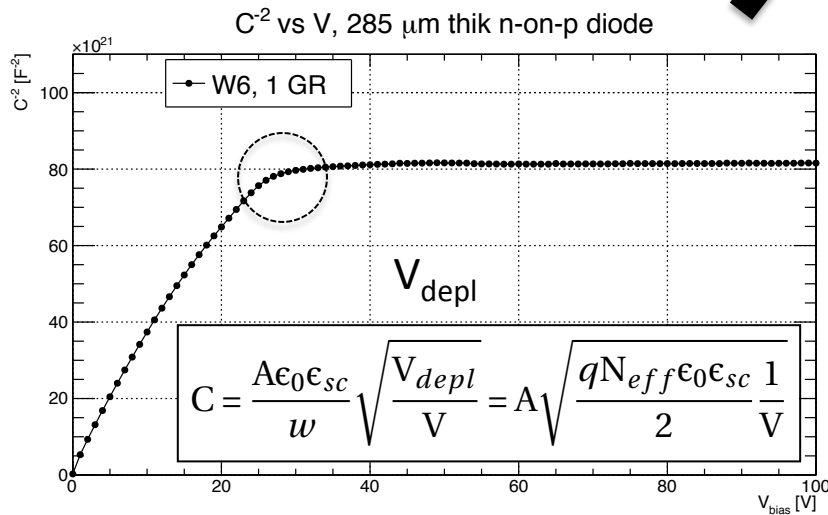
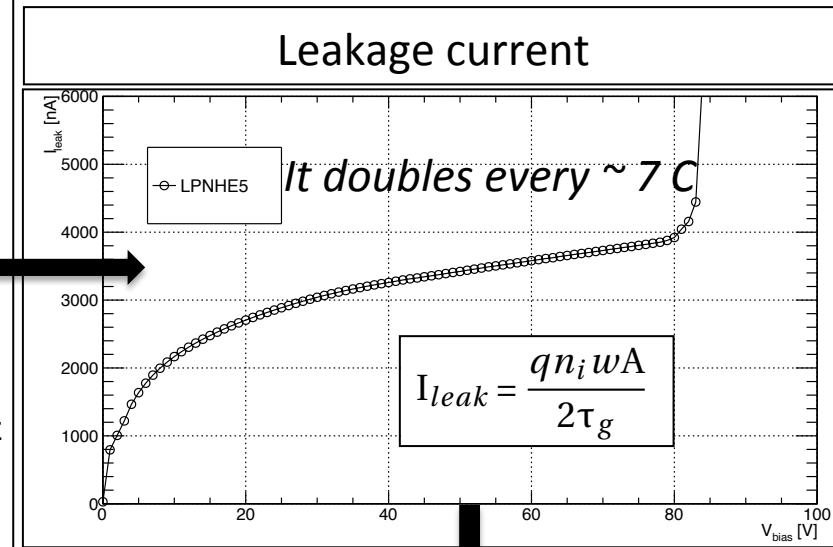
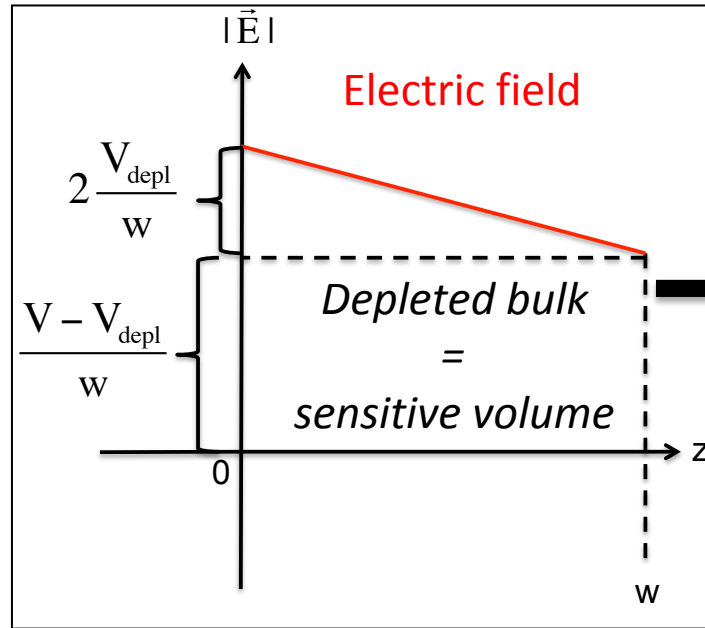
Signal given by the drift of charges (**electrons** and **holes**) under the effect of the electric field

The signal is then amplified and shaped

Silicon p-n junction in reverse bias



Reverse polarisation
 => Depletion voltage V_{depl}



Why Silicon?

Feature	Silicon Value	Comments
Density ρ	2.33 g/cm ³	compact and thin detectors
Energy bandgap E_g	1.12 eV	non-cryogenic operation
Mean ionisation energy ϵ	3.6 eV	large signals
Radiation length X_0	9.37 cm	thin detectors to minimize multiple scattering
Electron mobility μ_e	$\sim 1350 \text{ cm}^2\text{V/s}$	fast charge collection
Saturation velocity v_{sat}	$\sim 10^7 \text{ cm/s}$	fast charge collection

Simplest silicon sensors: the pad diode

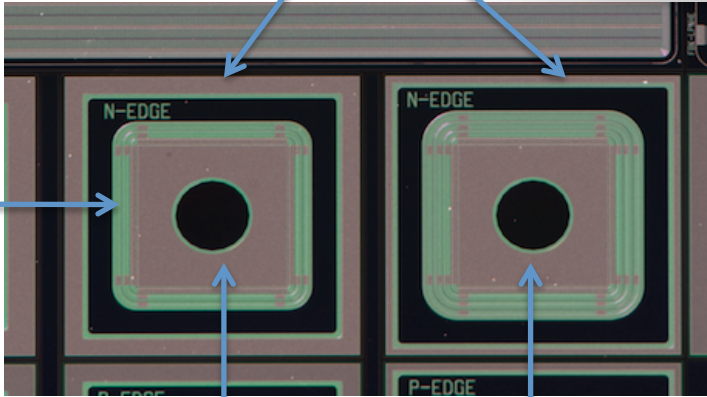
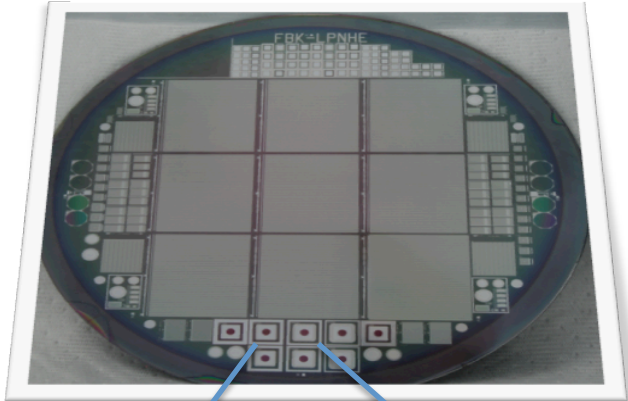
A single p-n diode in reverse bias is the simplest silicon radiation detector

Often it is called **pad diode**

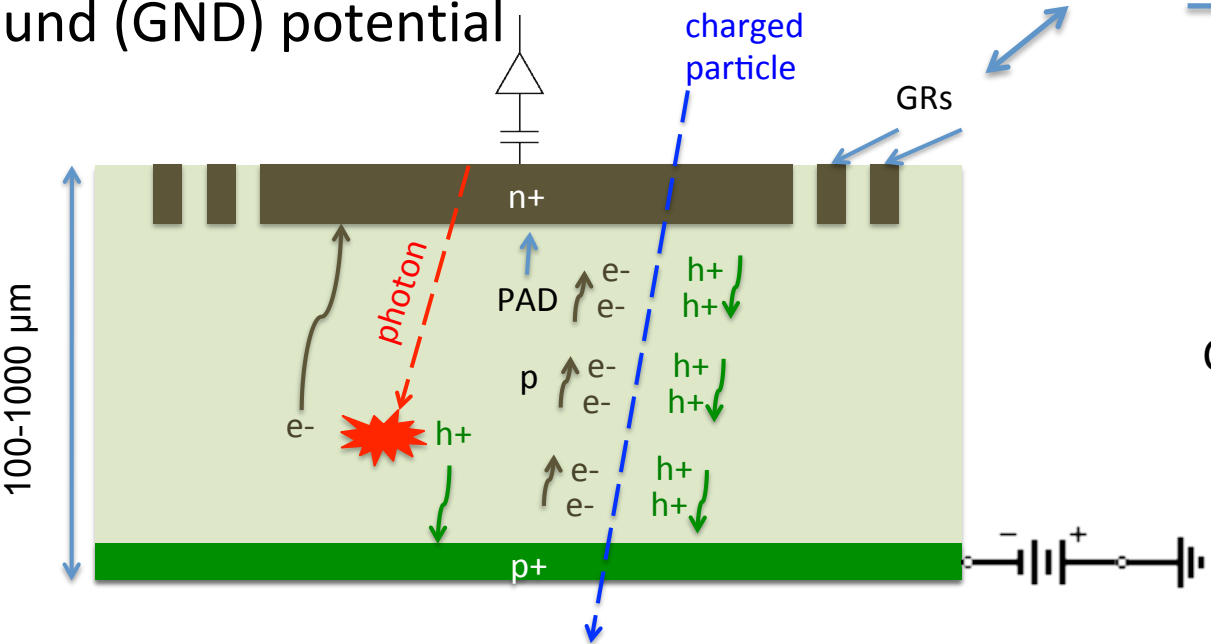
The **size** varies between **few mm²** to **few cm²**

Guard Rings (GRs) assure a smooth transition between the High Voltage (HV) and the Ground (GND) potential

N-on-p production



Central openings in the aluminium layer for visible/IR photon detection



GRs

GRs

charged particle

photon

n+

PAD

p

p+

100-1000 μm

Position measurement: Double-sided microstrip detectors (DSSD)

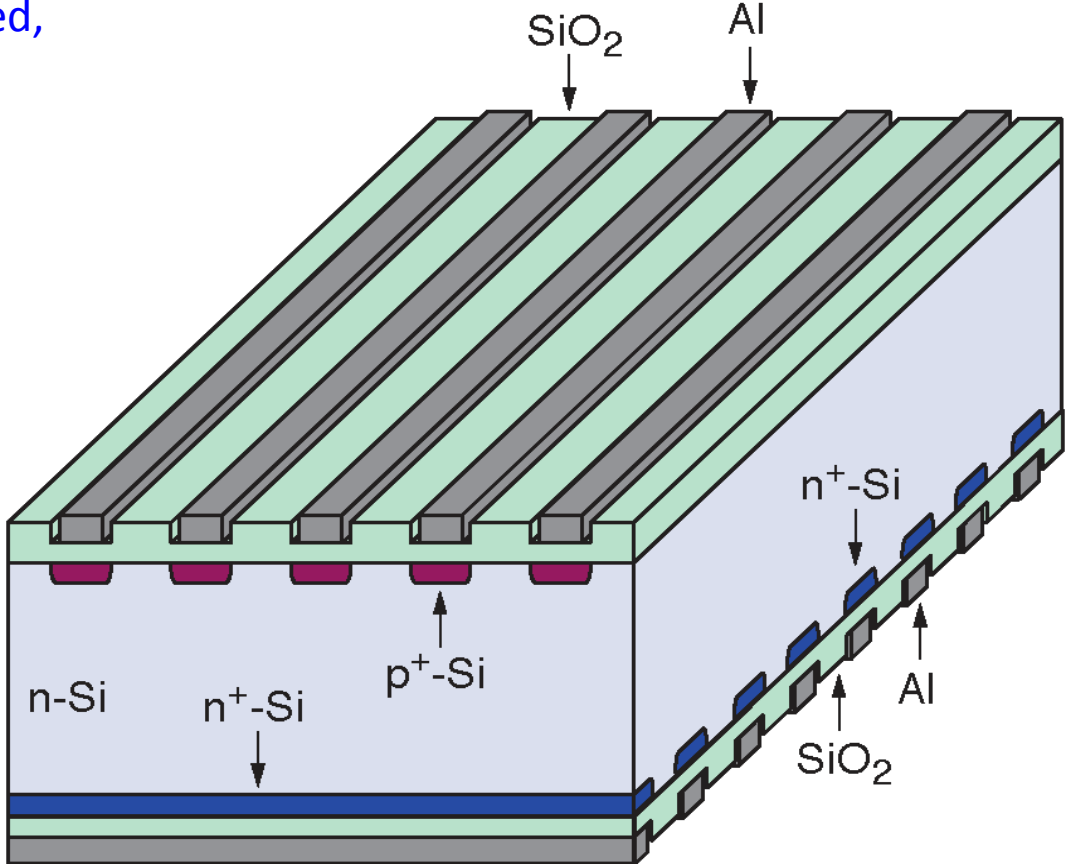
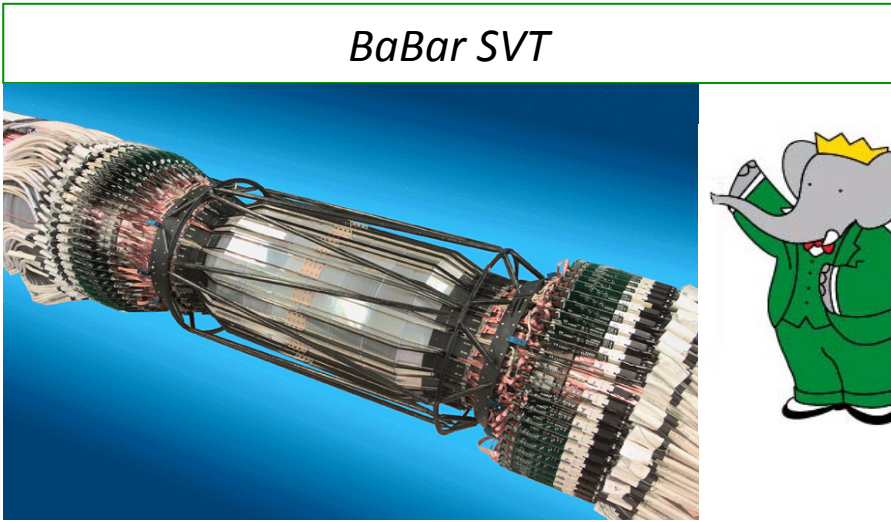
Single sided detector measures only one coordinate. To measure second coordinate requires second detector layer

Double sided strip detector measures two coordinates in one detector layer (minimizes material)

In n-type detector the n^+ backside becomes segmented, e.g. strips orthogonal to p^+ strips

Drawback: expensive as production, handling, and tests are more complicated, and ambiguities!

Scheme of a double sided strip detector (biasing structures not shown):



Hybrid Pixel Detectors

Originally in planar technology; now 3D too

HPD: Typical size is (50-400) μm x 50 μm

If signal pulse height is not recorded, resolution is the digital resolution: $\sigma = p/\sqrt{12}$

e.g. $\sigma = 14 \mu\text{m}$ for $p = 50 \mu\text{m}$

Reminder: better resolution is achieved with analogue readout

Small pixel area \rightarrow low detector capacitance (\sim few fF/pixel) \rightarrow large SNR ($\gg 10$)

Small pixel volume \rightarrow low leakage current (\sim few pA/pixel)

Drawbacks of HPD: large number of readout channels

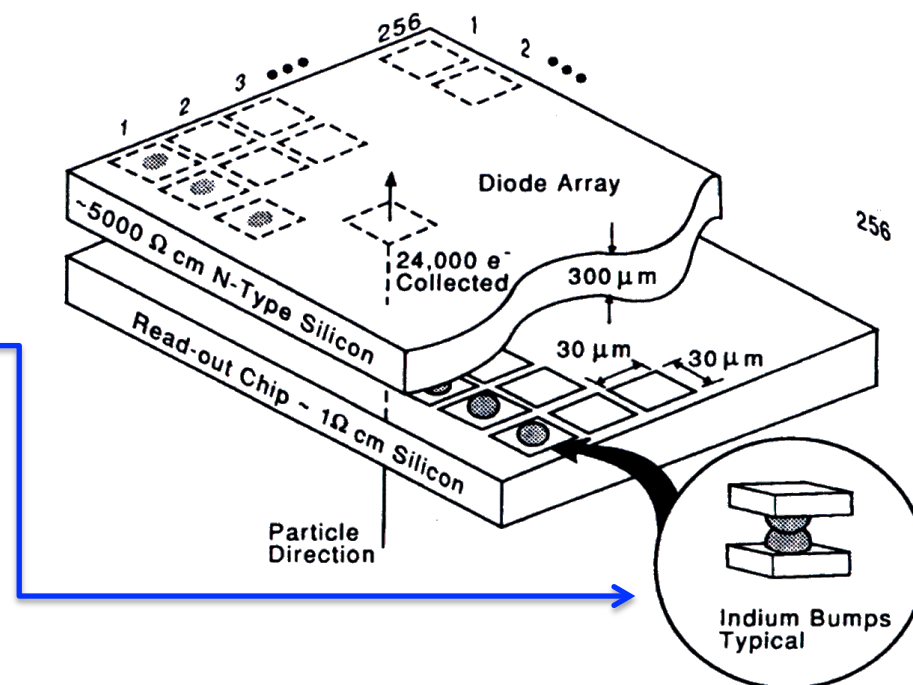
DSSD $\sim 2n$

HPD $\sim n^2$

Large number of electrical connections in case of HPD

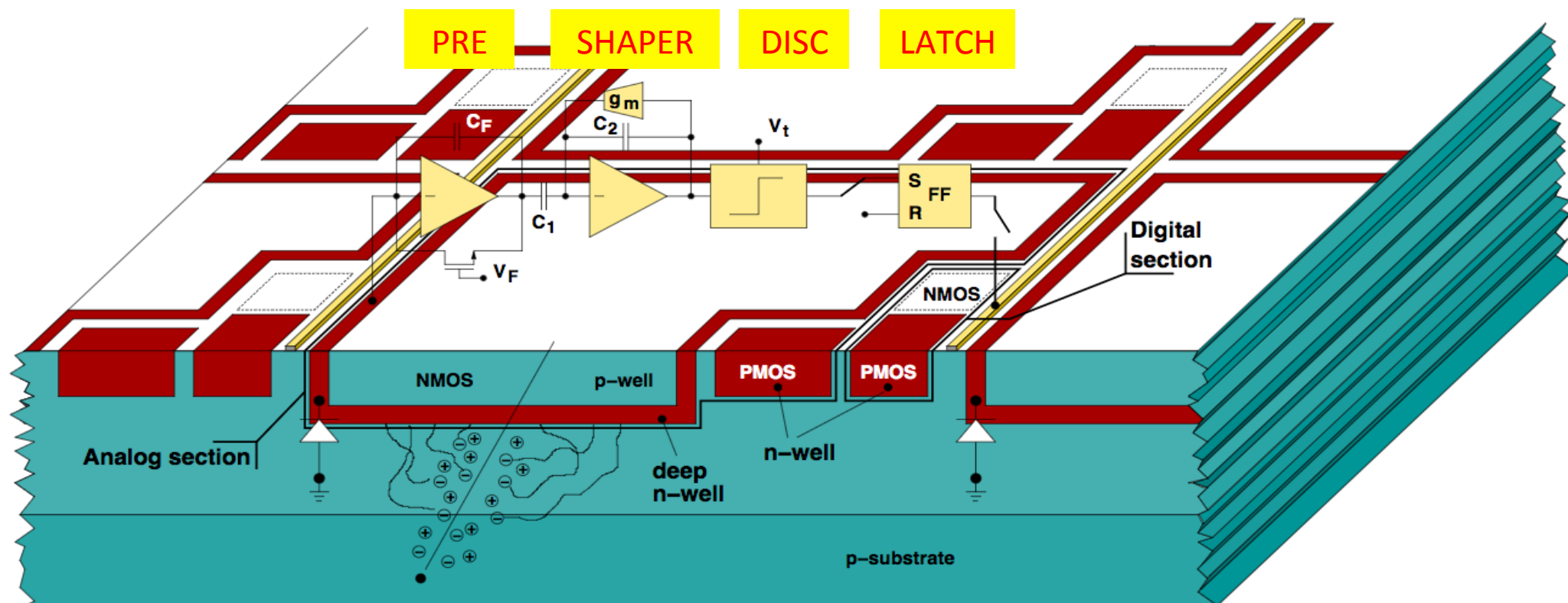
Large power consumptions of electronics

S.L. Shapiro et al., Si PIN Diode Array Hybrids for Charged Particle Detection, Nucl. Instr. Meth. A 275, 580 (1989)



Sensor and electronics together: CMOS MAPS

L. Ratti, IEEE Trans. Nucl. Sci. NS-53 (6) (2006) 3918



Developed for imaging applications

Several reasons make them very appealing as tracking devices :

- detector & readout on the same substrate
- wafer can be thinned down to few tens of μm
- radiation hardness (oxide $\sim\text{nm}$ thick) (now HV/HR developments)
- Fabrication costs

Important: **maximize fill factor**
(area of collecting n-well over total sensor area)

Silicon detectors with Low Interaction with Material

<http://www.pi.infn.it/slim5>



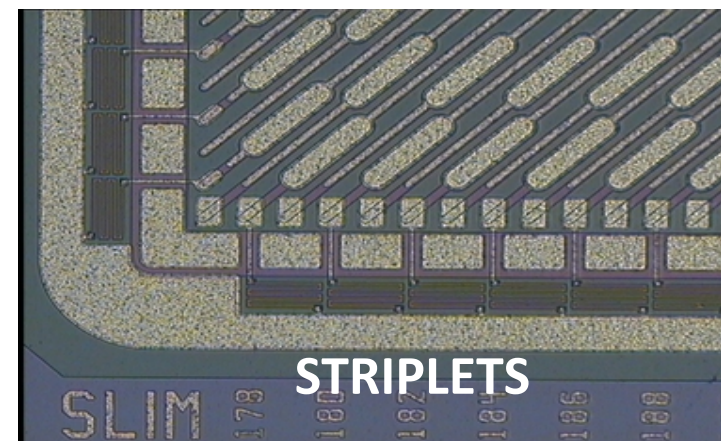
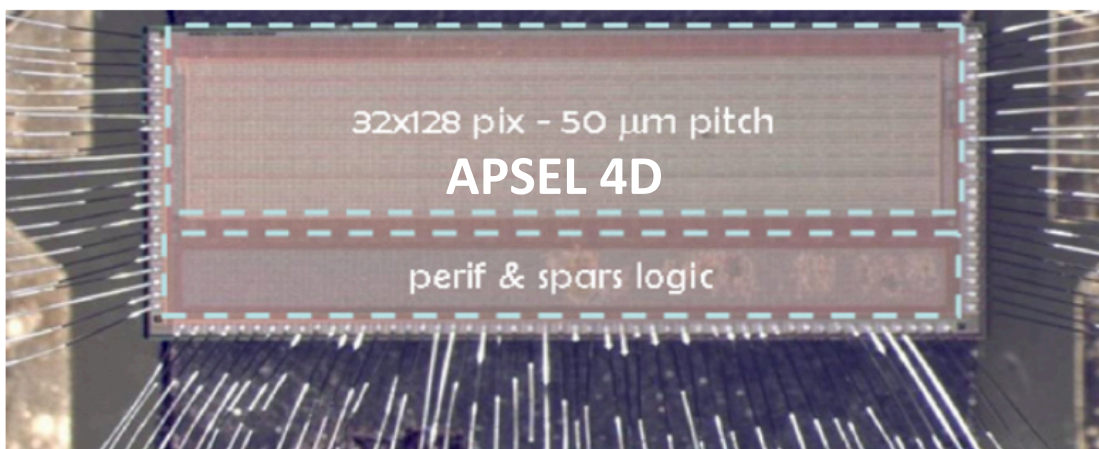
SLIM5: SILICON SENSORS FOR HIGH LUMINOSITY E+E- COLLIDER EXPERIMENTS

SLIM5 – the project



- The **SLIM5** project: advance the state-of-the-art of **thin tracking systems for high luminosity e^+e^- colliders**
- **Goal:** deliver **thin and intelligent** (self-triggering/data-driven) **silicon tracking detectors for** experiments at Super Flavour Factories (**SFF**) and Linear Collider (**LC**)
- Typical specifications:
 1. Space point resolution of $10 \mu\text{m}$
 2. Material budget below 1% of X_0
 3. Measure $p_T < 100 \text{ MeV}/c$
 4. Impact parameter resolution of the order of: $\sigma_{ip} = 5 \mu\text{m} \oplus \frac{10}{p\beta(\sin\theta)^{3/2}} \mu\text{m}$
- Two detector concepts were investigated:
- **Double sides strip detectors (DSSDs)**, and
- **Monolithic active pixel sensor (MAPS)**

SLIM5 silicon sensors



- CMOS MAPS
- Read out up to 40 MHz
- Thinned down to 100 μm
- 50 x 50 μm^2 pitch pixel cells
- Fill factor $\sim 90\%$
- Data sparsification: 4x4 macro pixels (MP) + periphery logic

Nucl. Instr. Meth. A 623 (2010) 942-953

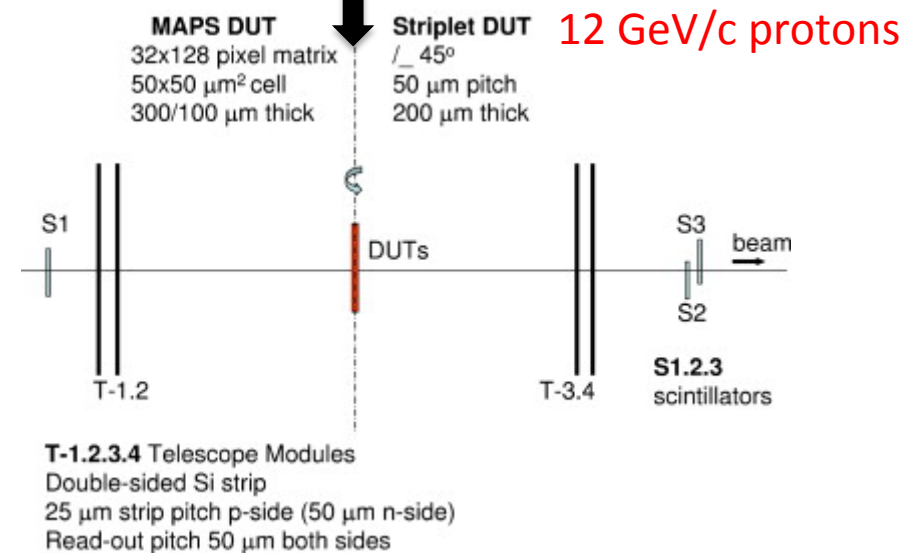
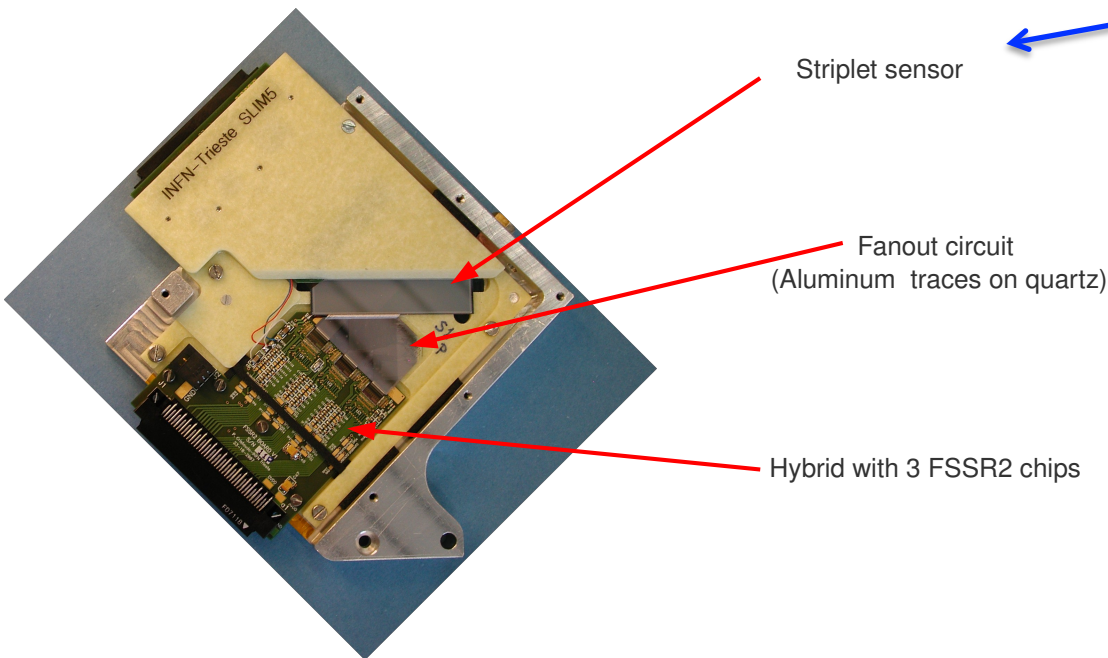
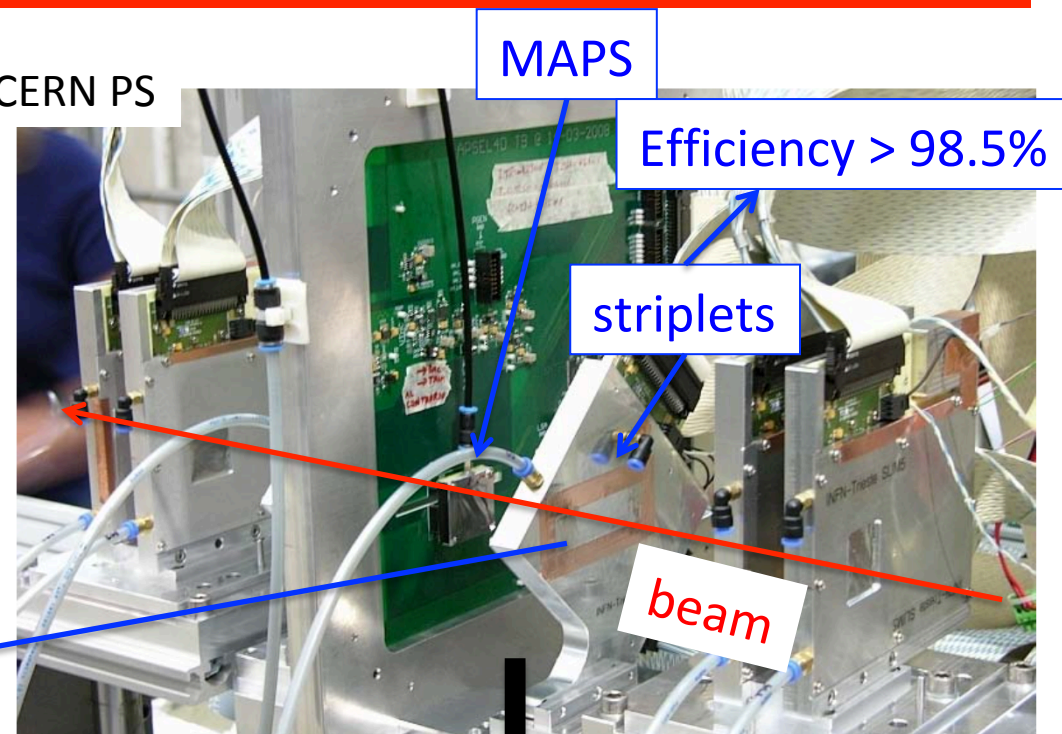
- 200 μm thick double sided strip detector: thinner to reduce multiple scattering effect (0.2% X_0)
- 50 μm pitch strips, tilted by 45°: less occupancy per channel for the same area
- Data-driven readout chip: data sent out only if above threshold

SLIM5 testbeam

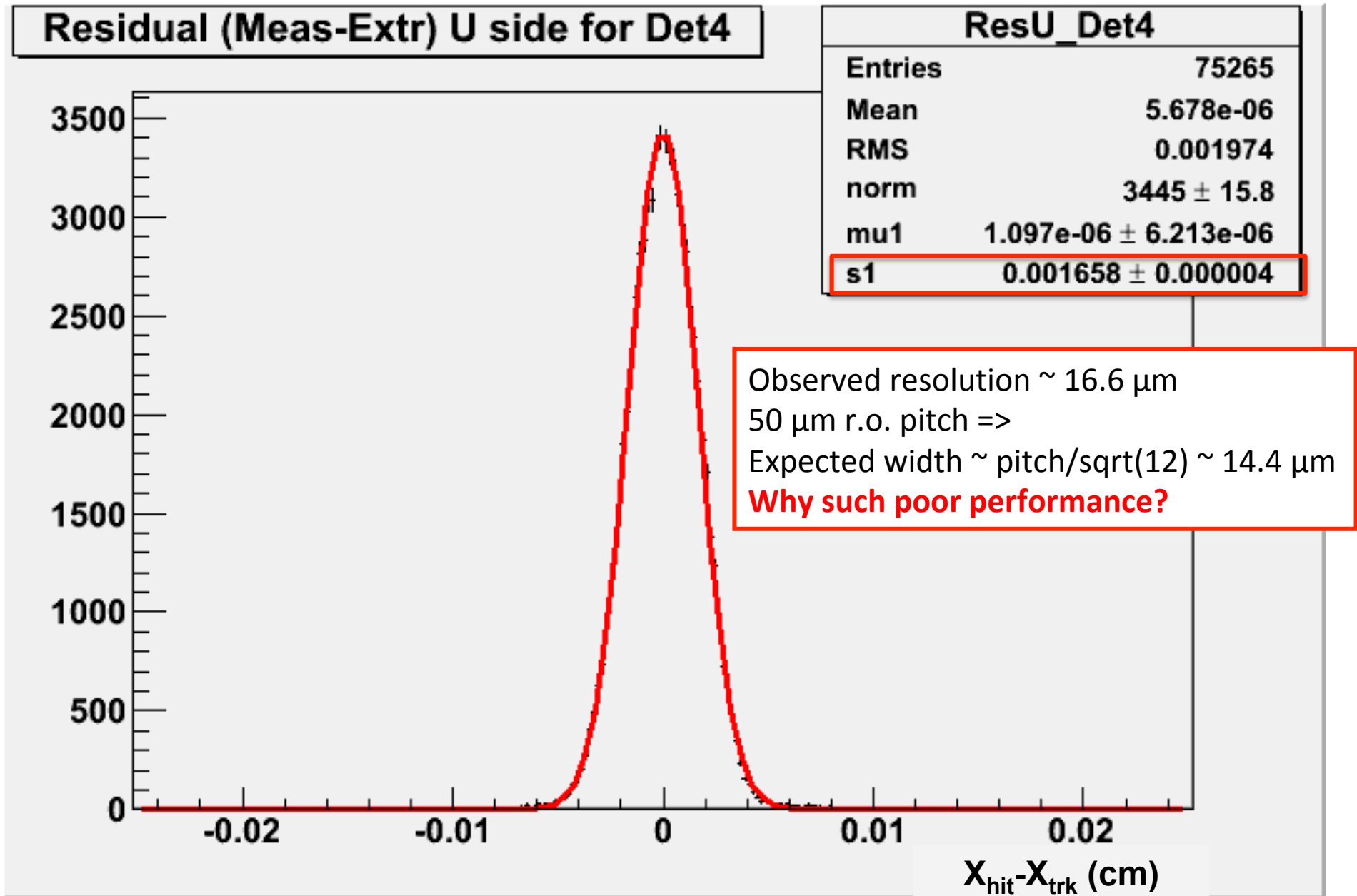
Nucl. Instr. Meth. A 623 (2010) 942-953



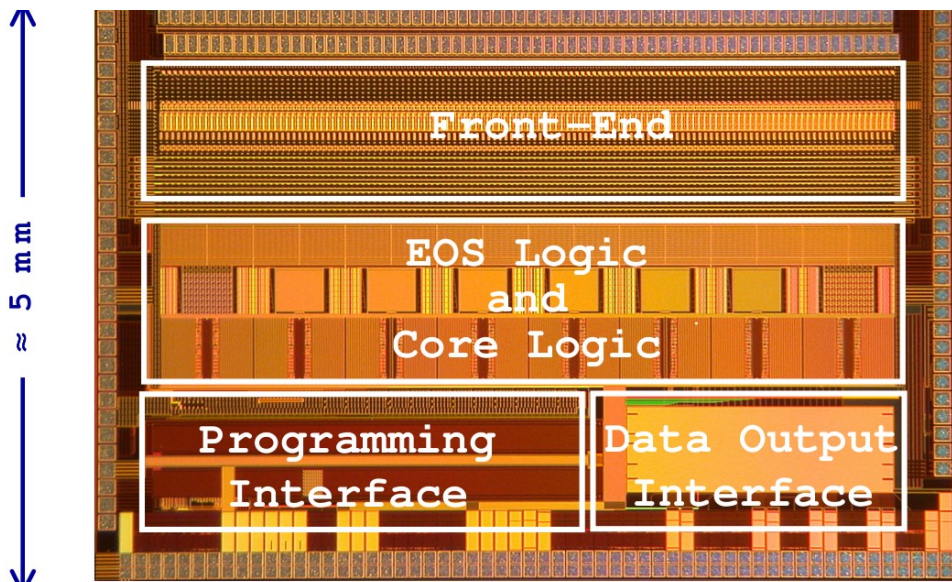
2008, CERN PS



SLIM5 triplets performance: resolution



Triplets front end and spatial resolution



Calibration results for triplets during the testbeam

Side	p	n
Noise (e)	630	1020
S/N	25	16
Gain (mV/fC)	96	67
Threshold (e)	4400	6300
Thr.Dis. (e)	880	780

Signal/Thresh. (S/T) 3.6 2.5

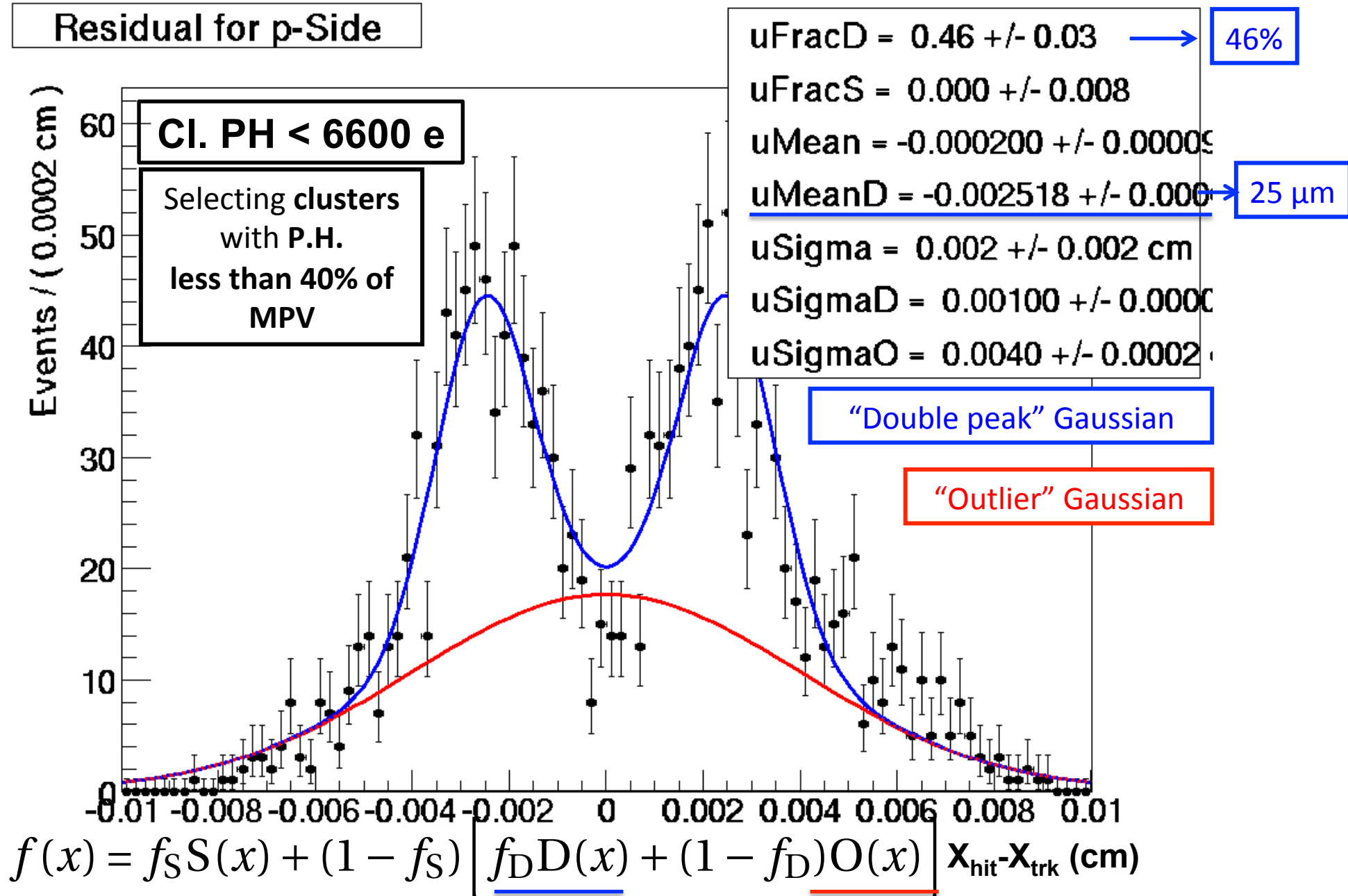
- FSSR2 originally developed for BTeV experiment
- Intended for p-on-n detector => not optimized for ohmic side readout (limited dynamic range)
- Completely data-driven thanks to
- 8 programmable threshold
- 1st one active as a hit/no-hit discriminator => *zero suppression* mode
- For n-side of triplets only binary information available

IEEE Trans. Nucl. Sci. 53 (2006) 2470–2476

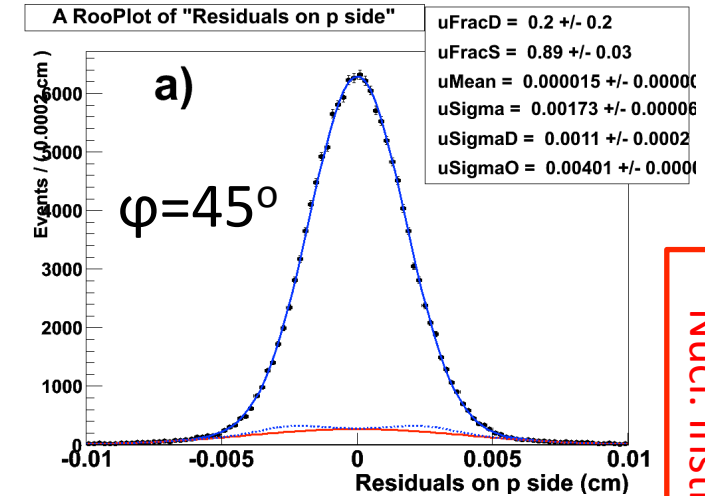
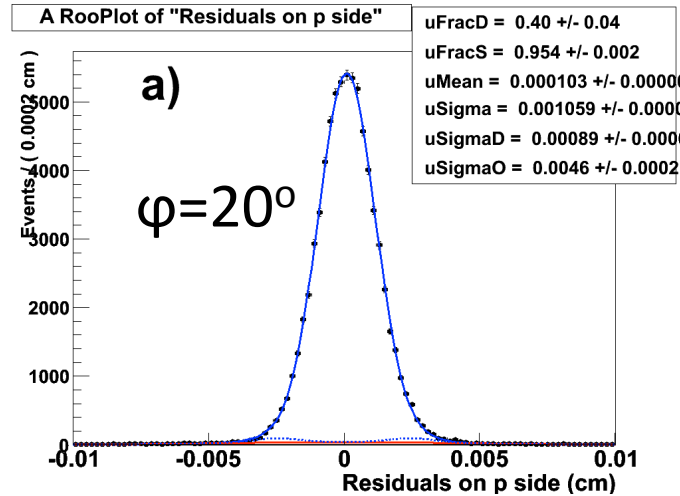
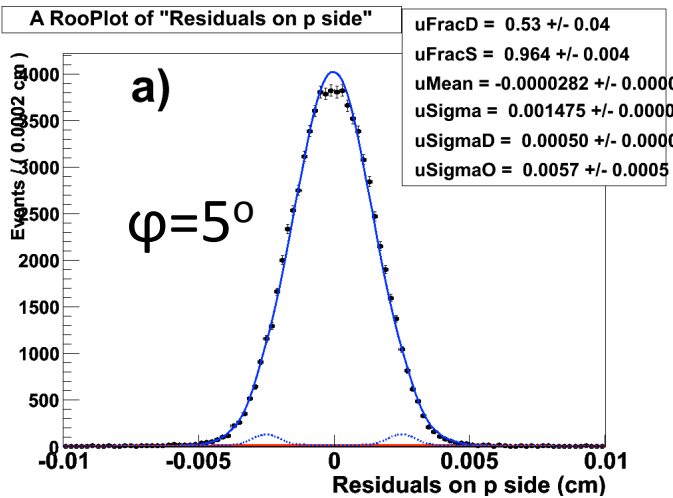
Hypothesis

- Due to **marginal S/T small hits are below threshold**
- **True clusters of 2 strips reconstructed as 1 strip only**
- **Average error on position \sim Pitch/2**

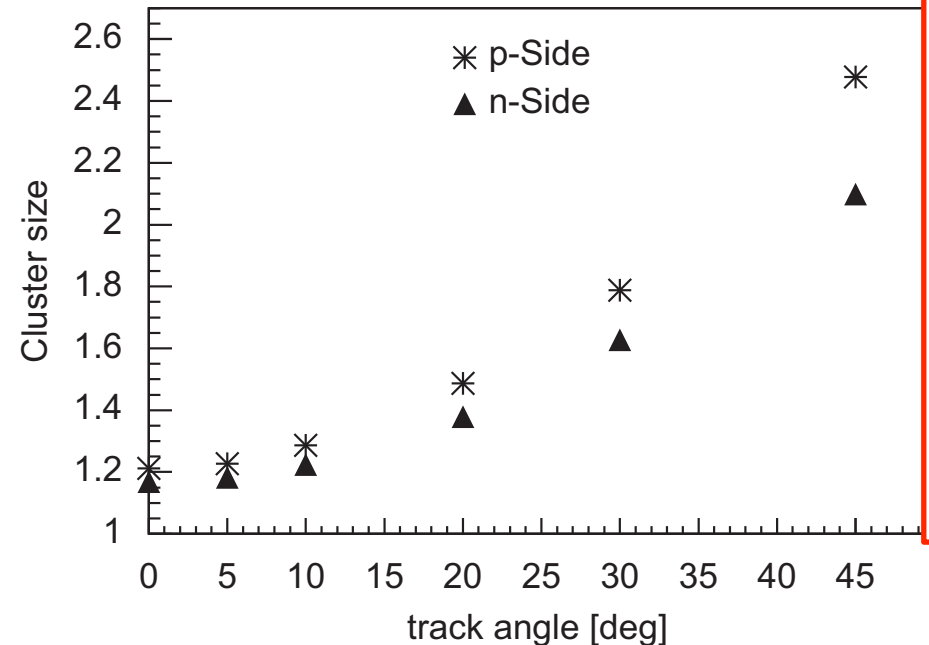
Triplets residuals: “double peak” effect



SLIM5 triplets residuals vs incidence angle

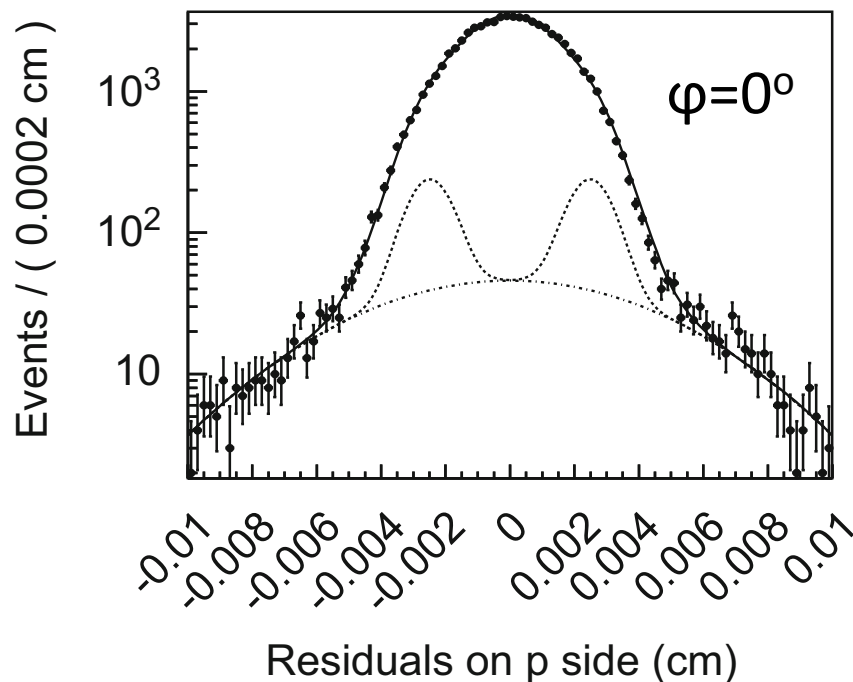


- Larger incidence angle φ
- Larger cluster size
- Less chances of mis-reconstructed clusters
- Smaller double peak contribution

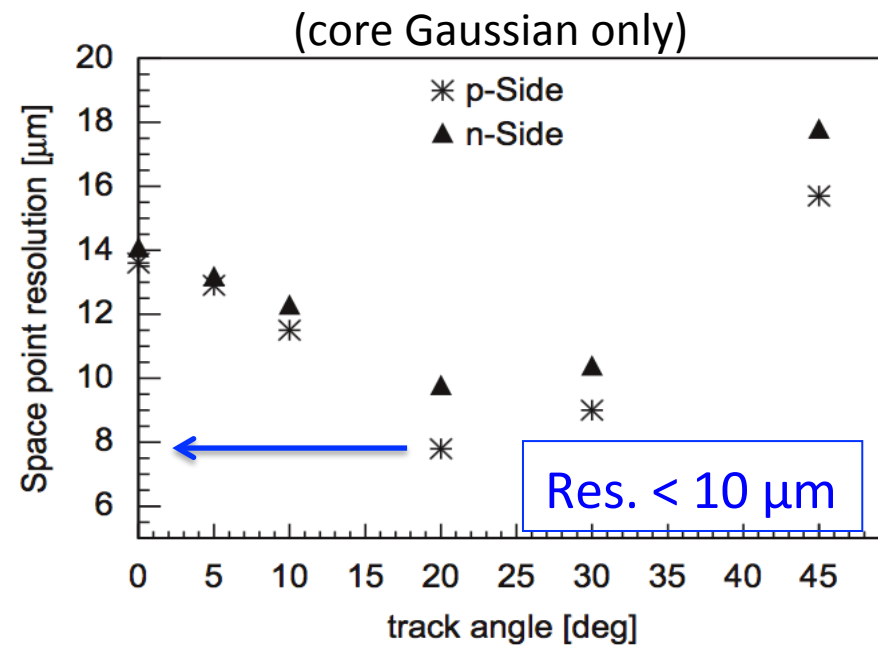


Nucl. Instr. Meth. A 623 (2010) 942-953

SLIM5 striplets performance: conclusions



Nucl. Instr. Meth. A 623 (2010) 159 – 161



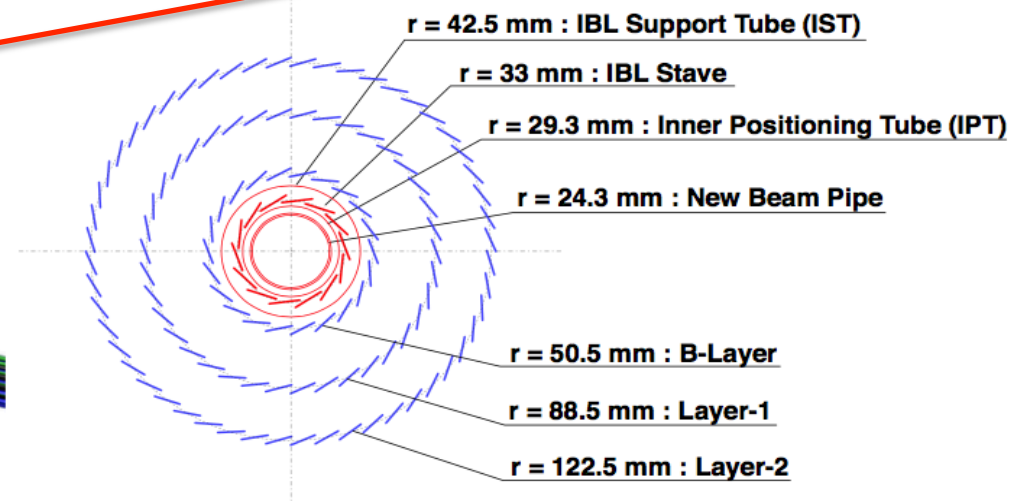
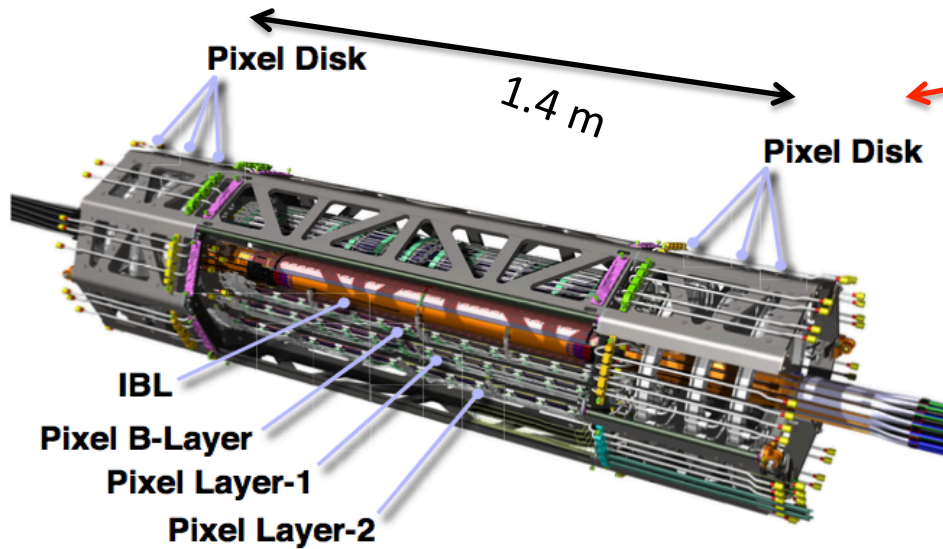
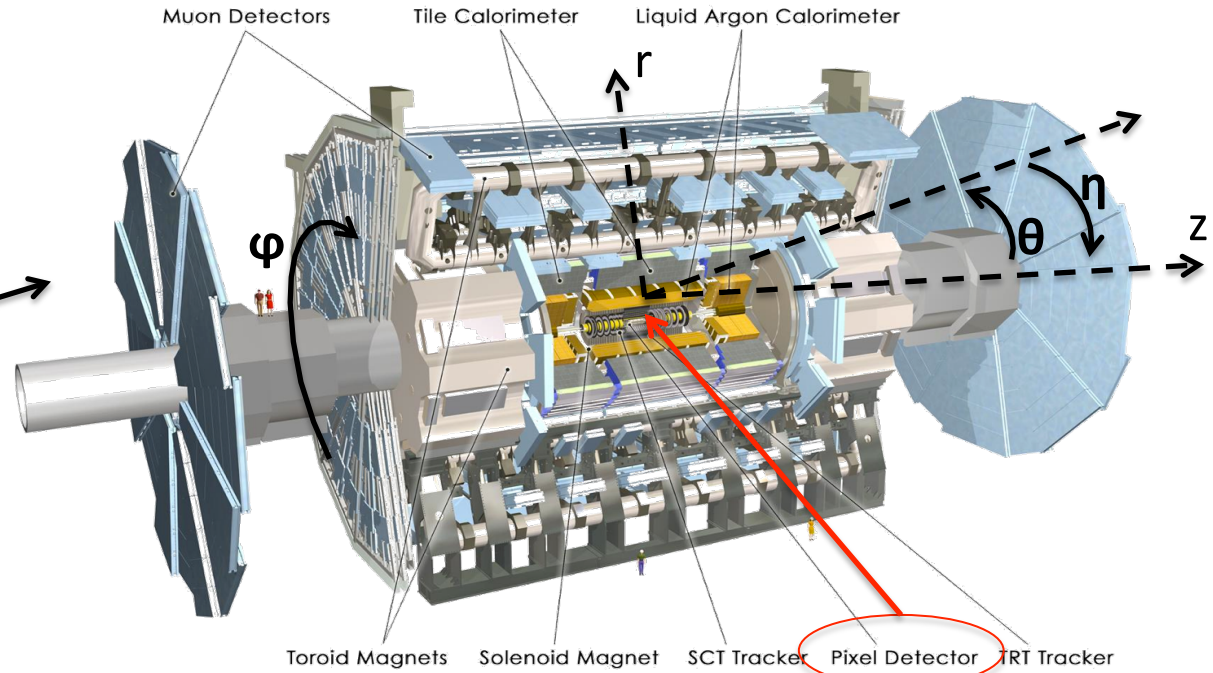
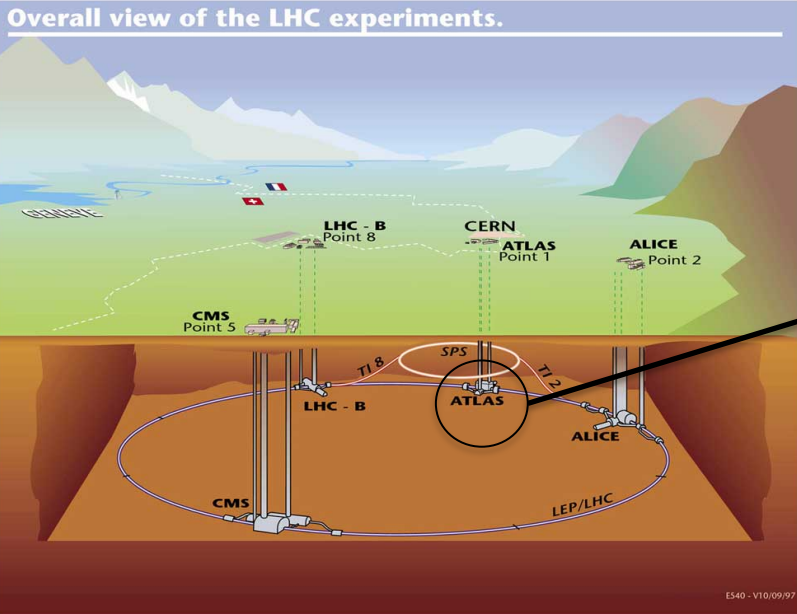
Nucl. Instr. Meth. A 623 (2010) 942-953

- The **spatial resolution** performance of the **striplets** were severely **impacted by** the sub-optimal functioning of the FFSR2 **readout chip**
- **Ultimate resolution**, measurable once the double peak effect has been identified, **within the specifications**
- Need for a better readout chip, in terms of noise and speed
- **Material budget under control (0.2% X_0)**



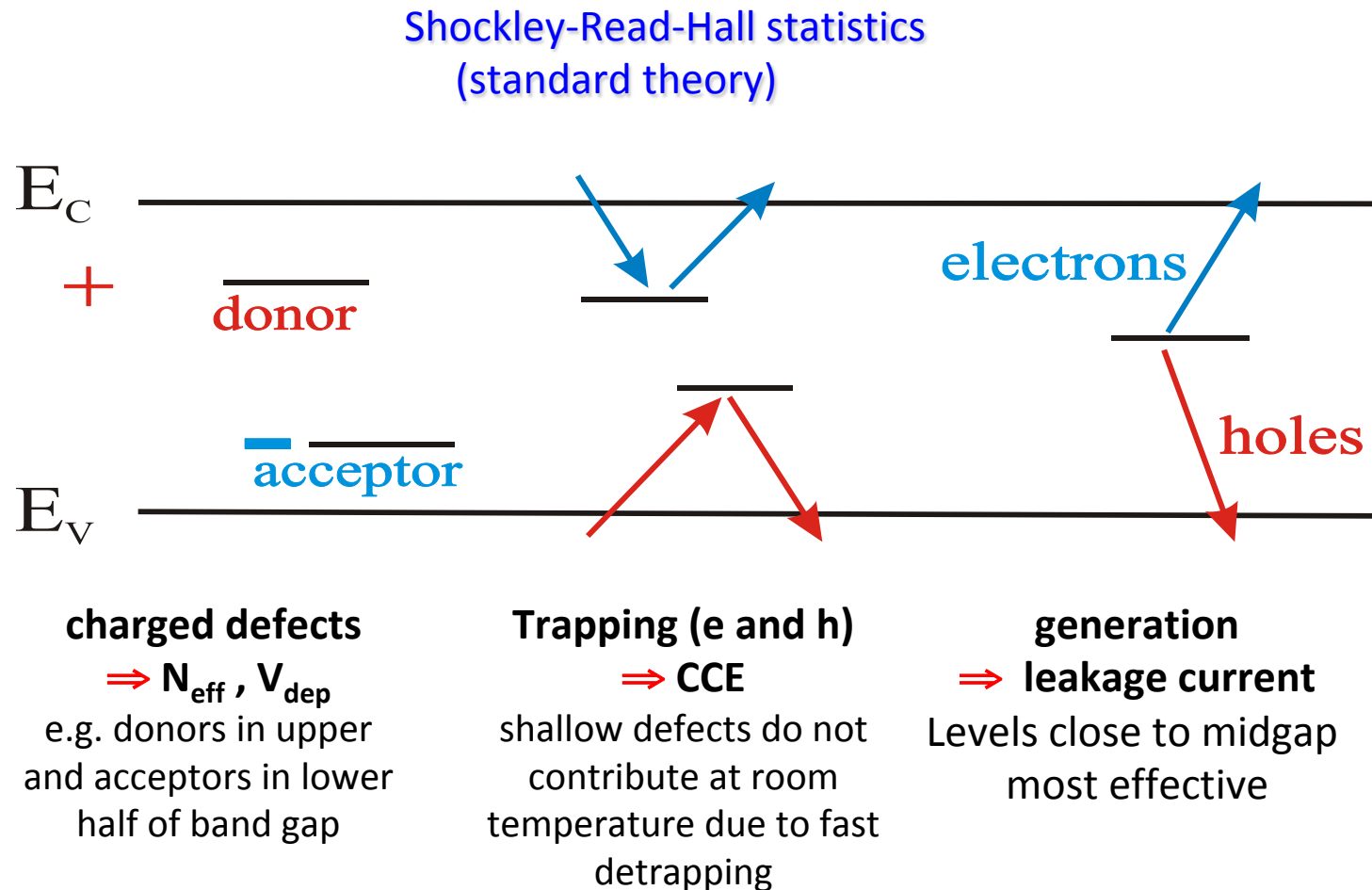
RADIATION DAMAGE MODELLING FOR THE ATLAS PIXEL DETECTOR

Current ATLAS detector @ CERN LHC



Radiation damage in silicon: microscopic level

M. Moll,
Simdet 2016



Impact on detector properties can be calculated if all defect parameters are known:

$\sigma_{n,p}$: cross sections

ΔE : ionization energy

N_t : concentration

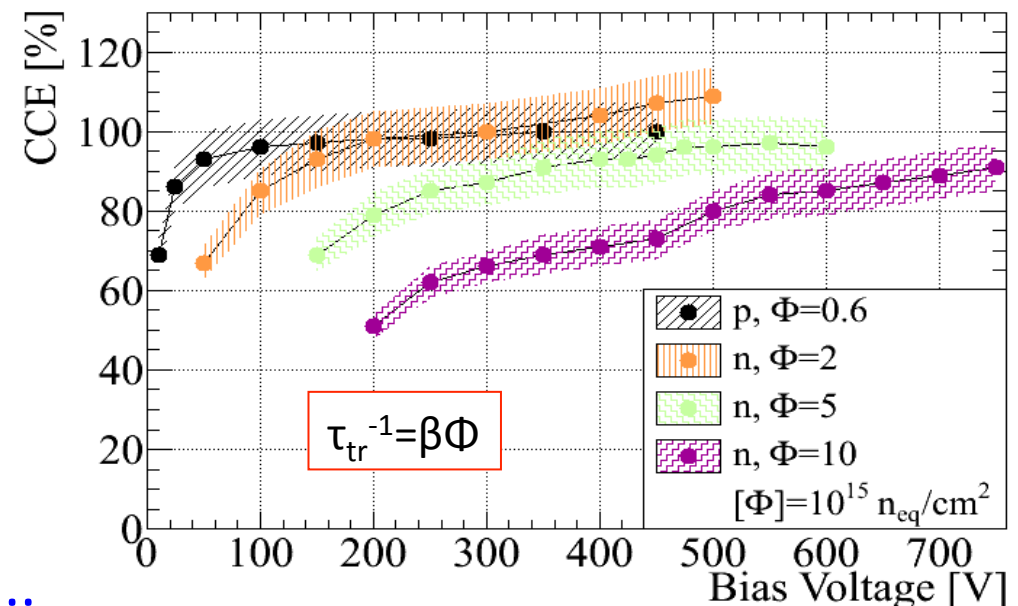
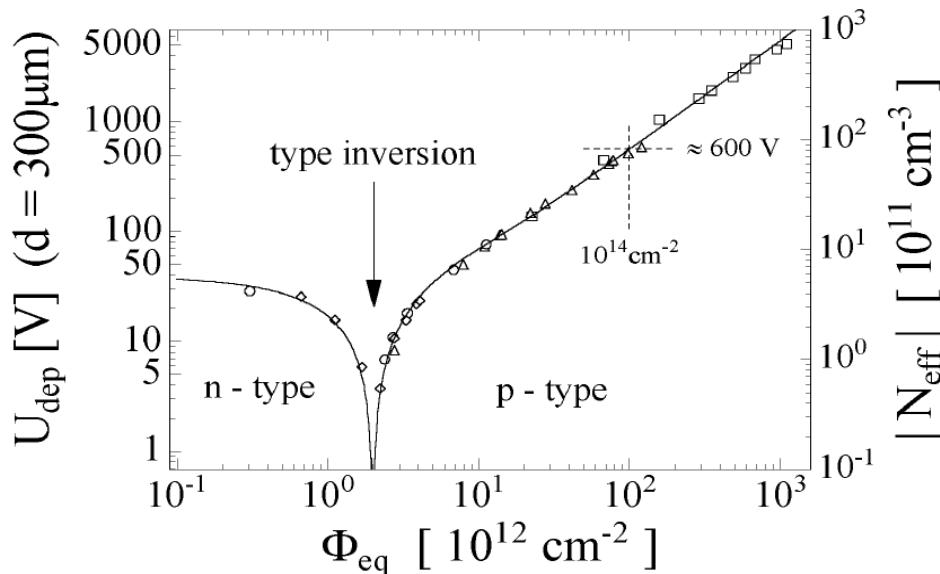
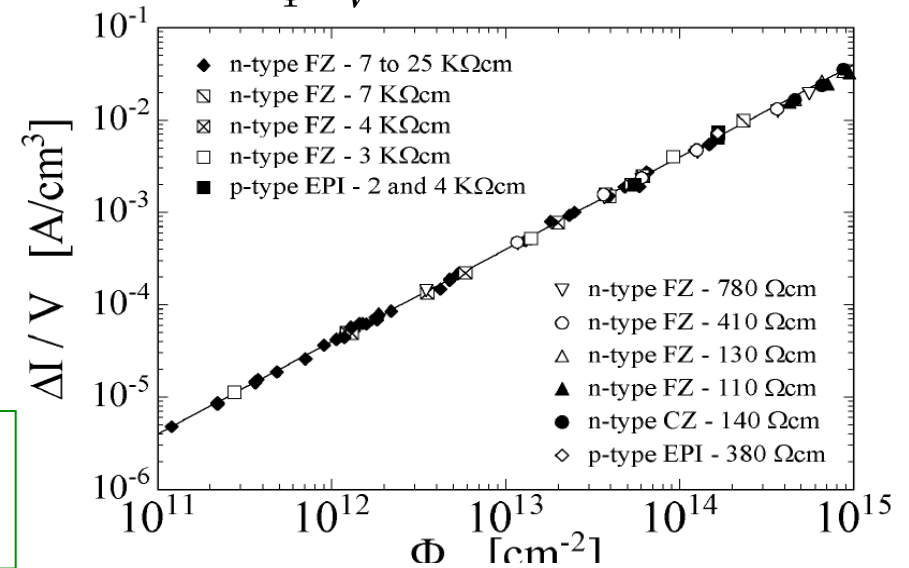
+ annealing...

Radiation damage in silicon bulk

- The leakage current increase is prop. to ϕ
- The U_{dep} increases is prop. to ϕ after type inversion
- The defects acts as trapping centers

M. Moll thesis,
MPI group

$$\alpha = \frac{\Delta I}{\Phi \cdot V} \sim 4 \times 10^{-17} \text{ A/cm}$$



+ annealing...

Defects annealing

Defects **annealing** includes defects migration, formation and dissociation

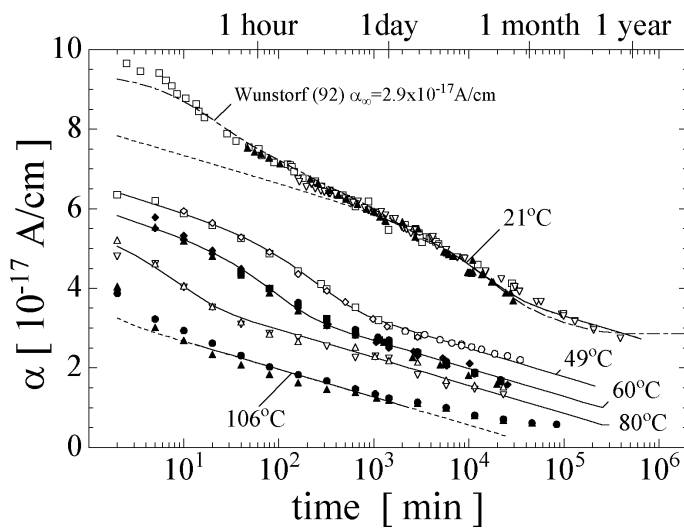
All **phenomena depend on temperature** and show a characteristic **time**, the latter depending on temperature

At first order all annealing processes become quickly negligible below 0° C

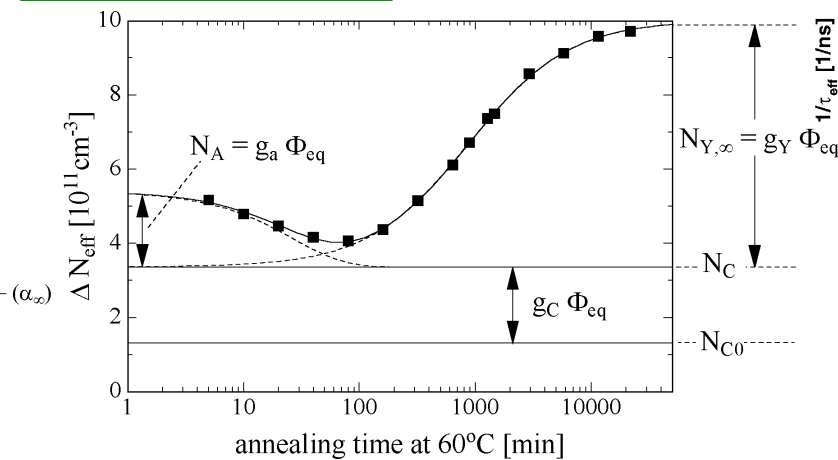
Annealing effects on macroscopic observables:

M. Moll thesis

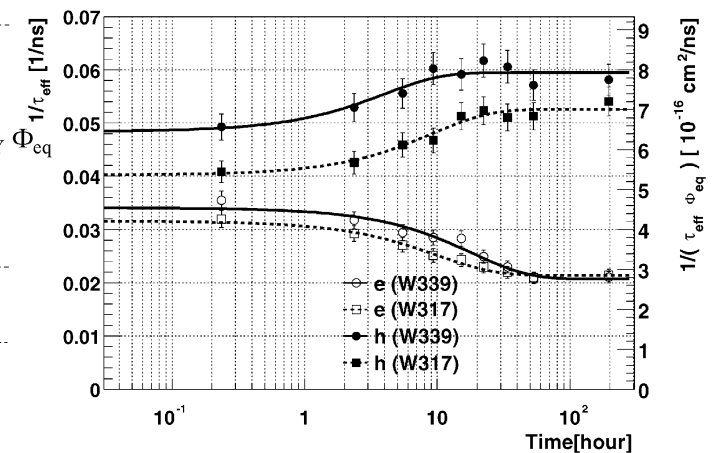
NIM A481(2002)297–305



Leakage current is always decreasing with time/temperature



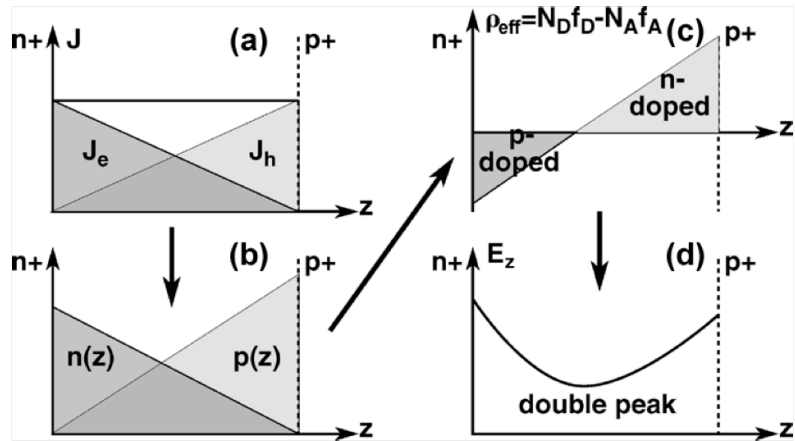
Operational voltage decreases at first (“beneficial annealing”) then it increases (“reverse annealing”)



Trapping constant annealing is beneficial for electrons while shows opposite behaviour for holes

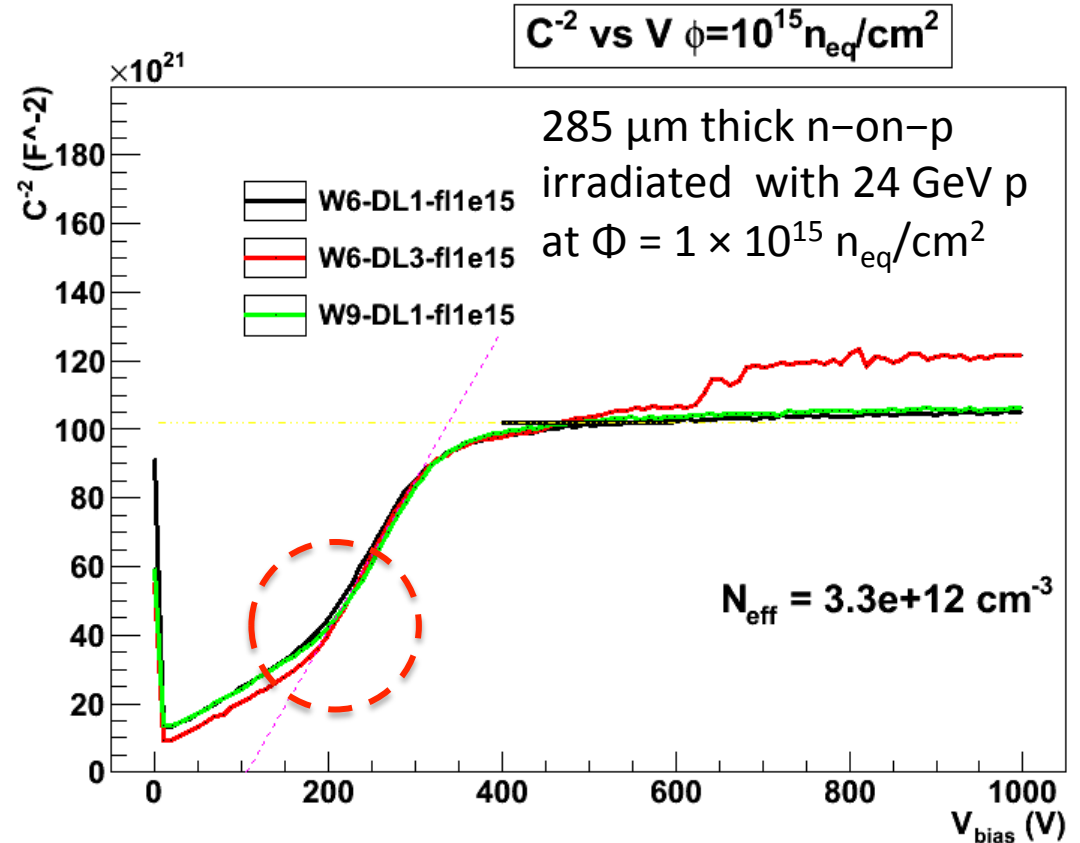
Electric field distribution in irradiated silicon

Double peak effect in electric field



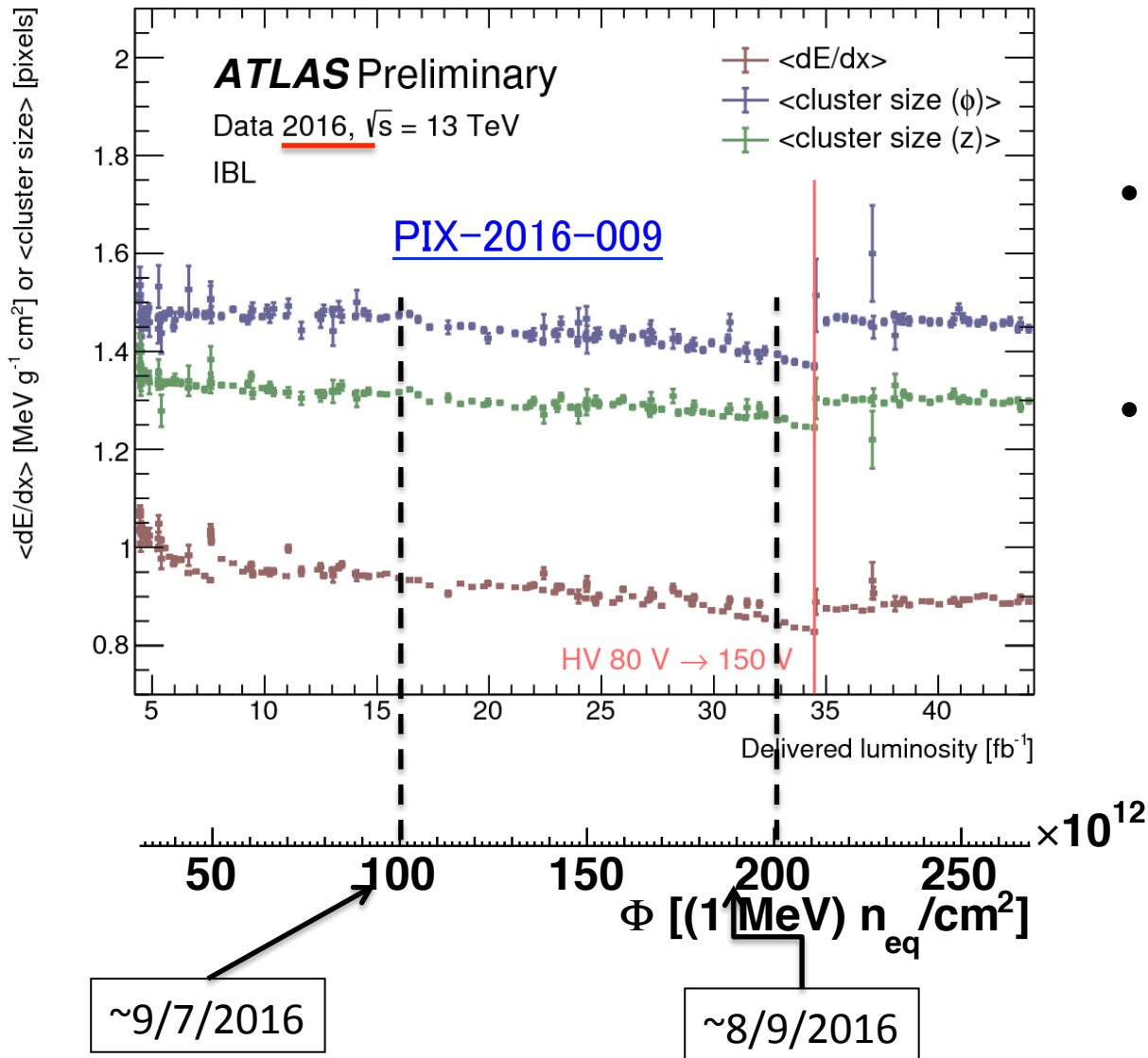
NIMA 476 (2002) 556–564

IEEE TNS 52 (2005) 1067–1075

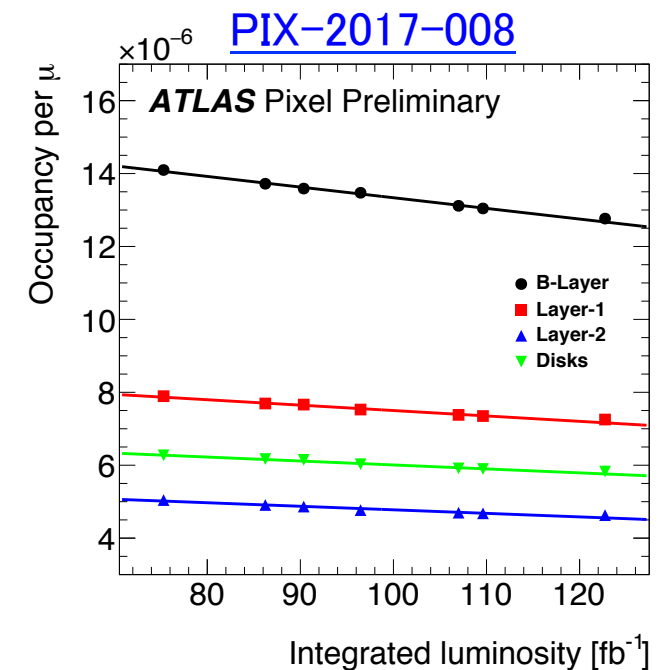


- Thermally generated carriers drift towards collecting electrodes
- Negative/positive space charge builds up approaching n⁺/p⁺ implant
- **Space charge distribution is no longer constant**
- **Electric field is no longer linear function of bulk depth**
- Visible in C⁻² vs V analysis as a **change of slope**

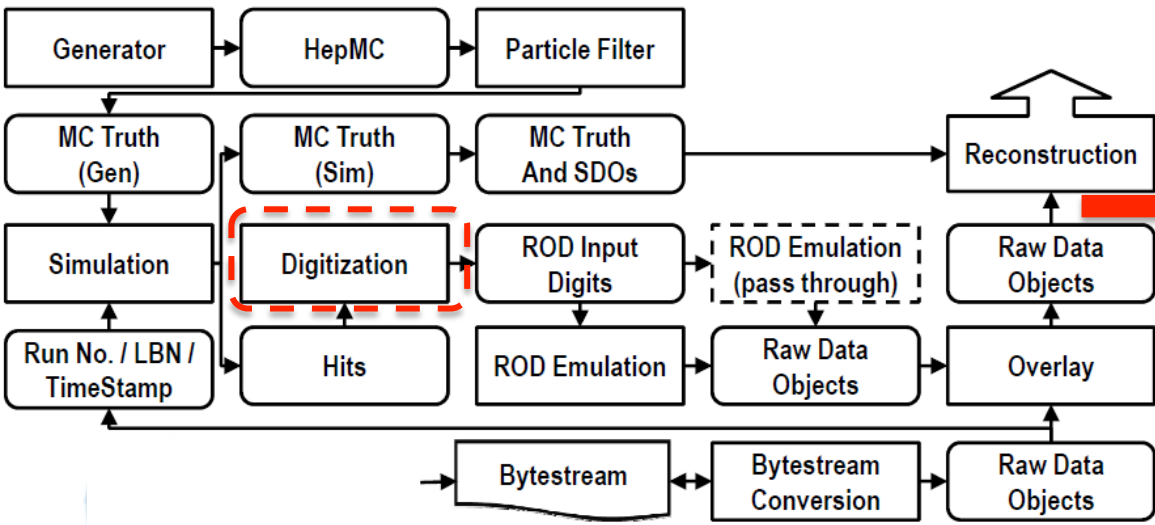
Radiation damage in current ATLAS pixels



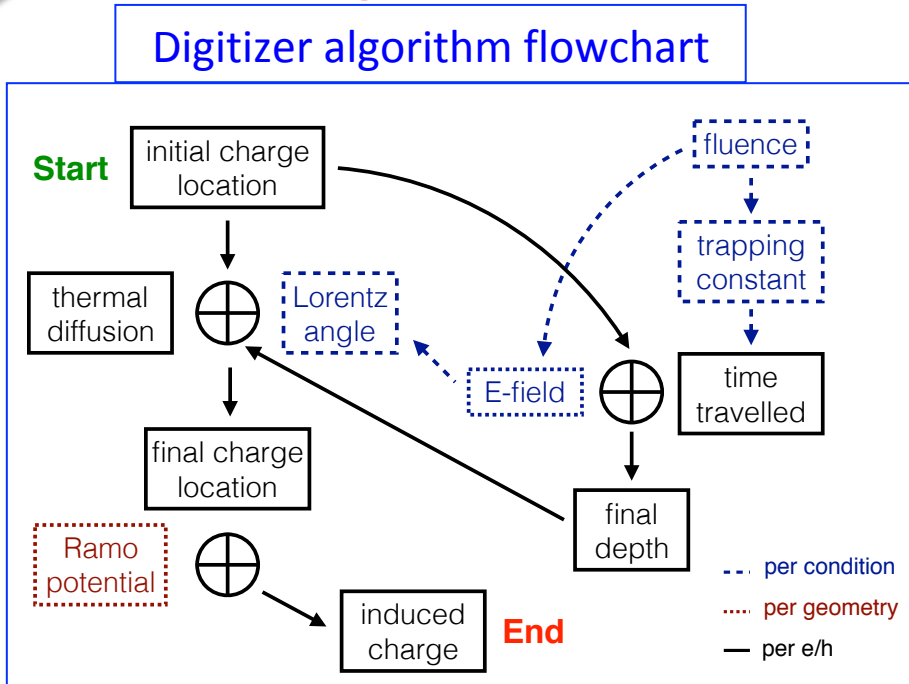
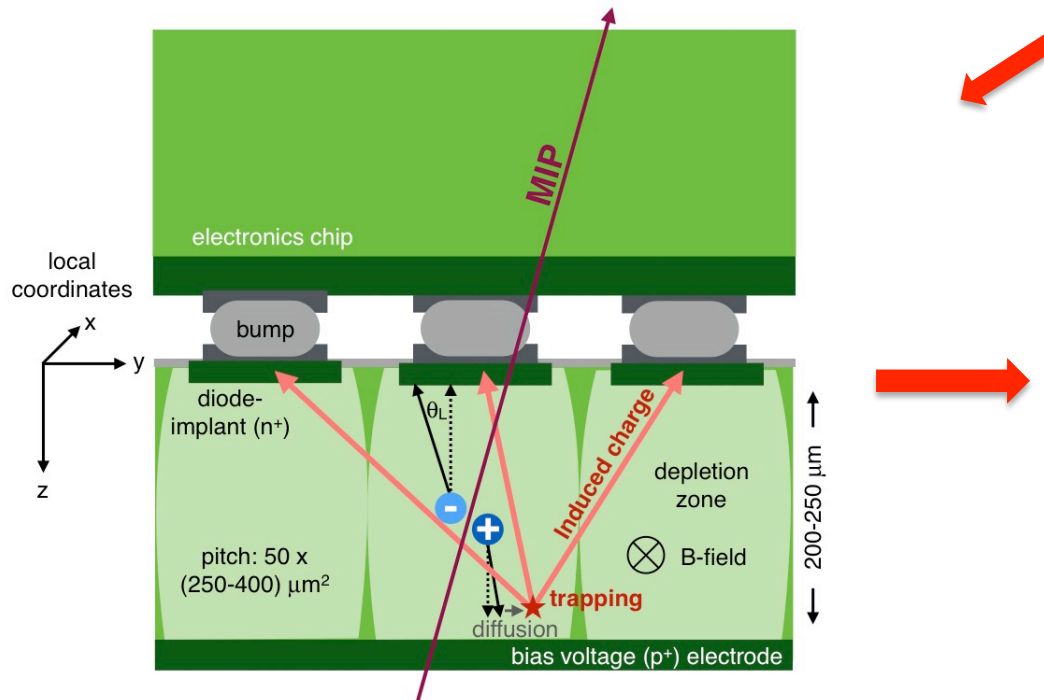
- Significant **decrease of dE/dx and cluster size for IBL**
 - Similar effect for B-Layer
- It was **necessary to increase the bias voltage** to halt the negative trend
- Occupancy decreasing too



Modelling radiation damage in ATLAS simulations



- **Digitization** step transforms carriers in digital signals on collecting electrodes
- We developed a new digitizer which includes:
 - Deformed electric field (TCAD)
 - Signal induced by trapped charges



arXiv:1710.03916
+ procs accepted by Jinst

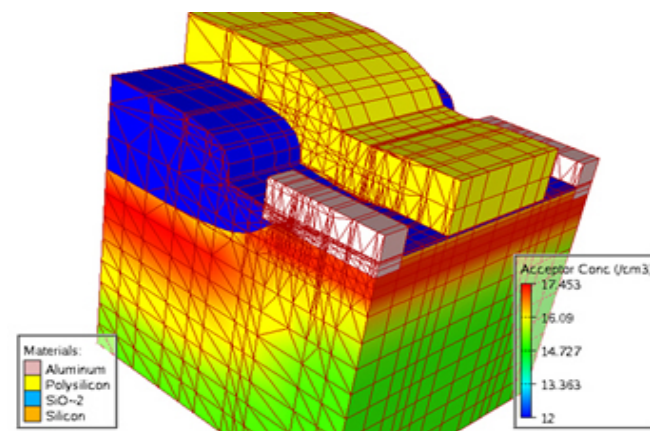
TCAD simulations for ATLAS pixels new digitizer

- Technology Computer Aided Design (TCAD) used to calculate electric field after irradiation (and Ramo potential too) for new digitizer
- Solving **drift/diffusion & Poisson equations** for electrons and holes:

$$J_n = qn\mu_n E + qD_n \frac{\partial n}{\partial x} \quad \frac{\partial n}{\partial t} = \frac{1}{q} \frac{\partial J_n}{\partial x} + G_n - R_n$$

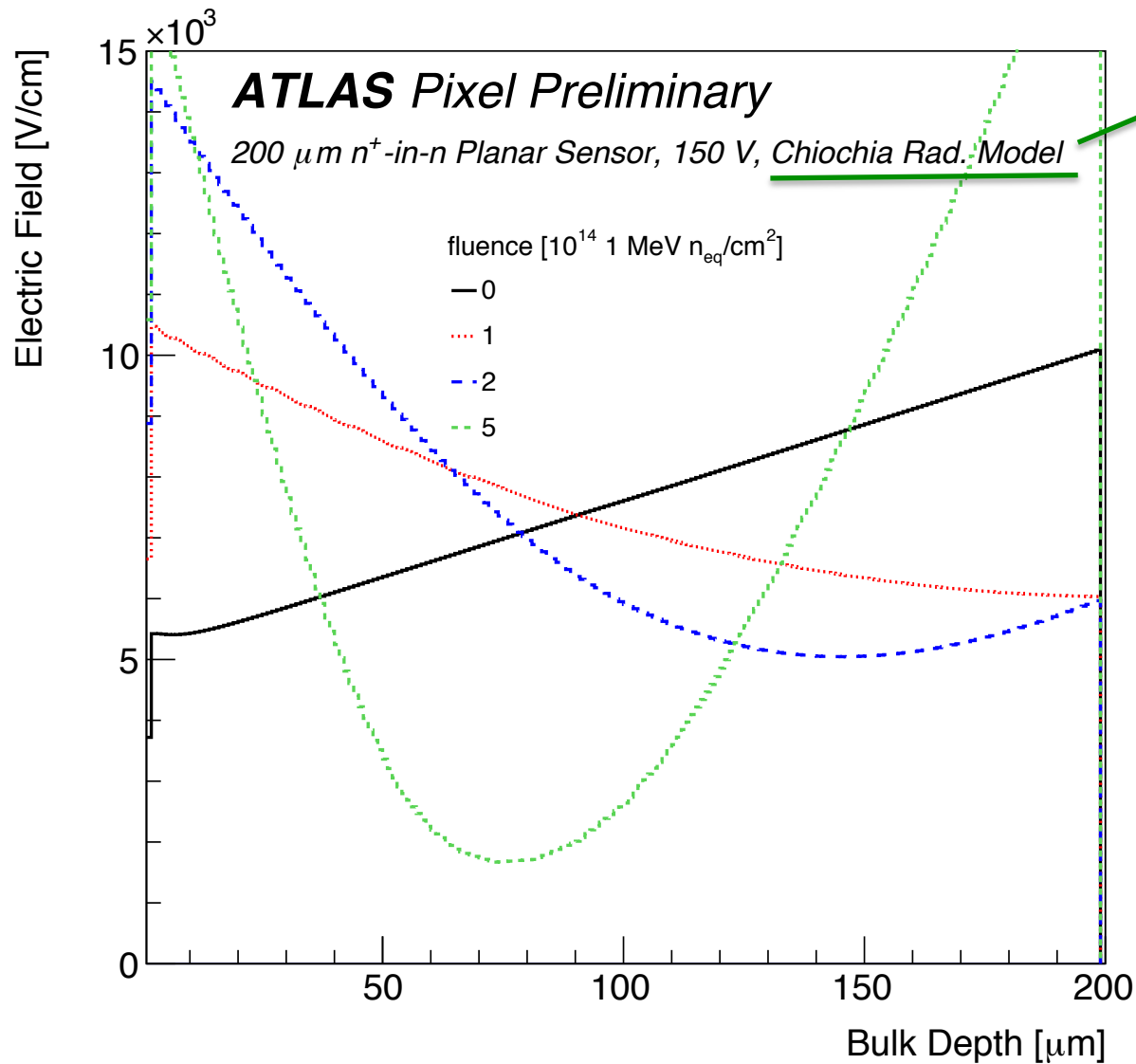
$$J_p = qn\mu_p E - qD_p \frac{\partial p}{\partial x} \quad \frac{\partial p}{\partial t} = -\frac{1}{q} \frac{\partial J_p}{\partial x} + G_p - R_p$$

$$\frac{\partial^2 \psi}{\partial x^2} = -\frac{q}{\epsilon_{Si} \epsilon_0} (N_D + p(x) - n(x) - N_A)$$



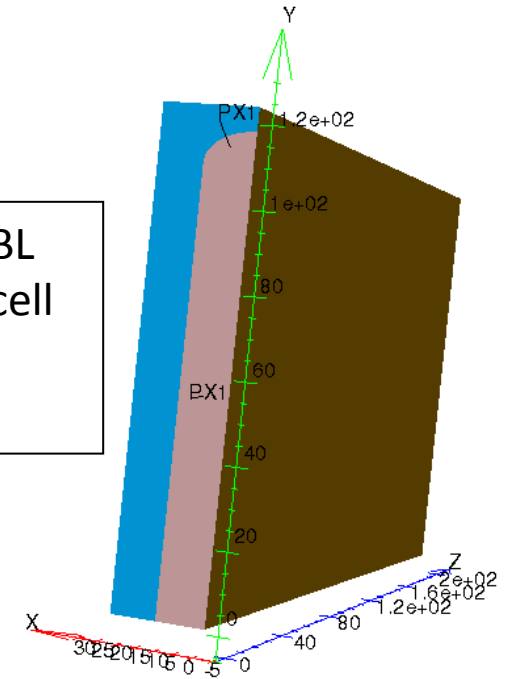
- taking into account **boundary conditions**
 - Electrodes' potentials, interface charges, etc
- **on a grid of points**
- Powerful **tool to explore and optimize** new sensors geometries (e.g. edgeless detectors) **and performance after irradiation**

Electric field predictions for IBL planar sensors



NIM A568 (2006) 51–55

A $\frac{1}{4}$ of the IBL planar pixel cell has been simulated



After irradiation the **electric field** is **no** longer a **linear** function of the bulk depth
This has an **impact** on:

- **Charge Collection Efficiency**
- **Lorentz Angle**

A word on TCAD radiation damage models

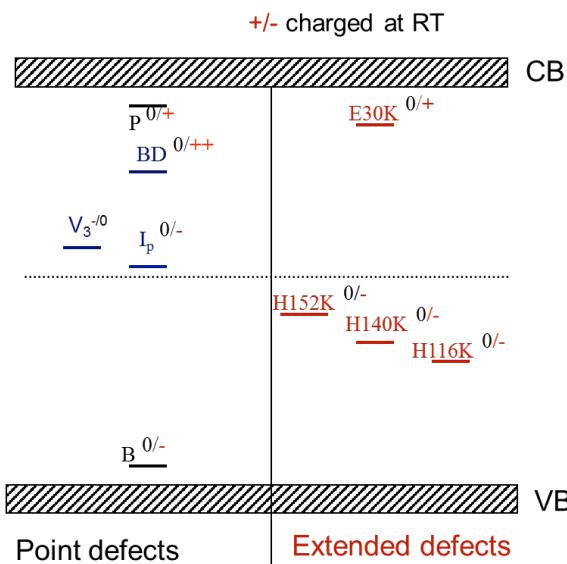
Measured defects

Point defects

- $E_a^{BD} = E_c - 0.225 \text{ eV}$
- $\sigma_n^{BD} = 2.3 \cdot 10^{-14} \text{ cm}^2$
- $E_a^{V3} = E_c - 0.545 \text{ eV}$
 - $\sigma_n^{V3} = 1.7 \cdot 10^{-15} \text{ cm}^2$
 - $\sigma_p^{V3} = 9 \cdot 10^{-14} \text{ cm}^2$
- $E_a^{Ip} = E_c - 0.545 \text{ eV}$
 - $\sigma_n^{Ip} = 1.7 \cdot 10^{-15} \text{ cm}^2$
 - $\sigma_p^{Ip} = 9 \cdot 10^{-14} \text{ cm}^2$

Extended defects

- > $E_a^{H116K} = E_v + 0.33 \text{ eV}$
- > $\sigma_p^{H116K} = 4 \cdot 10^{-14} \text{ cm}^2$
- > $E_a^{H140K} = E_v + 0.36 \text{ eV}$
- > $\sigma_p^{H140K} = 2.5 \cdot 10^{-15} \text{ cm}^2$
- > $E_a^{H152K} = E_v + 0.42 \text{ eV}$
- > $\sigma_p^{H152K} = 2.3 \cdot 10^{-14} \text{ cm}^2$
- > $E_a^{E30K} = E_c - 0.1 \text{ eV}$
- > $\sigma_n^{E30K} = 2.3 \cdot 10^{-14} \text{ cm}^2$



Simulated defects (TCAD, Chiochia model)

- Deep acceptor ($q=0/-$)
- Deep donor ($q=0/+$)

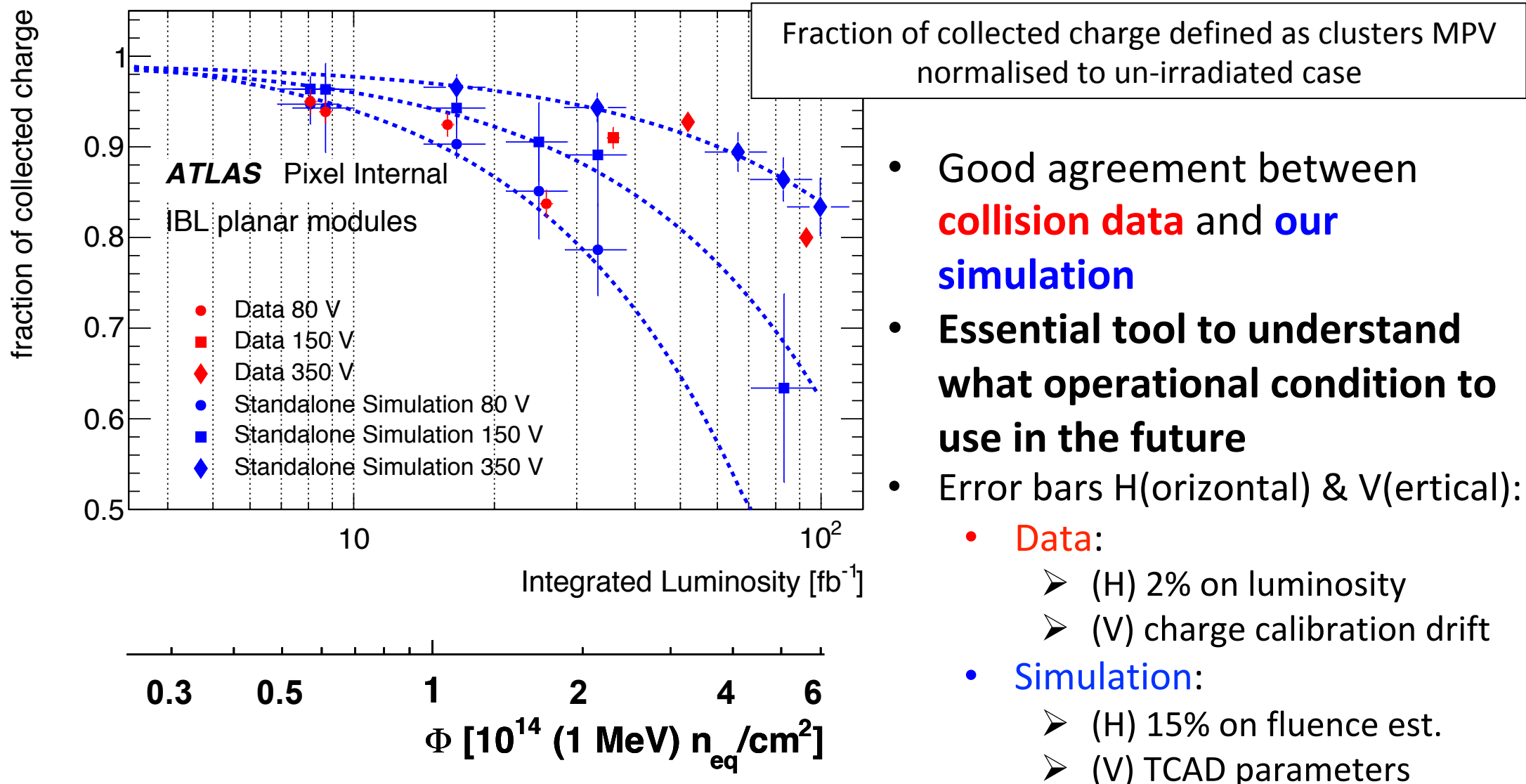
I. Pintilie (VERTEX2016). 25-30 September, 2016.

M. Moll,
Simdet 2016

Working with “effective levels” for simulation of irradiated devices

- Most often 2, 3 or 4 “effective levels” used to simulate detector behavior
- Defect densities and cross sections of defects tuned to match experimental data
- Leakage current, signal loss and electric field profile reproducible (with some caveats)

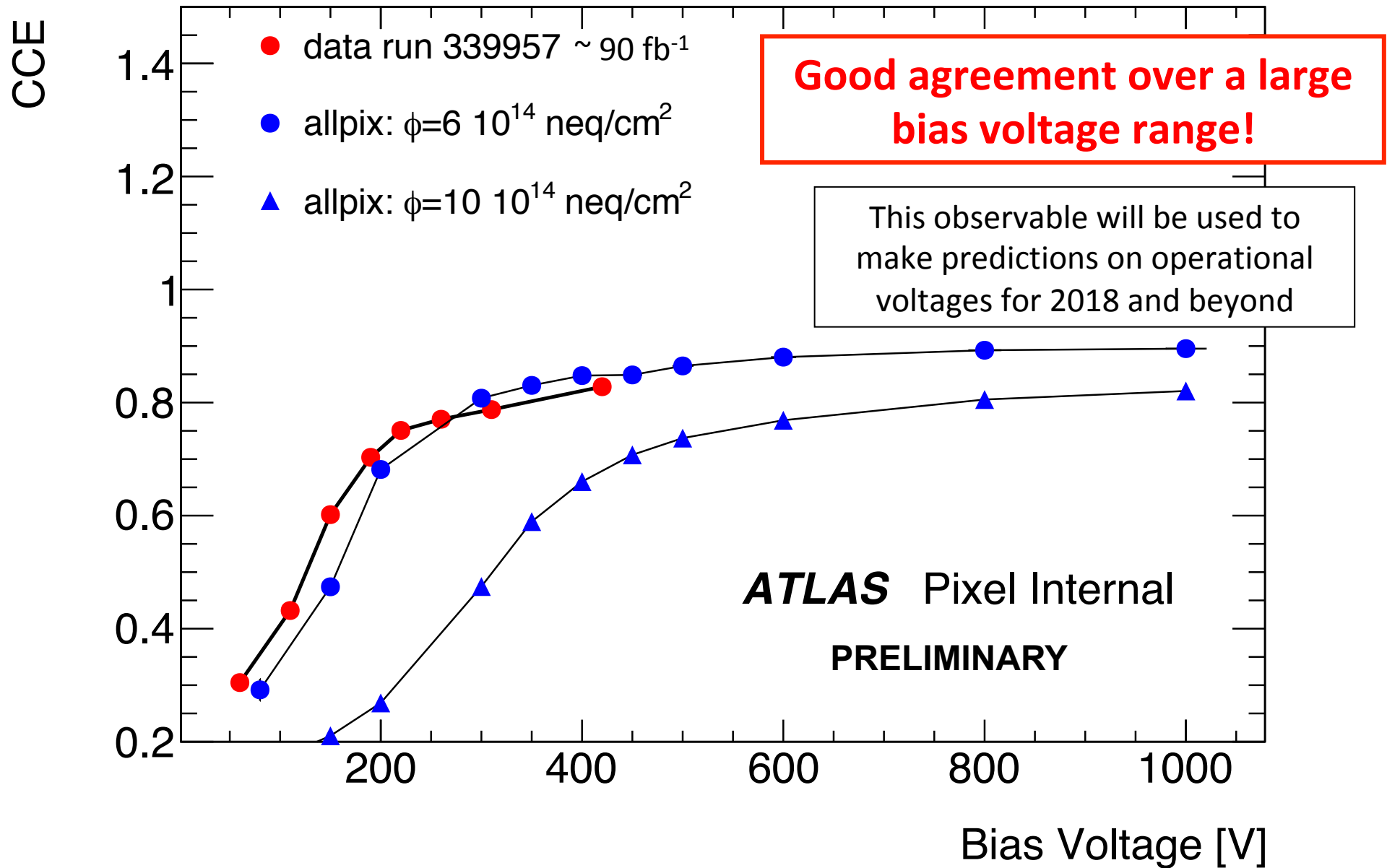
Charge collection efficiency: data vs simulation



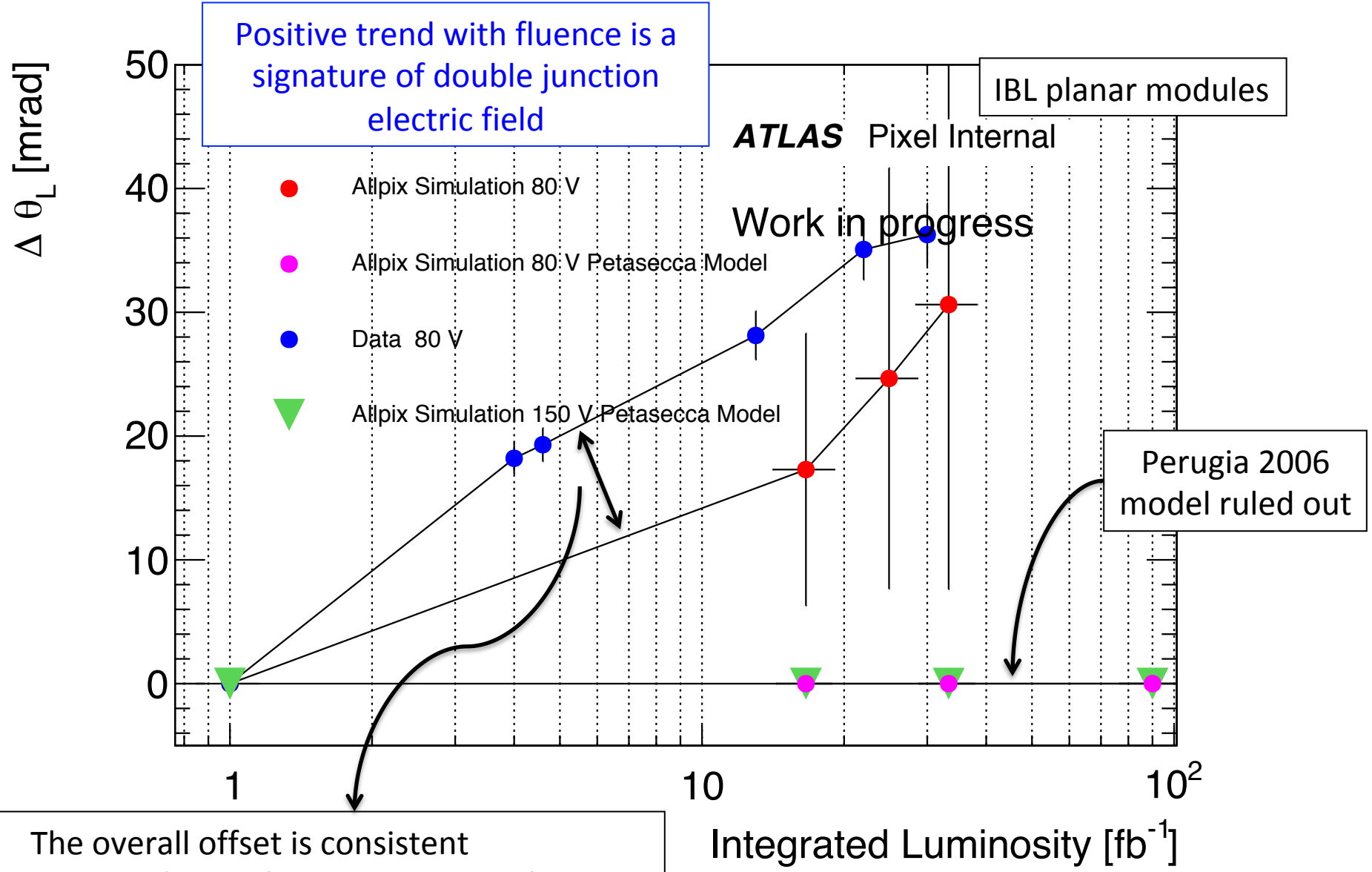
Old public version available here:
[PIX-2017-004](#)

[arXiv:1710.03916](#)
+ procs accepted by Jinst

CCE vs Bias Voltage in IBL planar sensors



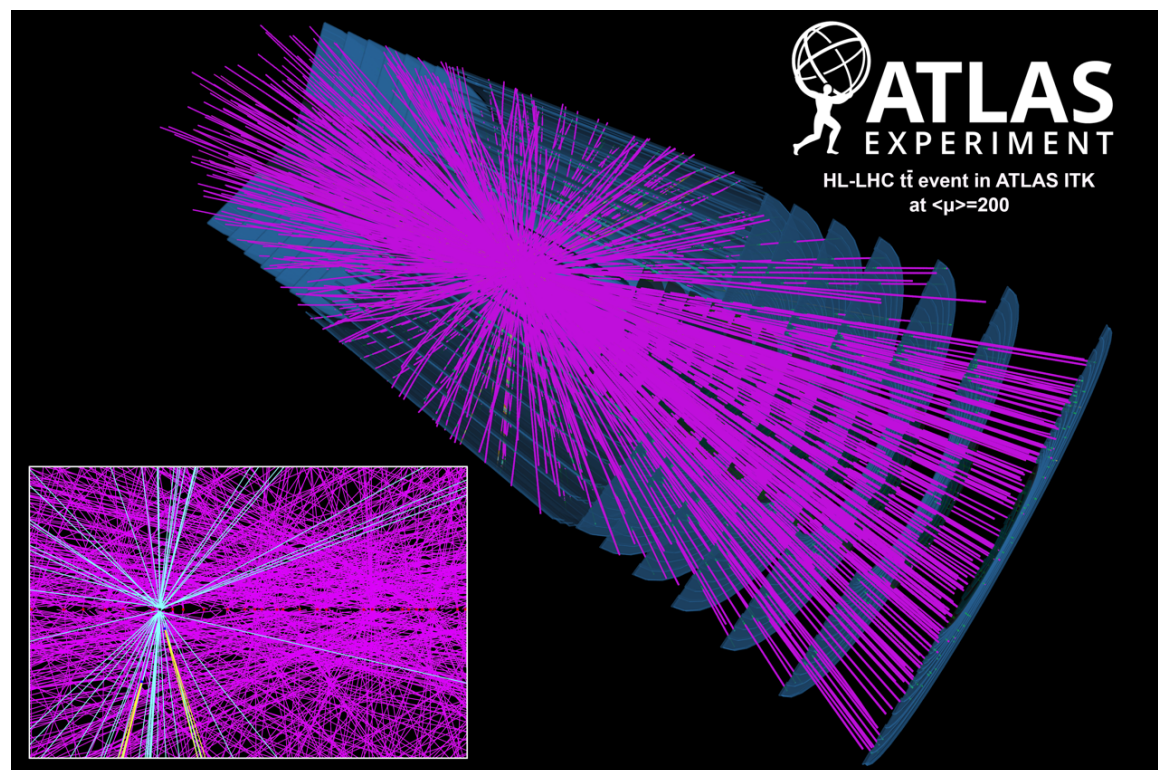
Lorentz Angle in ATLAS pixels: data vs simulation



The overall offset is consistent with previous studies and appears even without radiation damage (zero fluence)

Comments and Summary

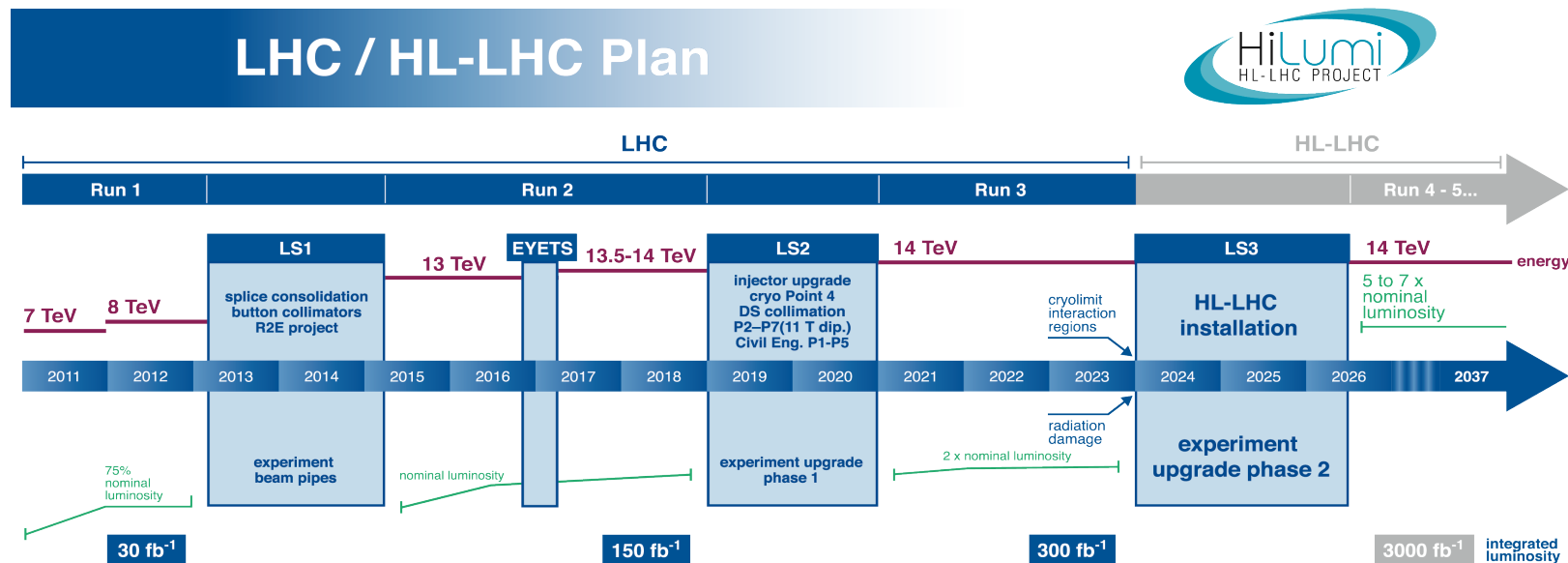
- Radiation damage is already impacting ATLAS Pixel detector:
 - Reduction of signal, cluster size, dE/dx, occupancy; drift of Lorentz Angle (LA)
- Two-fold action:
 1. **Reproduce radiation damage effects in ATLAS digitizer**
 2. Make predictions for optimal future data taking conditions
- New ATLAS pixel digitizer calculate signal induced on electrodes taking into account deformed electric field and trapping
- ✓ Model validated on collision data for what concerns CCE and LA
- Extrapolation for end of 2018 (expected $\sim 1 \times 10^{15} n_{eq}/\text{cm}^2$) on-going



PIXEL DETECTORS FOR THE NEW ATLAS INNER TRACKER

High Luminosity LHC

- To fully exploit its physics reach, CERN plans to upgrade LHC into an **High Luminosity collider (HL-LHC)**
- With $L = 5-7 \times 10^{34} / \text{cm}^2 / \text{s}$ and about 4 ab^{-1} of final data set observation of **rare SM mechanism** will be eventually **possible** (one example: **Higgs self-coupling**) and the **physics reach** for several **BSM** scenarios will be significantly **extended**
- Such large instantaneous and integrated luminosities translate into an **unprecedented** level of events rate and **radiation fluence**.
- The ATLAS Inner Detector needs to be replaced**



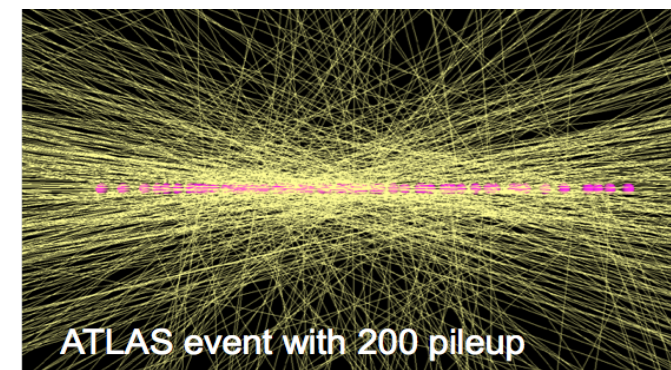
Challenges for the future ATLAS tracker

- Instantaneous luminosity : $L_{\text{inst}} = 5-7 \times 10^{34} \text{ cm}^{-2}\text{s}^{-1}$
 - x7 more than today
- Events-pile up: $\mu \approx 140 - 200 \text{ events/Bunch Crossing}$
 - x8-10 more than today



➤ Need to increase the pixel granularity

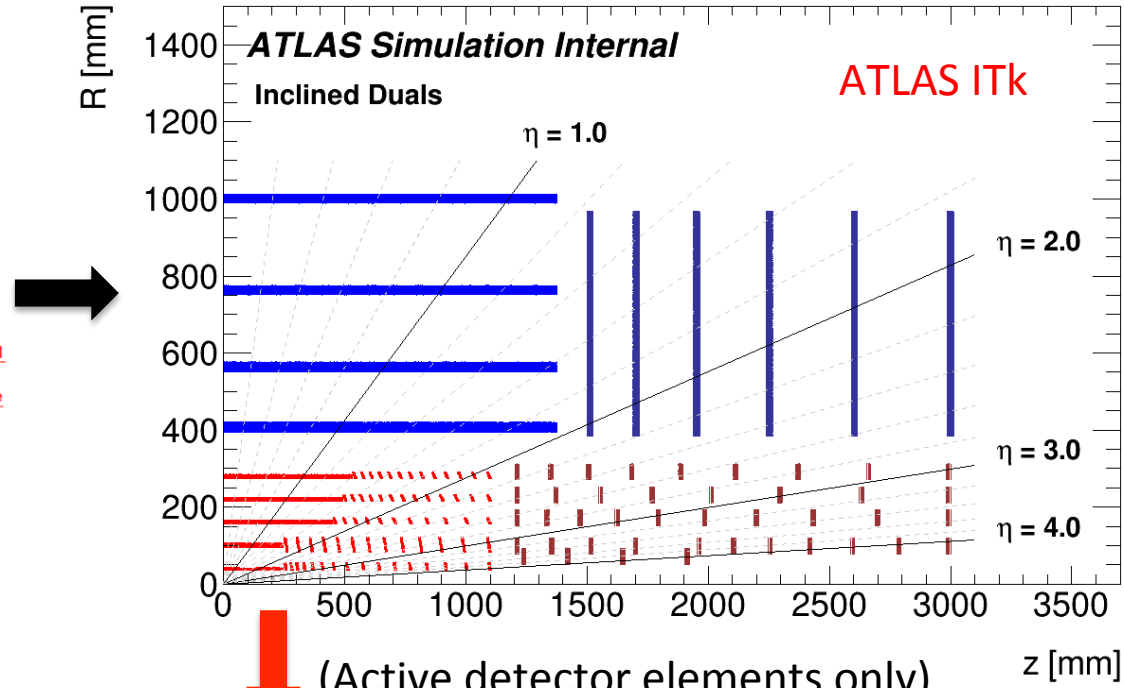
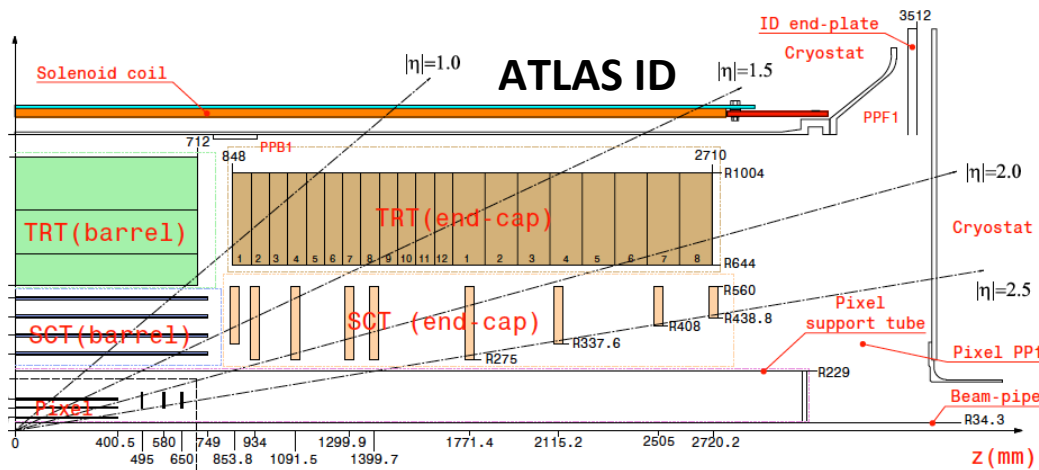
- Actual pixel size: $50 \times (250-400) \mu\text{m}^2$
- Expected fluence: $\phi = 2 \times 10^{16} n_{\text{eq}}/\text{cm}^2$
 - x5 more the actual sensor lifetime limit



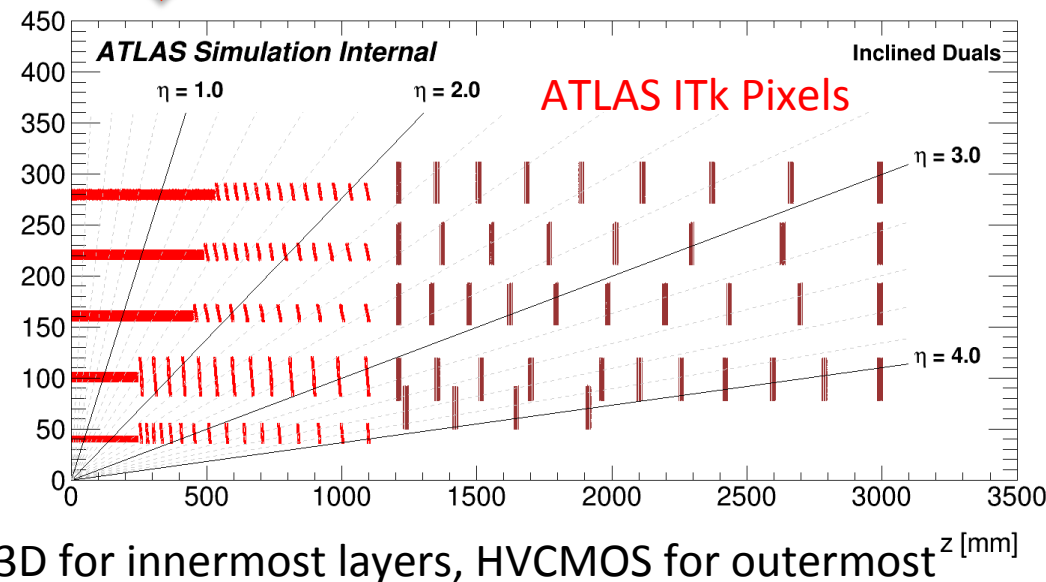
➤ Need radiation-hard detectors

➤ Goal: better performance in a harsher environment!

From ATLAS Inner Detector to Inner Tracker



(Active detector elements only)



3D for innermost layers, HVCMOS for outermost z [mm]

The new **ATLAS Inner Tracker (ITk)** will be an **all silicon tracking system**, composed of:

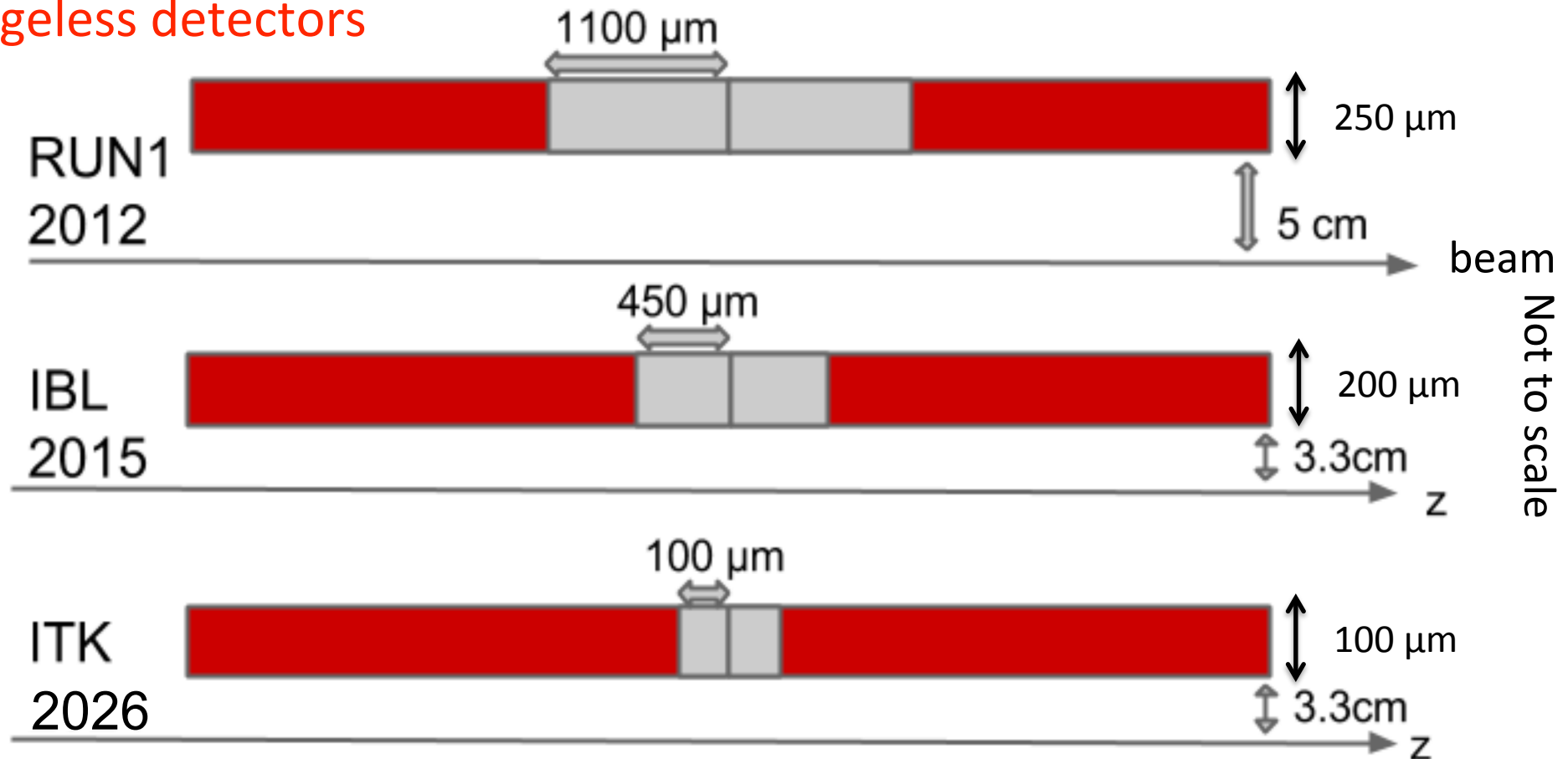
- 5 pixel barrel layers with *inclined modules*, down to $|\eta| \sim 4$, plus several pixel rings
- **Pixel pitch: $50\mu\text{m} \times 50\mu\text{m}$** (it was $50 \times 250\text{-}400$)
- Small pitch to keep occ. at 0.1% even with $\mu=200$
- **Pixel thickness: $100\text{-}150\mu\text{m}$** (it was $200\text{-}250$)
- Reduced thickness to cope with charge trapping
- Total pixel surface: $\sim 13 \text{ m}^2$ (it was 1.6 m^2)
- Total number of channels $\sim 5.2 \text{ G}$ (it was $\sim 90 \text{ M}$)

[ATLAS-TDR-025](#) + ITk Pixel TDR (internal)

Edgeless (and thin) detectors

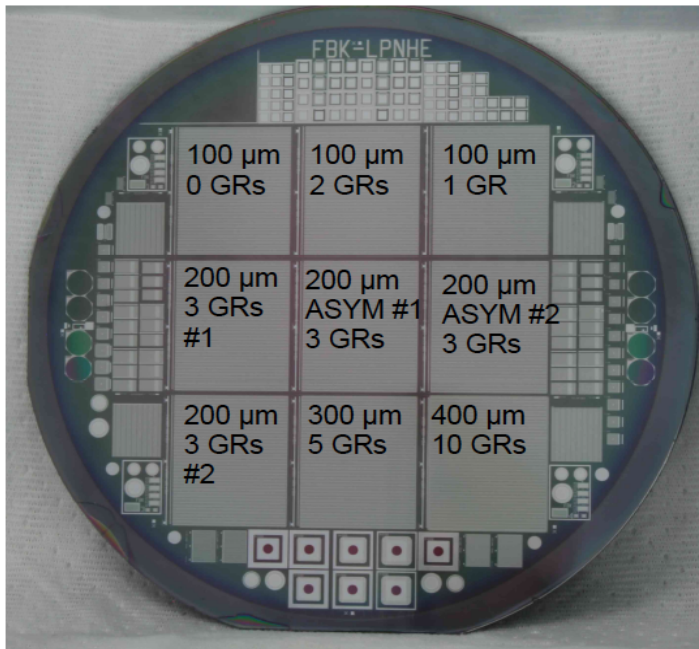
- To maintain (and improve) the flavour tagging performance we have to place detection modules as close as possible to the beam interaction point
- Detectors dead areas are to be reduced to maximize acceptance

➤ Edgeless detectors



LPNHE planar pixel productions

PAE1 – active edge

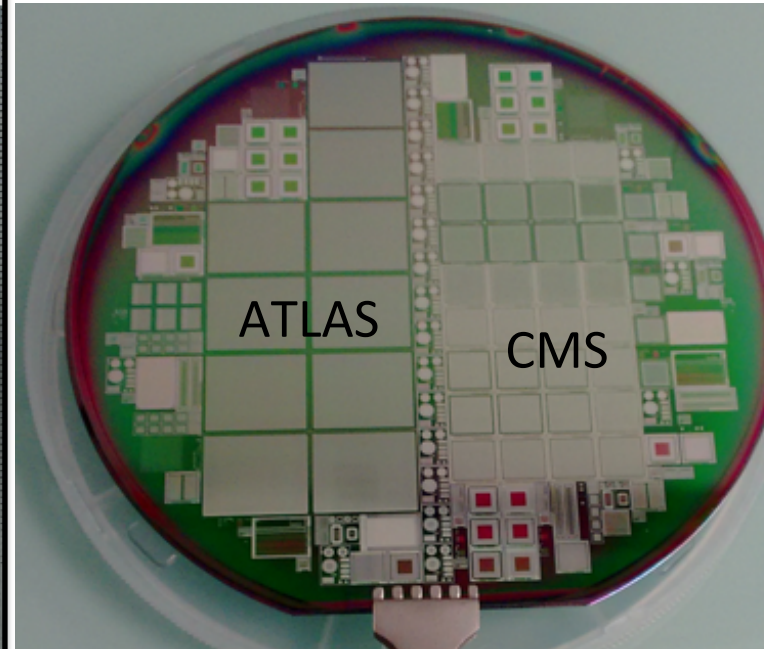


4" 200 μm thick n-on-p
Active Edge technology
Pixel-to-edge down to 100 μm
Tested extensively on beam

NIM A 712 (2013) 41–47

JINST 12 P05006 (2017)

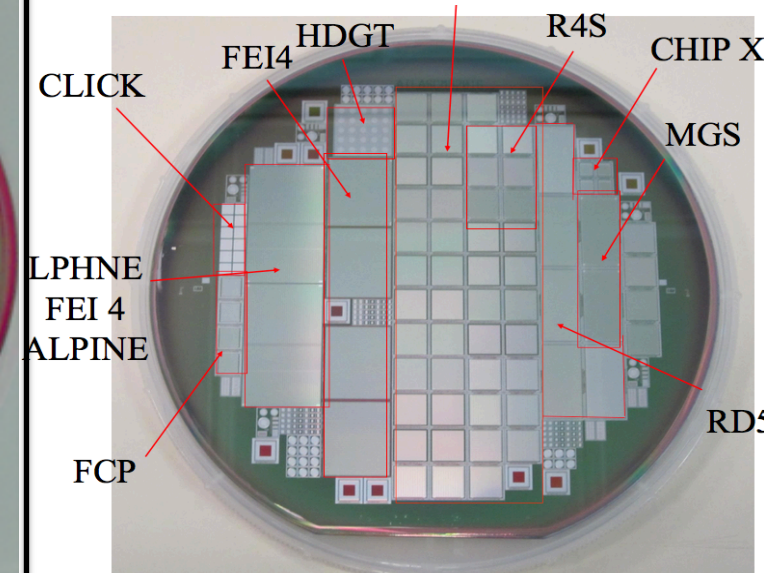
P2 - thin



6" 100 μm thick n-on-p
INFN ATLAS/CMS project
Tested extensively on beam,
after irradiation too

2017 JINST 12 C12038

PAE3 - thin and active edge



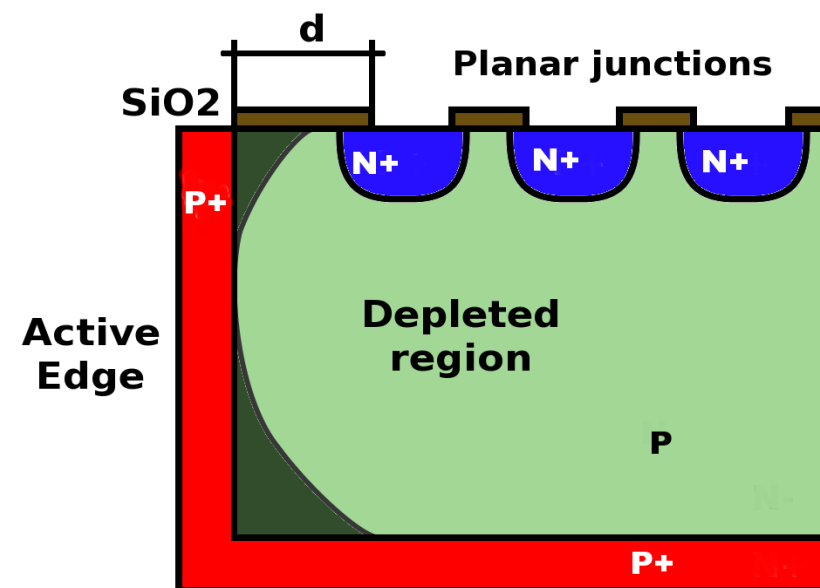
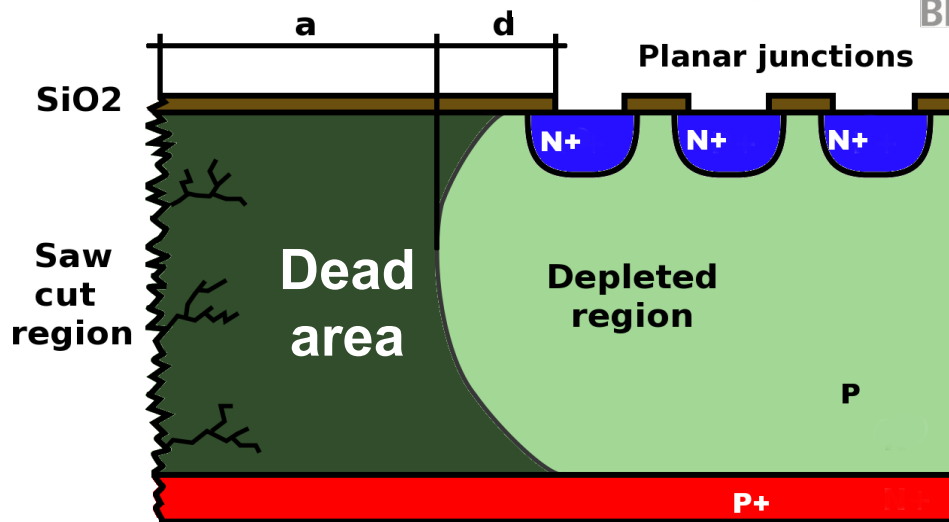
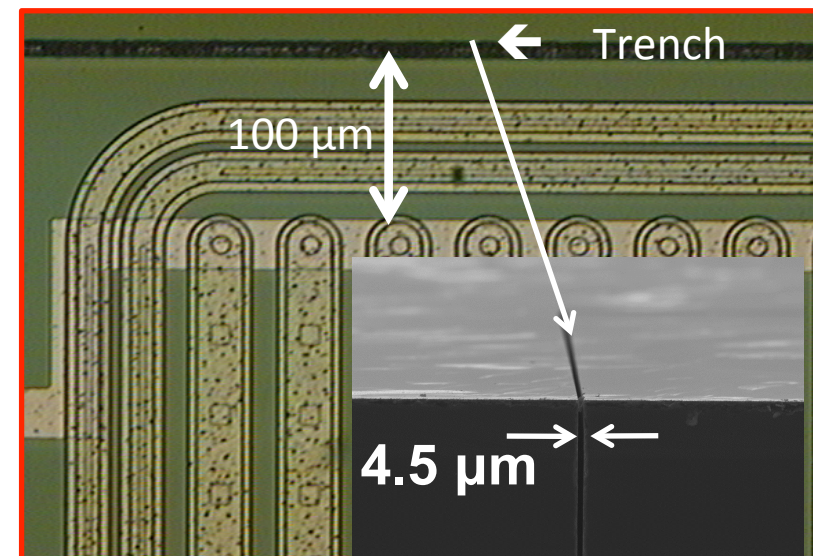
6" 100 μm thick n-on-p
INFN ATLAS/CMS project
Active Edge technology
Pixel-to-edge down to 50 μm
50x50 μm pitch sensors
Tested on beam,
after irradiation too

13th Trento Workshop, 2018

The FBK/LPNHE PAE1 pixel production

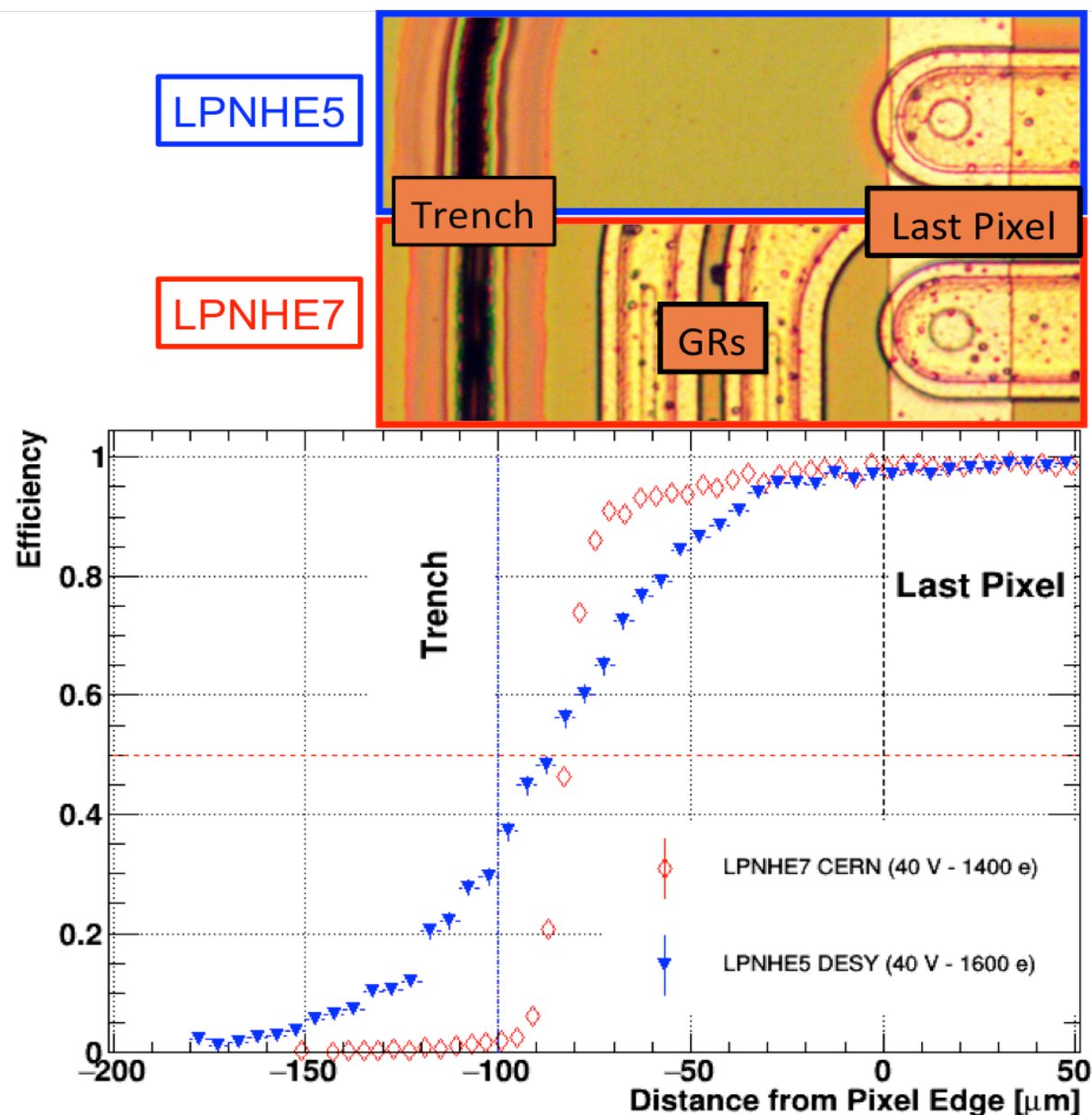
An FBK-LPNHE production

- 200 μm thick, n-on-p sensors
- **Challenge: reduce the dead area at the detector periphery** (Atlas: 1100 μm)
- Technique: *Deep reactive Ion Etching*
- ✓ **Inactive region down to: 100 μm**



NIM A 712 (2013) 41-47

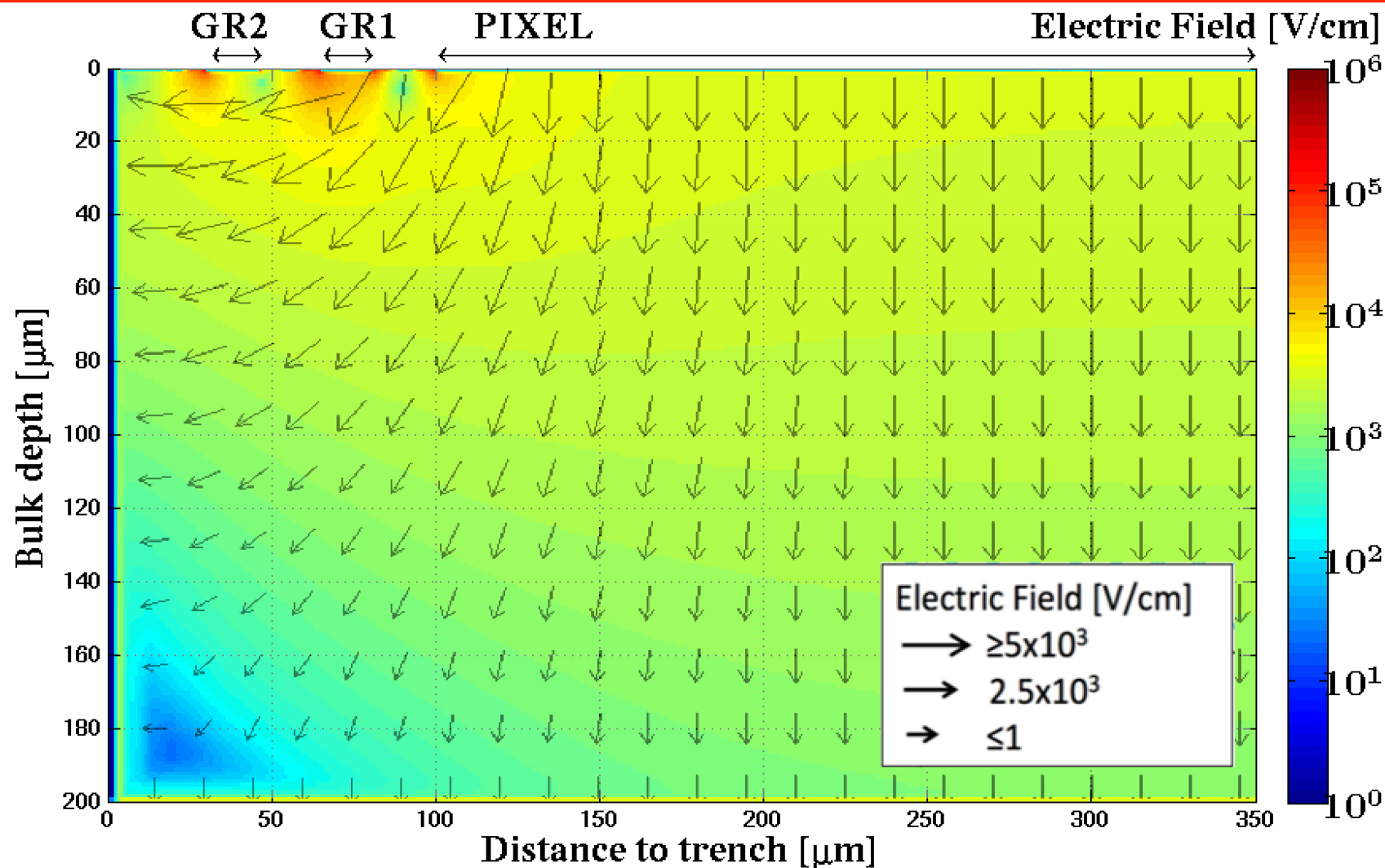
Testbeam performance of edgeless detectors



- The detector is efficient beyond the last collecting electrode
- Efficiency is $> 90\%$ up to $80 \mu\text{m}$ away from the last pixel
- **The dead area is no longer dead!**
- But how is it possible that charge is collected beyond the last pixels?
- **TCAD simulations can shed light here!**

JINST 12 P05006 (2017)

TCAD simulations and edgeless detectors

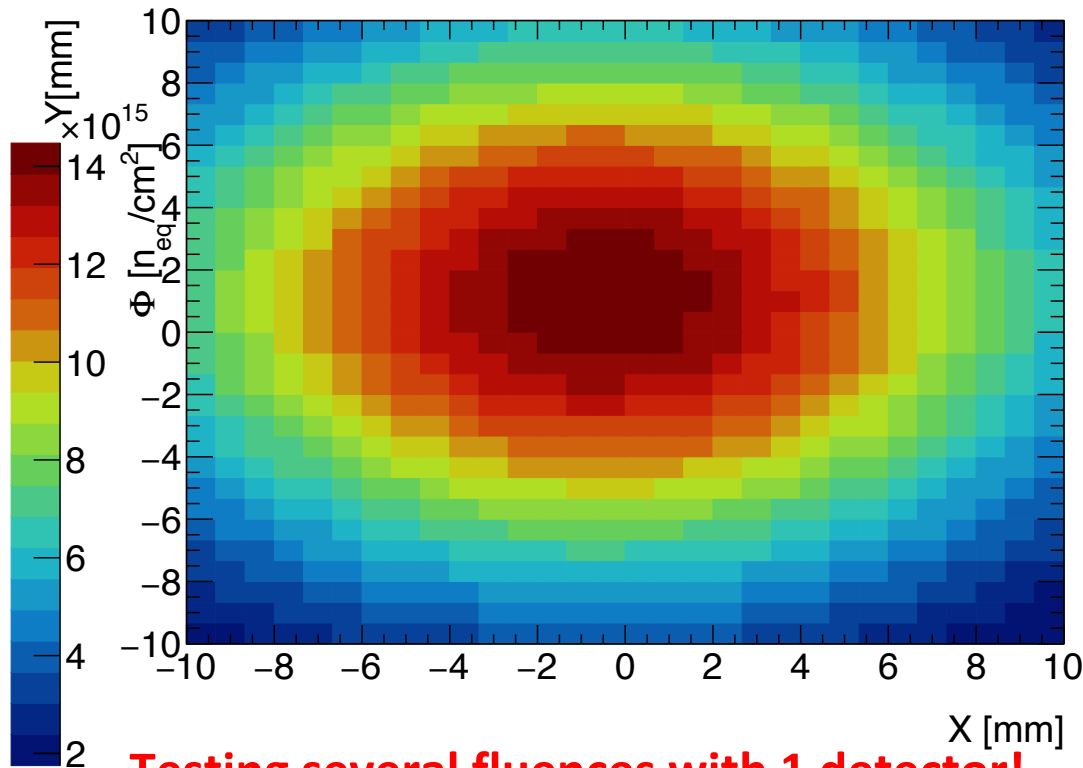


Charges are not collected and re-emitted by the GRs
apart from few μm below the surface

JINST 12 P05006 (2017)

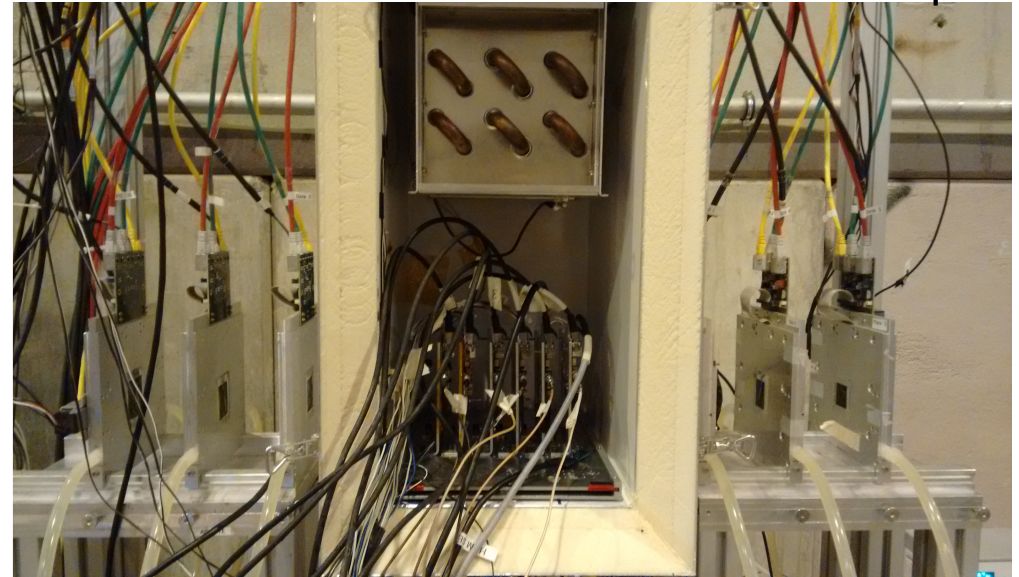
P2 - Thinner detectors for the HL-LHC phase

Two n-on-p pixels sensors from P2 production were irradiated with 24 GeV protons at CERN in subsequent irradiation steps with a Gaussian beam profile



Testing several fluences with 1 detector!

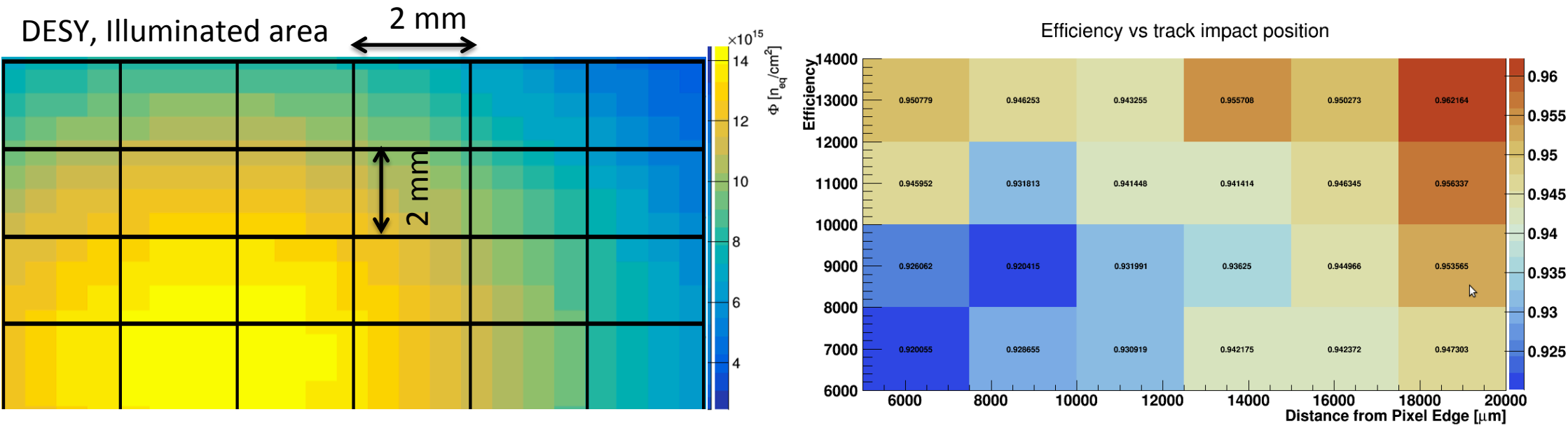
Tested on beam after each irradiation step



Module name (thickness [μm], # of GRs)	Beam spot size (FWHM - [mm ²])	Fluence ϕ [10 ¹⁵ n _{eq} /cm ²]	Cumulative fluence at peak Φ [10 ¹⁵ n _{eq} /cm ²]
W80 (130, 2)	20×20	3	same
W30 (100, 5)	12×12	4	same
W80 (130, 2)	20×20	7	10
W30 (100, 5)	20×20	7	11

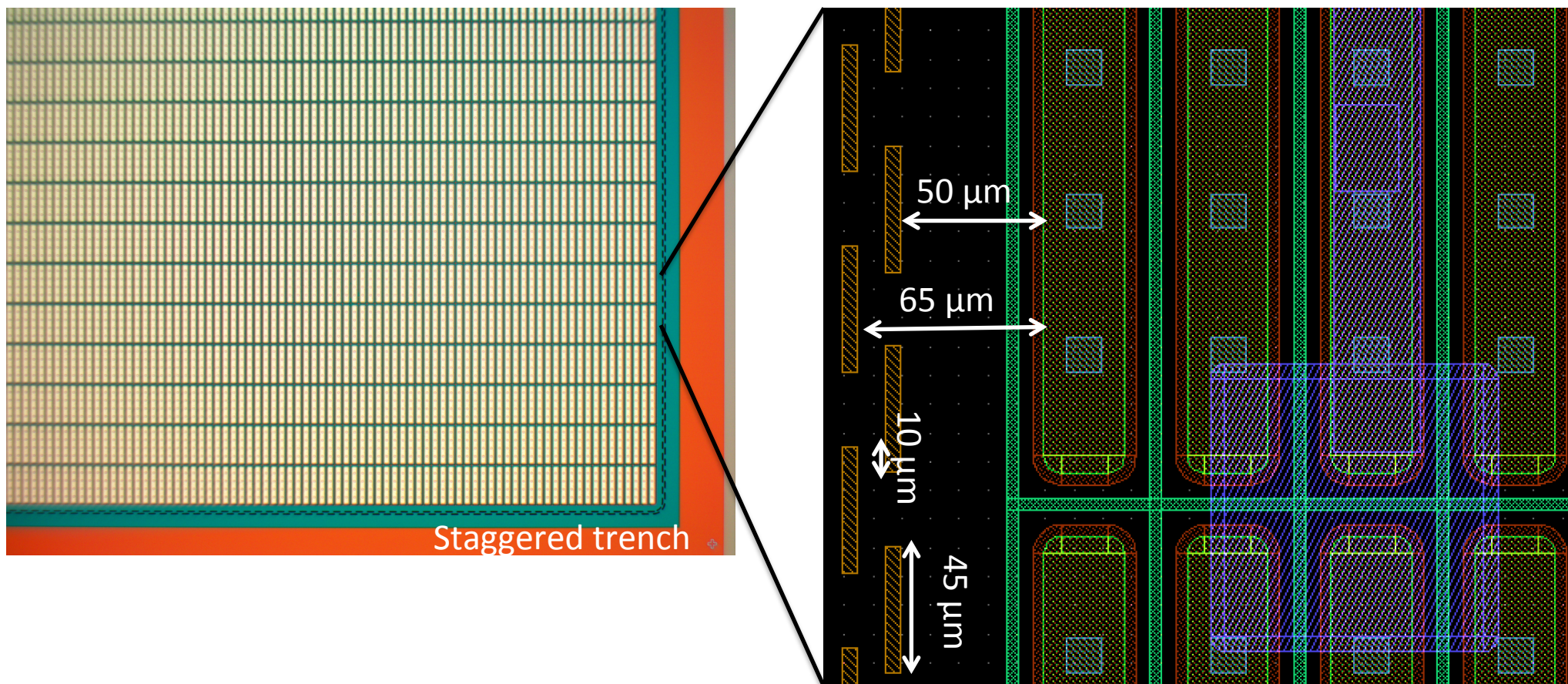
2017 JINST 12 C12038

P2 – Hit efficiency after HL-LHC like fluence



- Module tested up to 600 V at $t = -40^\circ \text{C}$
 - at DESY (4 GeV/c electron beam) and CERN (120 GeV pion beam)
- Hit-efficiency is $\sim 92-94\%$ at $1.4 \times 10^{16} n_{eq}/\text{cm}^2$
- Hit-efficiency is $\sim 96-98\%$ at $5.5 \times 10^{15} n_{eq}/\text{cm}^2$
- Average hit-efficiency is $\sim 94-96\%$ at $1 \times 10^{16} n_{eq}/\text{cm}^2$ (ITk specs. require 97%)
- **Uncertainties** on irradiation **map alignment, threshold** and **gain** uniformity
- *To be used to tune the digitizer for HL-LHC fluences*

PAE3 – thin and active edge sensors



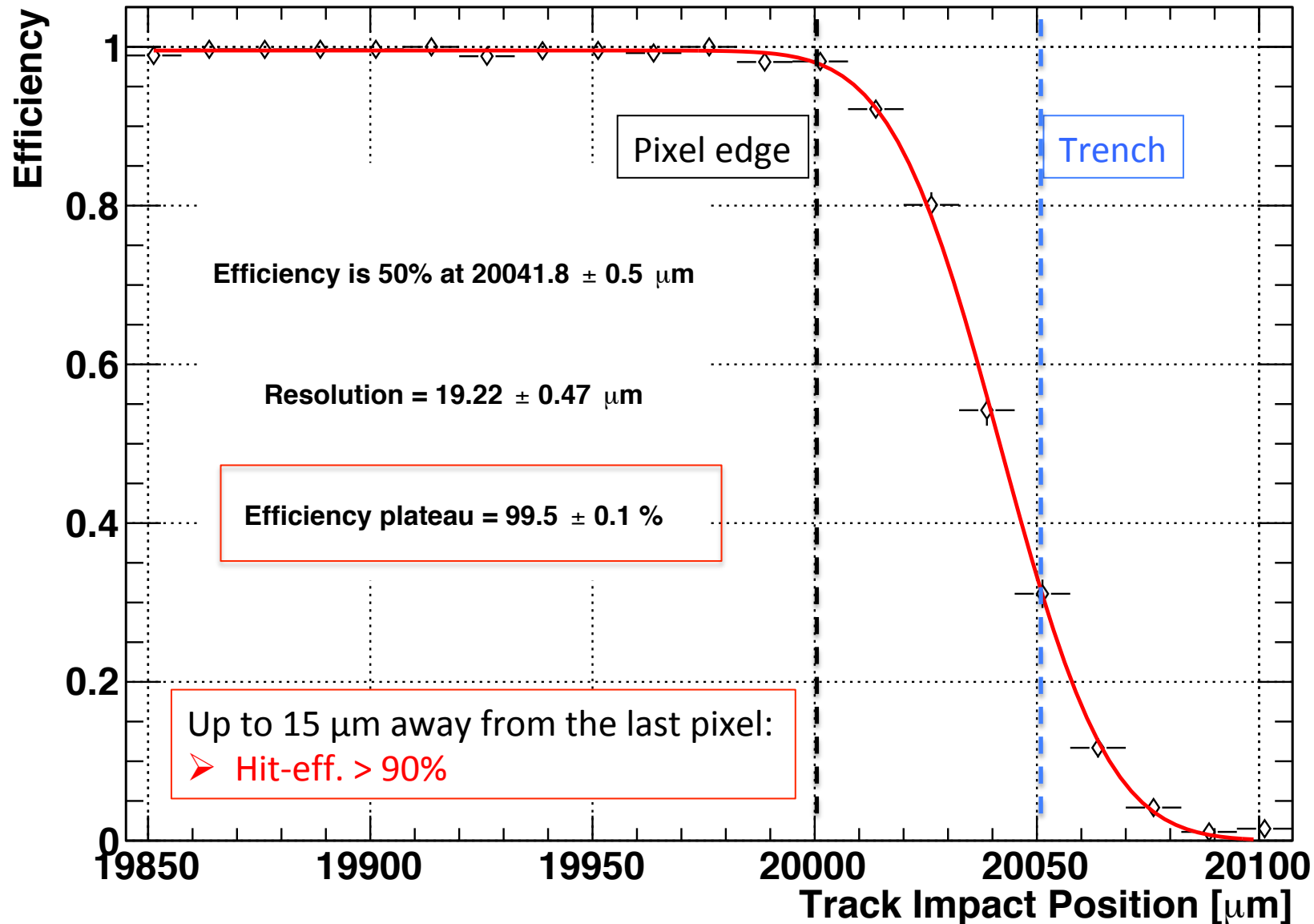
Sensor taken from **130 μm** SiSi wafer

50 μm minimal **pixel-to-edge** distance and **no Guard Rings**

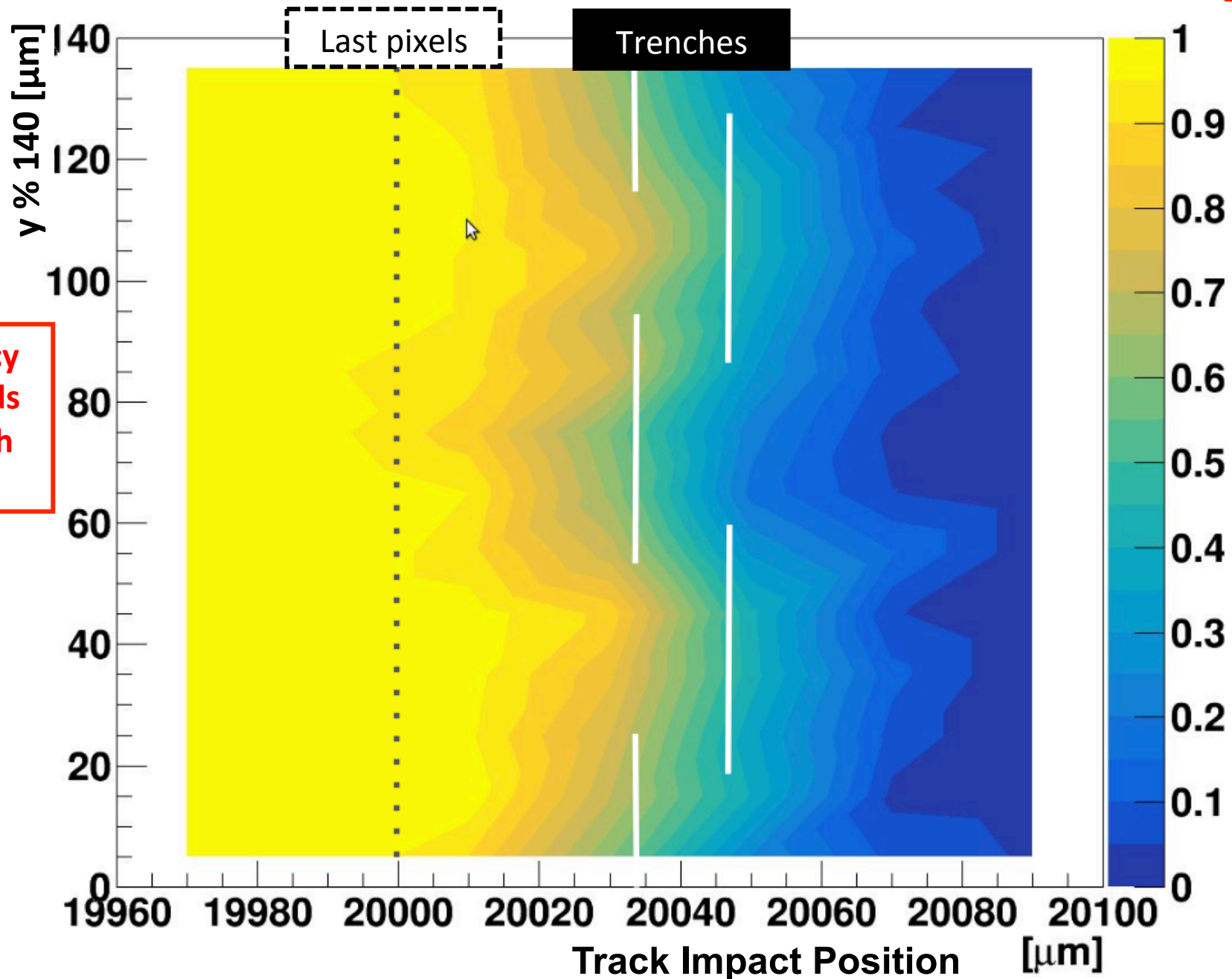
Irradiated uniformly with low energy protons (KIT) at $2.7 \times 10^{15} \text{ n}_{\text{eq}}/\text{cm}^2$ (average fluence for ITk Pixel intermediate layers)

Tested on beam (DESY) before and after irradiation

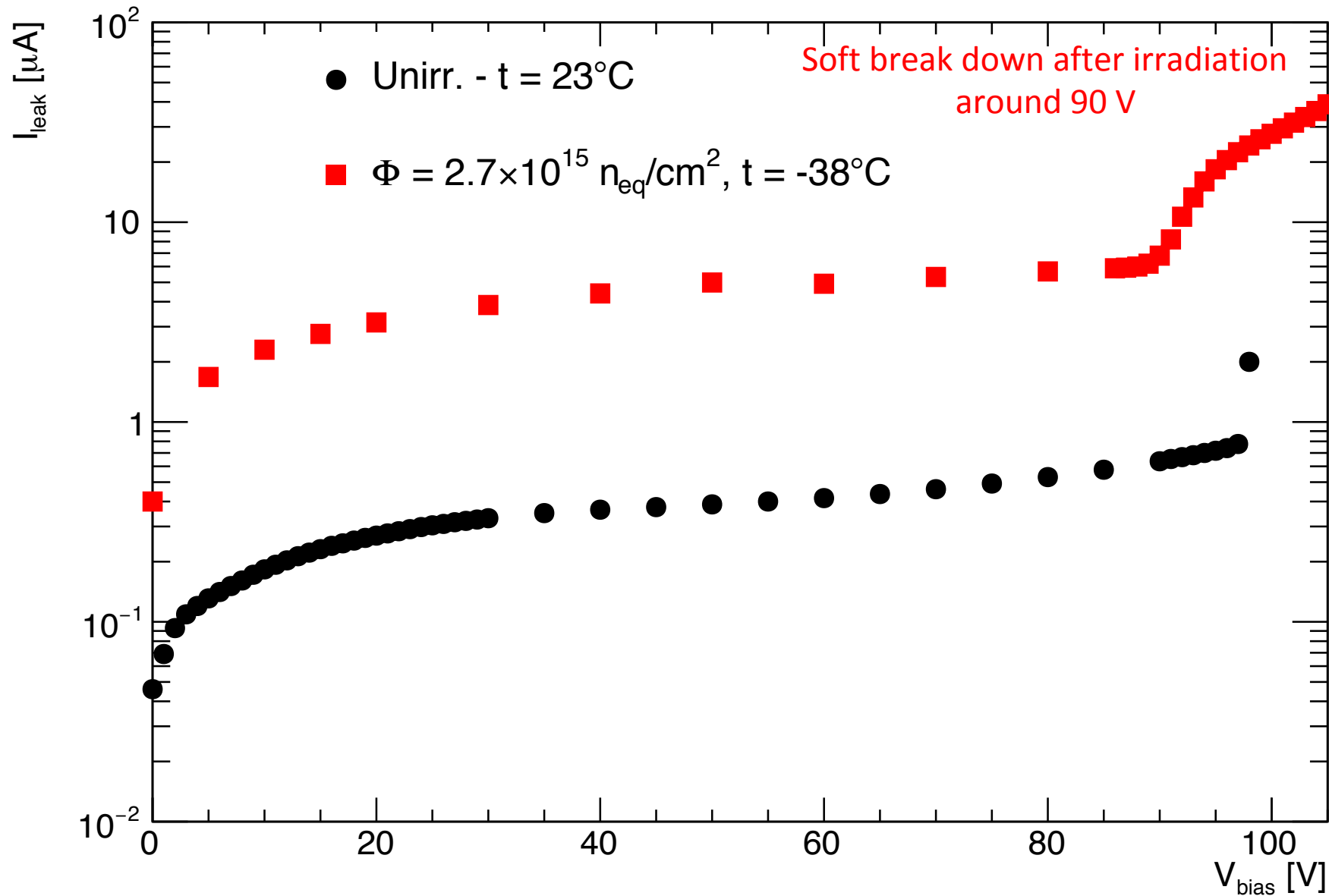
PAE3 – Edge efficiency for un-irr. sensors



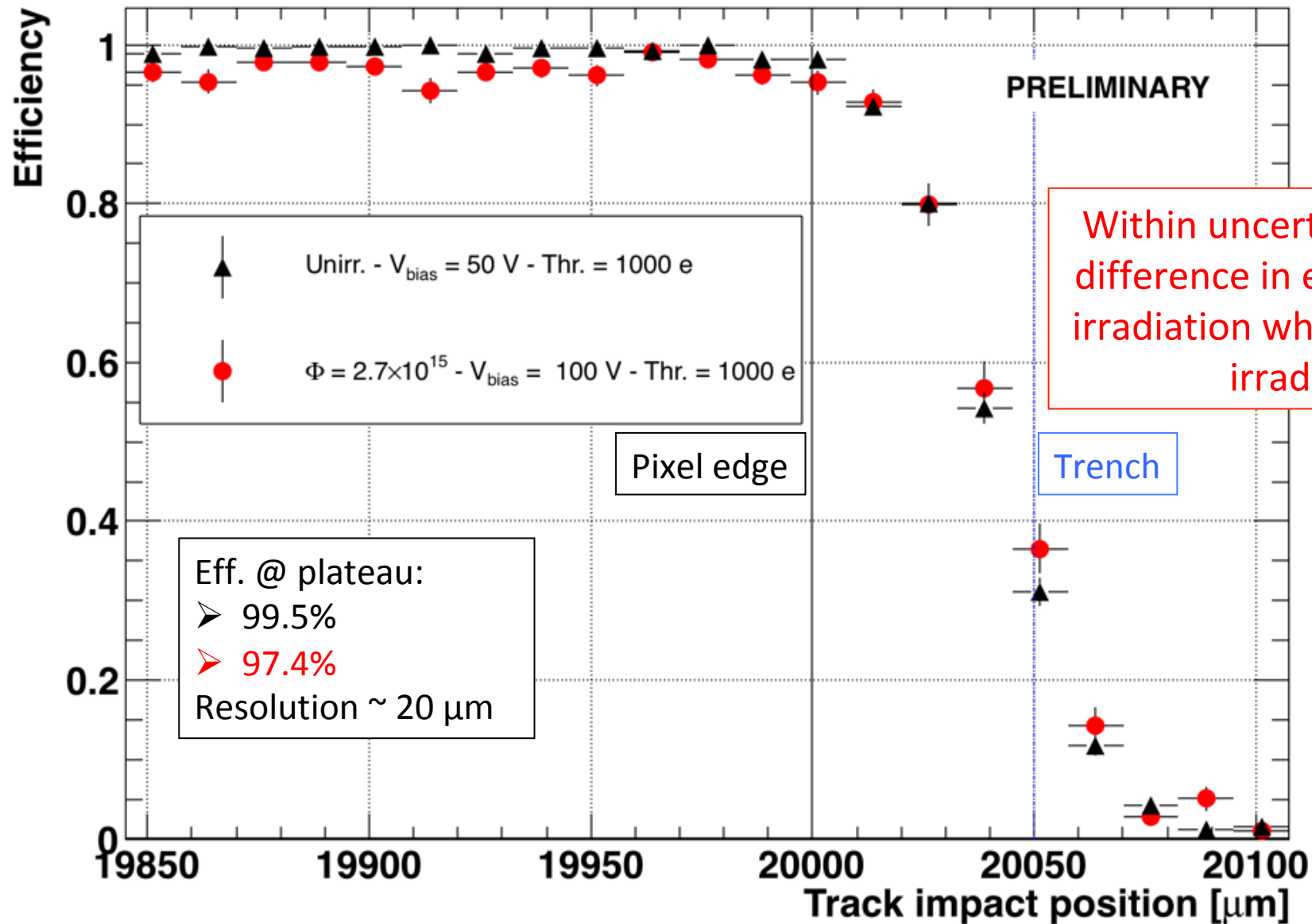
PAE3 – Edge efficiency for un-irr. sensors



PAE3 - IV curves before and after irradiation



Efficiency at edge: irr. vs unirr. modules



Summary and Outlook

- The planned **increase luminosity of LHC** translates into **unprecedented** levels of event rate, pile-up and **radiation damage**
- A complete **new inner tracking system is under development** within the **ATLAS** community, the **ITk**
- **Pixels**, at the core of the ATLAS ITk, will have to **assure the performance of current detectors in a much more harsh environment**
- **Planar thin and edgeless pixel sensors** are **excellent candidates** for intermediate **ITk** layers thanks to their **performance** and **cost effectiveness**
- **Active edge technology to be retested at larger fluences**

PERSPECTIVES

Development of the ITk pixel system

- Hybrid pixels are the sensors candidates for the innermost layers of the ATLAS Inner Tracker
- **My expertise in designing, simulating and testing silicon sensors** will allow me to **keep making important contributions** for the development of the **ITk**:
 1. I am contributing to **new pixel productions**, based on results achieved in the last years
 2. We are now entering the phase of **module construction**, and within the ATLAS ITk French group, I will be in charge of **coordinating** some of the **modules construction** phases
 3. As ATLAS ITk **testbeam coordinator** I will play an important role in the **final sensor decision** for the new ATLAS Pixel detector

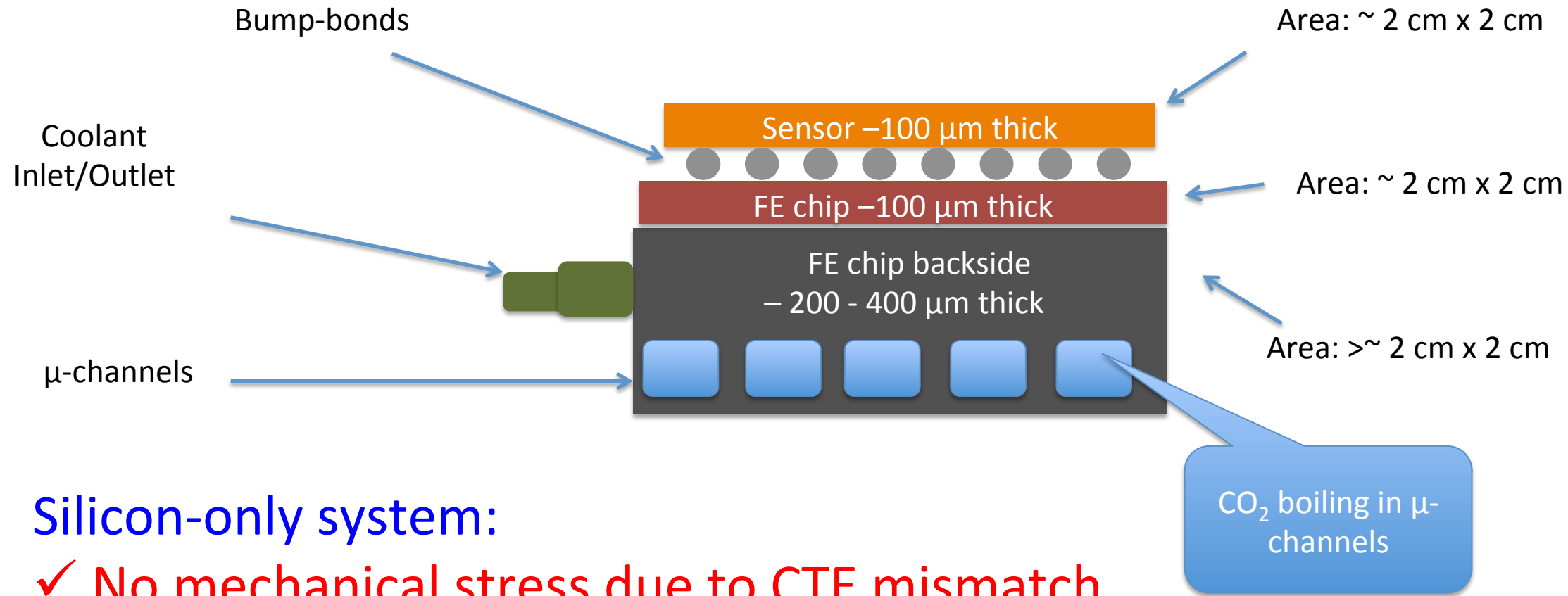
Improved TCAD and Monte Carlo simulations

- The **data collected in laboratory and on beam** with highly-irradiated sensors are **vital to model the radiation damage in silicon** at the fluences expected at the **HL-LHC**
- As **coordinator of the Radiation Damage Pixel Digitizer** group I will make use of ITk-like modules data to further **develop** first **TCAD** and then **Monte Carlo simulations**
- The natural continuation of such a program is the **further development of the ATLAS Monte Carlo simulations** to correctly **model** the **degraded detector** at the **fluences** expected **HL-LHC**, work I started already for the ITk Pixel TDR

From tracker radiation damage to performance

- **Radiation damage is already impacting** actual **ATLAS** data taking
- It is important to **follow closely tracker and tracking observables** to quickly **re-establish optimal data-taking** conditions
- **Hit-efficiency** is one of the most important variables to monitor but **cluster size** is even more **important** for **tracking resolution** which impacts on a large part of the ATLAS physics program
- **Monte Carlo studies** based on different scenarios for what concerns radiation damage are **being prepared** and will be vital **to predict future performance** of tracks and high-level **physics objects**
- New and **better** algorithms for **clustering, tracking, vertexing** and **flavour-tagging** will be developed on this work
- I see **myself coordinating** this effort together with tracking experts, mentoring students that will have the opportunity to **understand in deep the performance of the ATLAS tracking system**

The μ -channels solution (option for HL-LHC)



Silicon-only system:

- ✓ No mechanical stress due to CTE mismatch
- ✓ Low mass
- ✓ Customizable layout of the channels \rightarrow more efficient and uniform cooling

Coefficient of Thermal Expansion

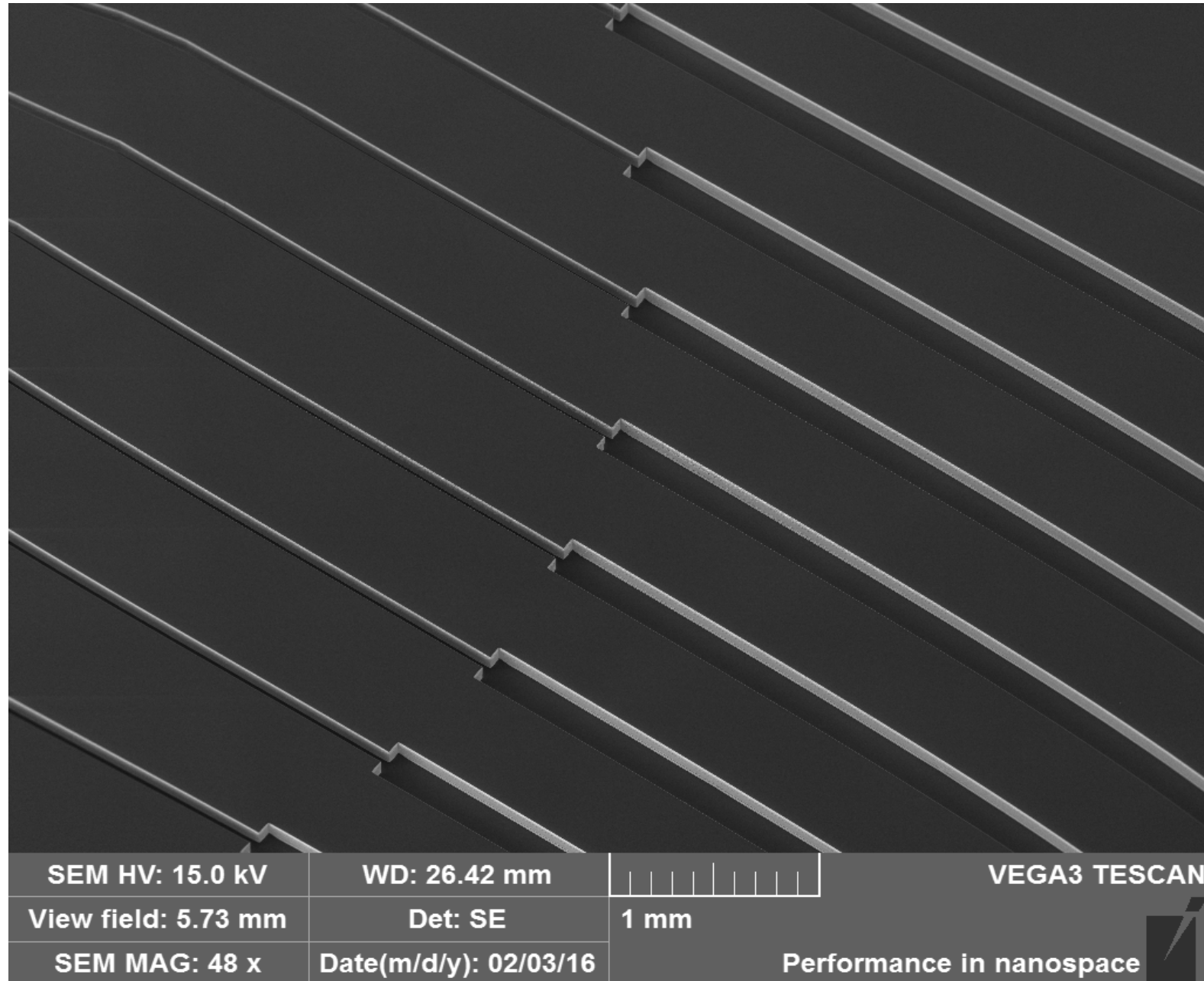
REFLECS & REFLECS2 project (financed by CNRS)

6" wafer μ -channel
production

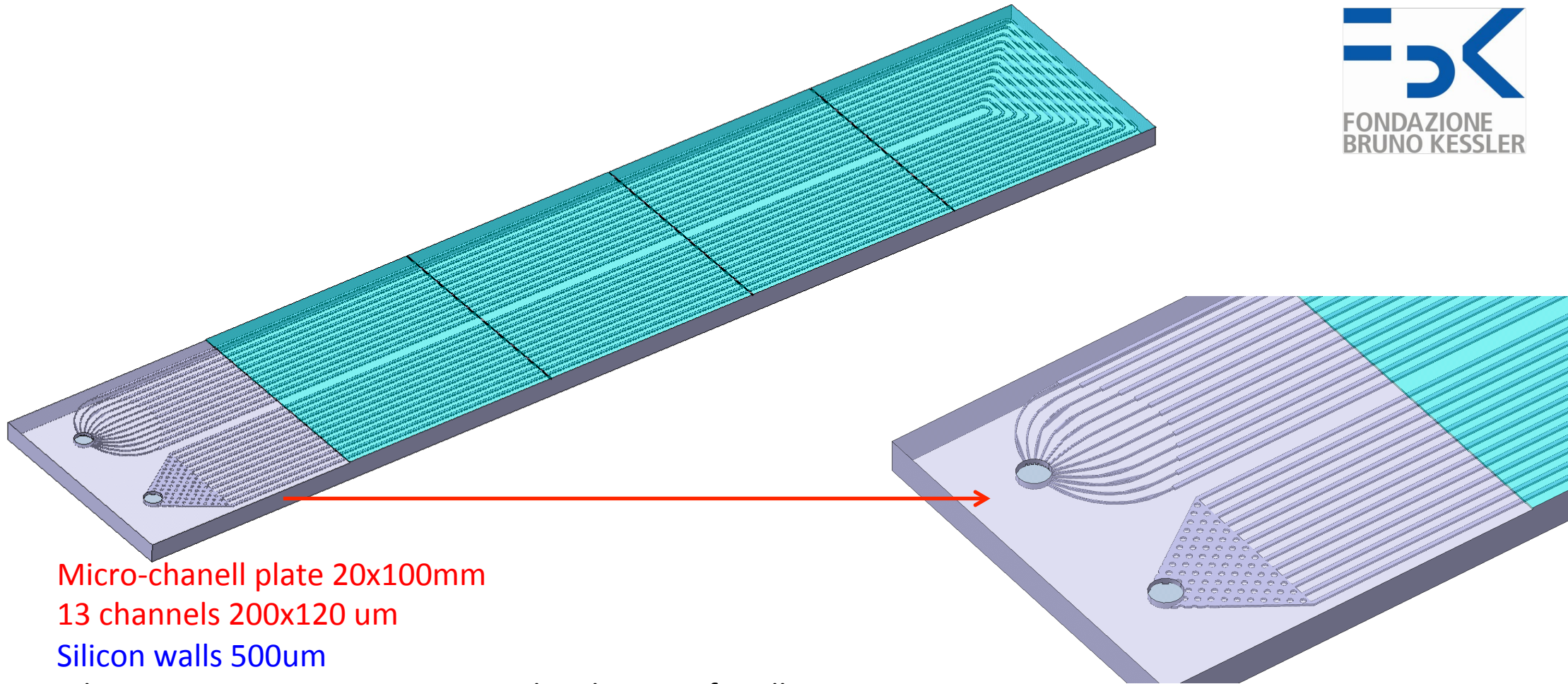


REFLECS & REFLECS2 project (financed by CNRS)

13 channels 200x120 μm
Silicon walls 500 μm
Inlet restrictions 60x120 μm



FBK production: mini-stave for 4 modules



Micro-channel plate 20x100mm

13 channels 200x120 μm

Silicon walls 500 μm

Inlet restrictions 60x120 μm : same length 6mm for all

Inlet outlet holes 1.6 mm diameter

Pillars in the outlet: 350 μm diameter

Shortest channel: 165 mm

Longest channel: 199 mm

SUMMARY

Summary

- Silicon detectors for High Energy Physics were born almost 40 years ago with the goal of measuring heavy flavour particles
- Today they are the standard choice for the innermost layers of experiments at high energy colliders
- Rare phenomena and high precision measurements require high luminosity colliders
- The main challenges for future silicon detectors are high data rates and radiation damage
- Further detector segmentation and more “intelligence” at the pixel level are crucial, together with accurate performance predictions
- An all-silicon system is the final goal
- I am happy to be one of the actors in this field, able to contribute from design to performance studies and eager to enter the “High-Lumi” era

Habilitation à diriger des recherches

Silicon Trackers
for High Luminosity Colliders

THANK YOU FOR YOUR ATTENTION



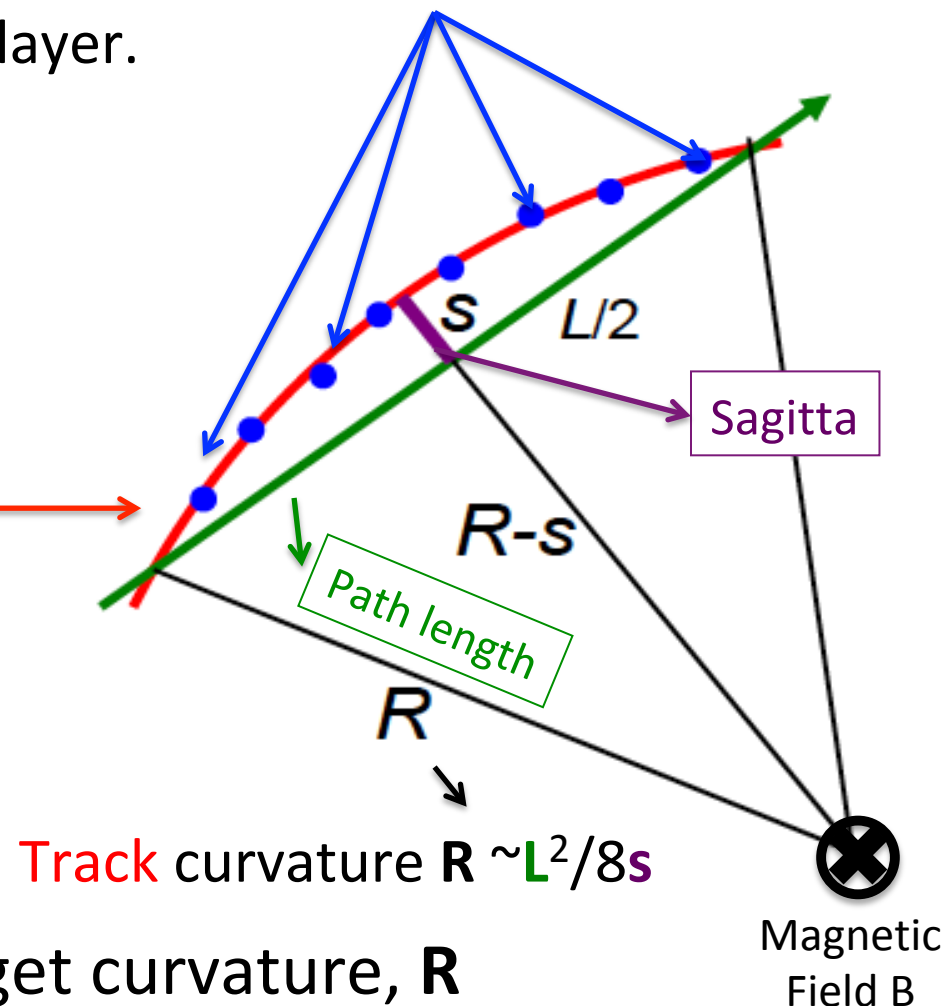
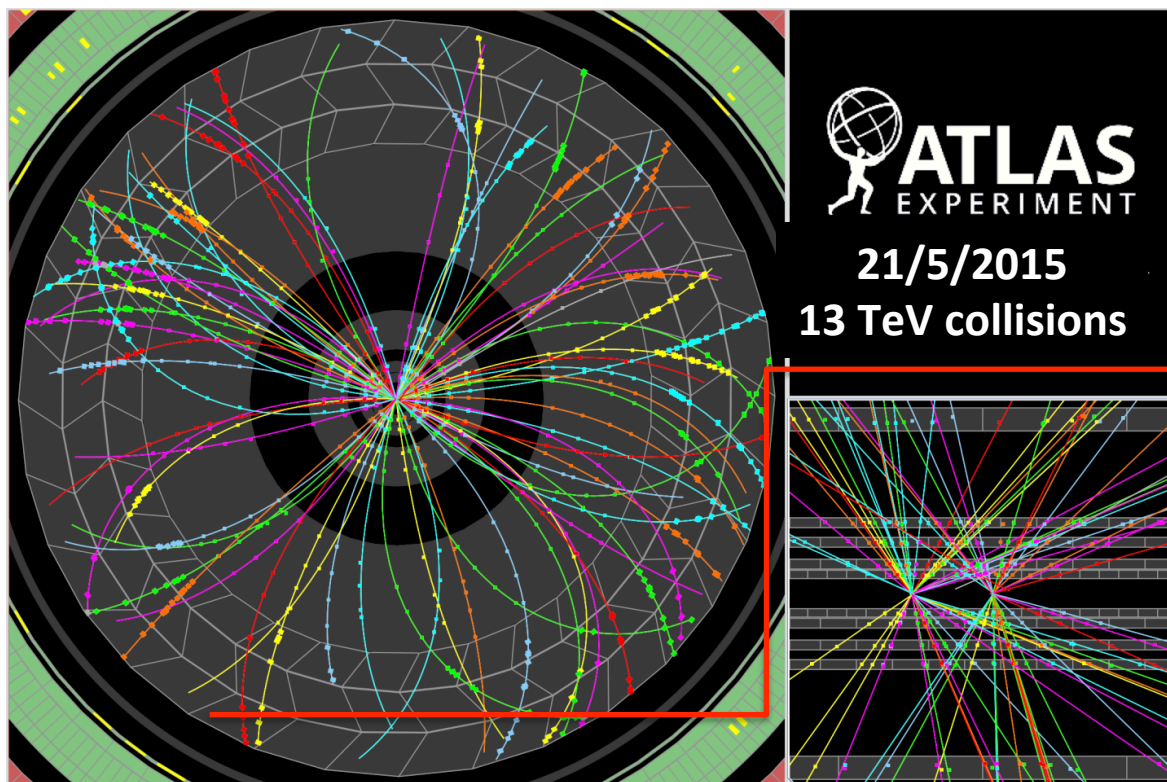
Marco Bomben
LPNHE & UPD – Paris, France



Backup

Transverse momentum measurement

The base of tracking and vertexing is the measurement of **space-points**, *i.e.* the 3D position of the track traversing the sensing layer.



Measure sagitta, s , from track arc \rightarrow get curvature, R

From curvature R transverse momentum p_T can be determined:

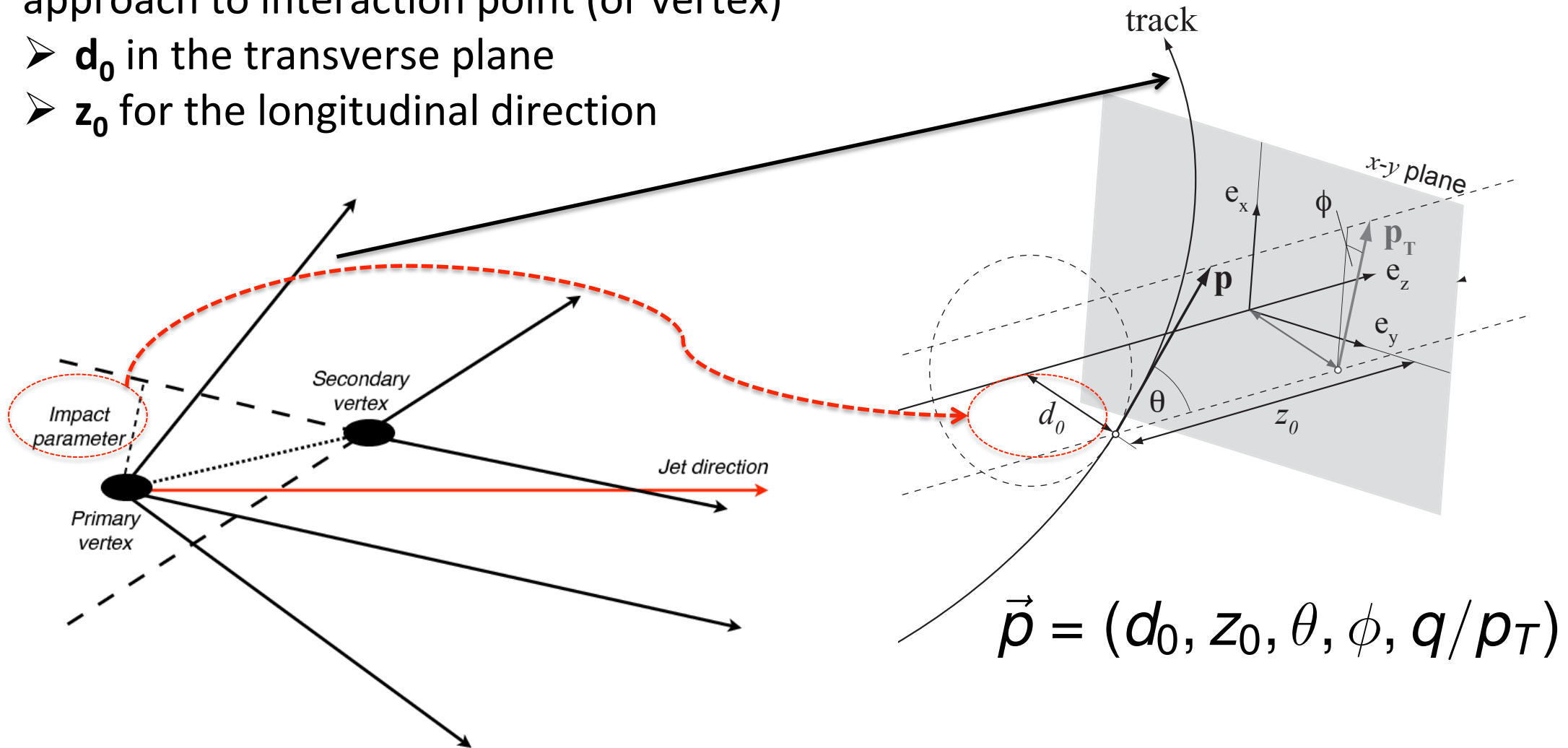
$$p_T[\text{GeV}/c] = 0.3 |z| B[\text{T}] R[\text{m}]$$

Vertexing measurement

Task: find a common point in space for tracks' origin

Fundamental ingredient: distance of closest approach to interaction point (or vertex)

- \mathbf{d}_0 in the transverse plane
- \mathbf{z}_0 for the longitudinal direction



P-n Junction – Signal formation

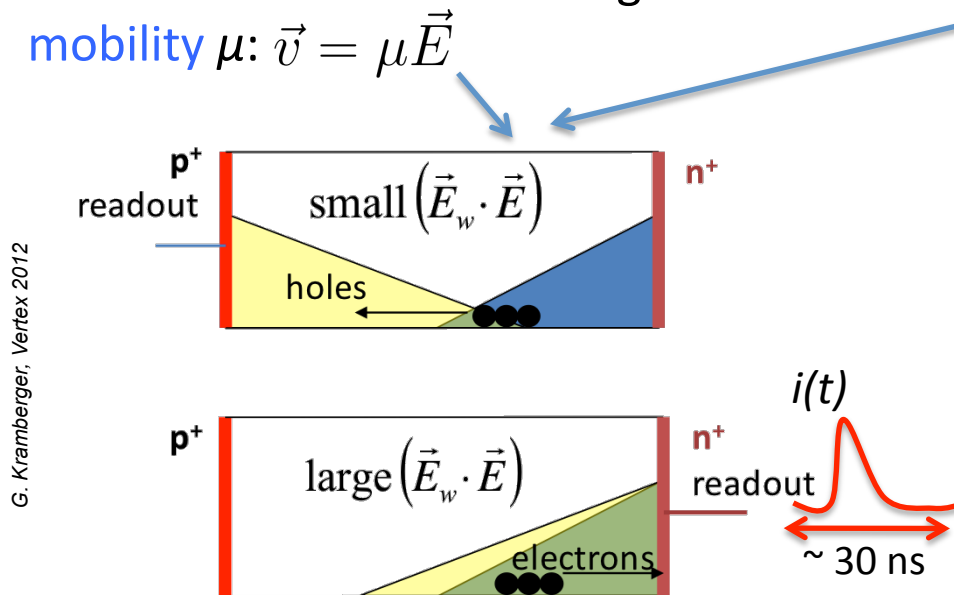
The **charged carriers** created by the interaction of a photon or of a charged particle **drift towards the respective electrodes** under the effect of the **electric field E**

The **carrier velocity v** depends linearly on the electric field E through the **mobility μ** : $\vec{v} = \mu \vec{E}$

The **charged carriers drifting** towards the respective electrodes **induce a transient current** on them

For a single carrier with charge q this current $i(t)$ depends on the **carrier velocity v** and on the **weighting field E_w** : $i(t) = q\vec{v} \cdot \vec{E}_w$
(For a MIP: $i(0) \sim O(\mu A)$)

The weighting field E_w is related to the **weighting potential V_w** by the relation: $\vec{E}_w = -\nabla V_w$
where V_w is the **solution of the Laplace equation**: $\nabla^2 V_w = 0$
with unit potential to one of the electrodes and zero for the others



G. Kramberger, Vertex 2012

SLIM5 APSEL 4D performance

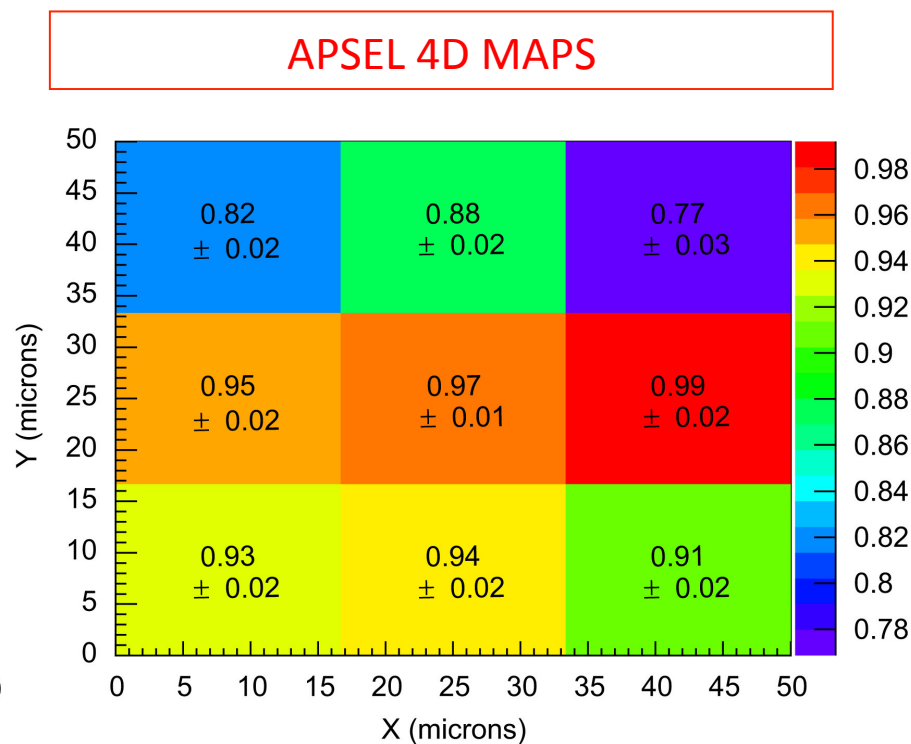
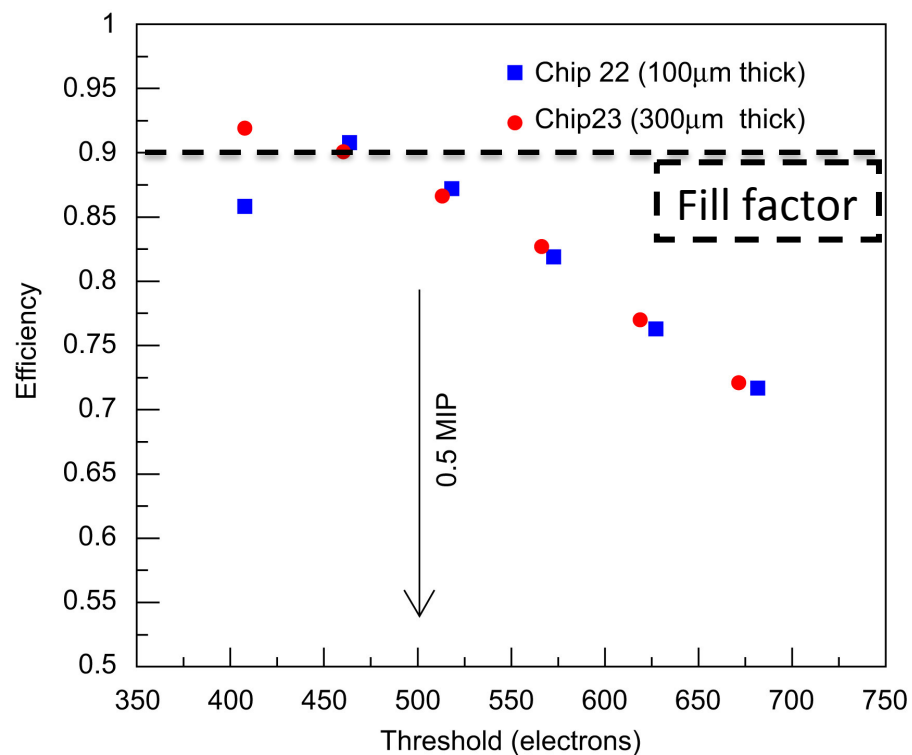


Figure 3.9: (left) Efficiency results for two MAPS detectors, taken from a single threshold scan. The statistical uncertainty on each point is smaller than the size of the plotting symbol. The point of low efficiency at the lowest threshold was probably due to temperature fluctuations during the measurements. (right) MAPS hit efficiencies measured as a function of position within the pixel. The picture, which is not to scale, represents a single pixel divided into nine sub-cells. The values are the efficiencies obtained in each sub-cell after taking into account track migration among cells. The uncertainties include the statistical uncertainty plus a systematic contribution coming from the track migration.

Nucl. Instr. Meth. A 623 (2010) 942-953

SLIM5 triplets performance; efficiency

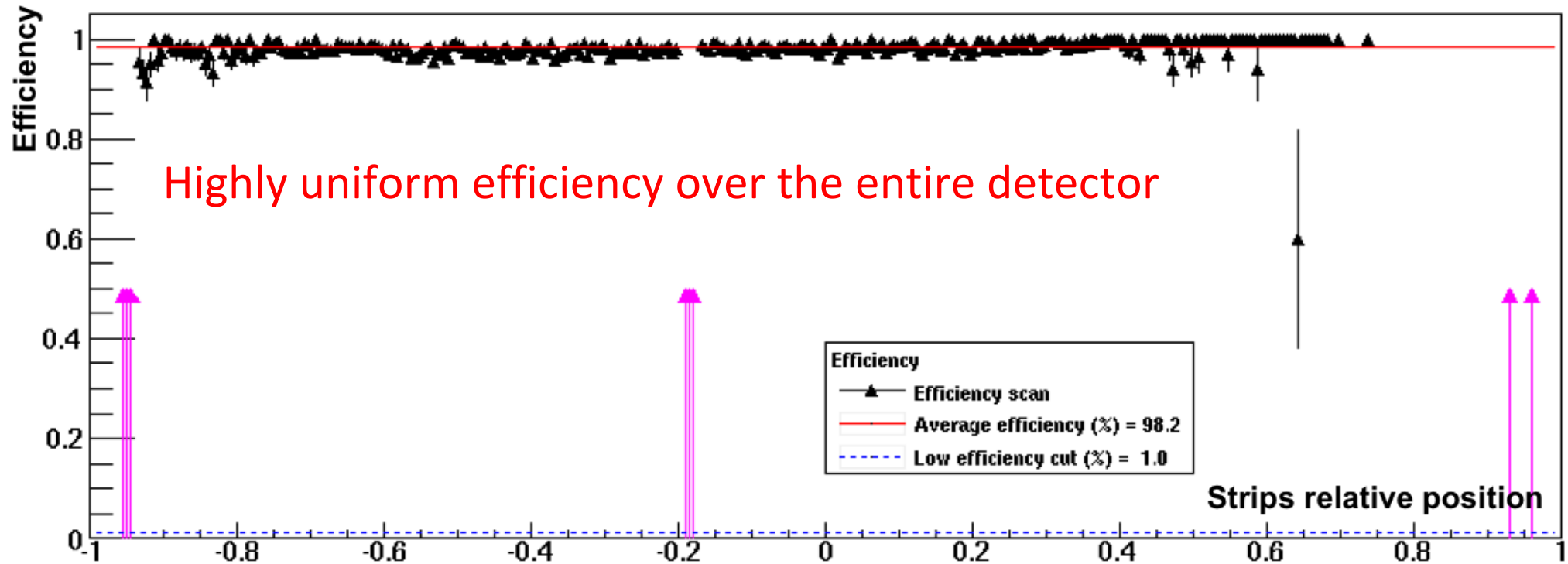
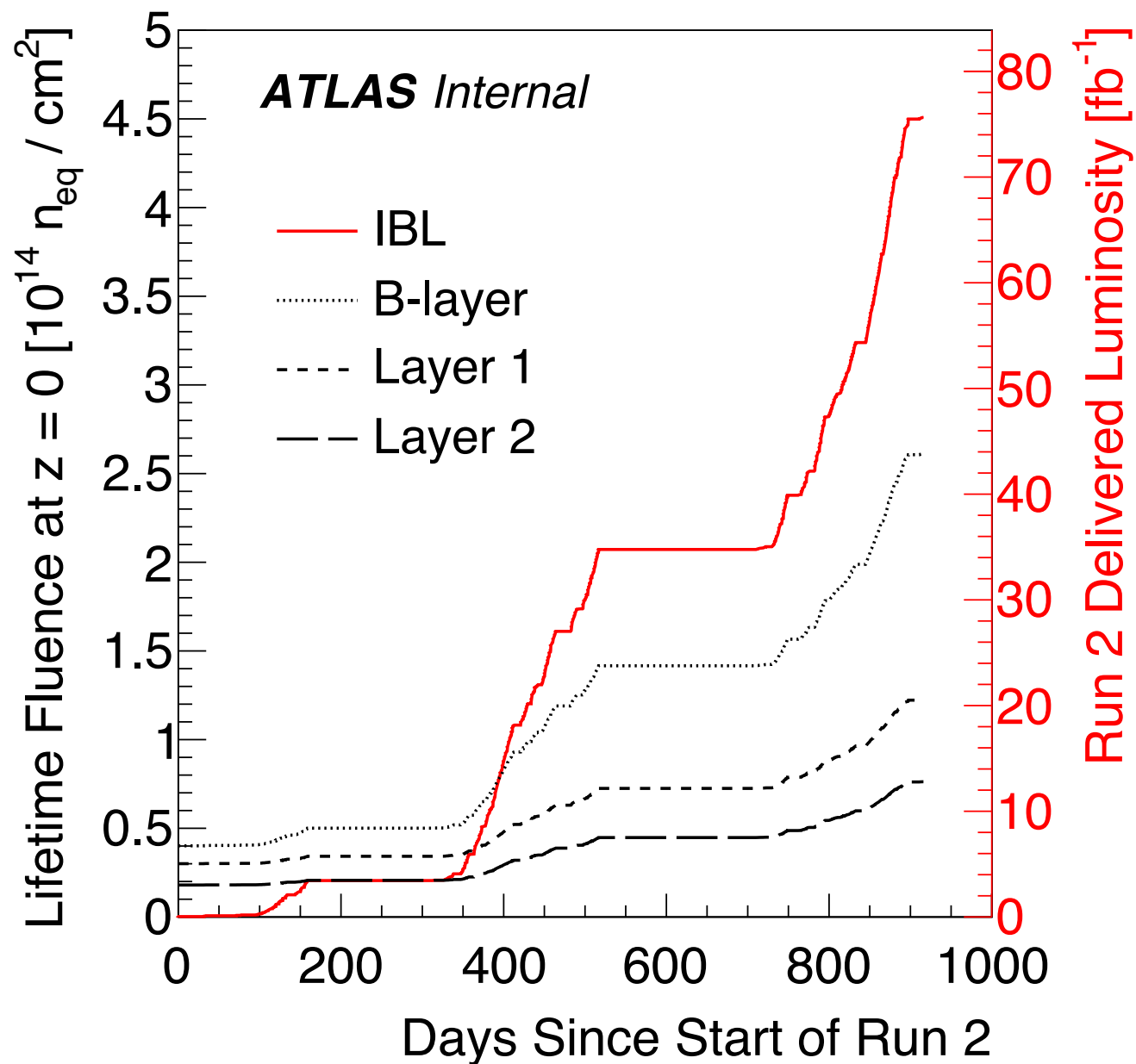


Figure 3.11: Efficiency of a triplet module as a function of the track impact position. Dead strips were removed from the analysis by selecting strips with efficiency greater than 1.0%; dead strips position is marked by magenta arrows.

ATLAS Pixels: Fluence and Luminosity



Example of TCAD radiation damage models

Perugia 2006

TABLE I
THE RADIATION DAMAGE MODEL FOR P-TYPE

Level	Ass.	σ_{np} (cm ²) Exp.[2]	σ_n (cm ²)	σ_p (cm ²)	η (cm ⁻¹)
Ec-0.42eV	VV ^(+/0)	2·10 ⁻¹⁵	2x10 ⁻¹⁵	2x10 ⁻¹⁴	1.613
Ec-0.46eV	VVV ^(+/0)	5·10 ⁻¹⁵	5x10 ⁻¹⁵	5x10 ⁻¹⁴	0.9
Ev+0.36eV	CiOi	2.5x10 ⁻¹⁵	2.5x10 ⁻¹⁴	2.5x10 ⁻¹⁵	0.9

TABLE II
THE THREE LEVELS RADIATION DAMAGE MODEL FOR N-TYPE

Level	Ass.	σ_{np} (cm ²) Exp.[2,9]	σ_n (cm ²)	σ_p (cm ²)	η (cm ⁻¹)
Ec-0.42eV	VV ^(+/0)	2x10 ⁻¹⁵	2x10 ⁻¹⁵	1.2x10 ⁻¹⁴	13
Ec-0.50eV	VVO(?)	5x10 ⁻¹⁵	5x10 ⁻¹⁵	3.5x10 ⁻¹⁴	0.08
Ev+0.36eV	C _i O _i	2.5x10 ⁻¹⁵	2x10 ⁻¹⁸	2.5x10 ⁻¹⁵	1.1

IEEE TNS, VOL. 53, NO. 5 (2006)

IEEE TNS, VOL. 63, OCTOBER 2016

Perugia 2016

TABLE III
THE RADIATION DAMAGE MODEL FOR P-TYPE (UP TO 7×10^{15} N/CM²)

Type	Energy (eV)	σ_e (cm ⁻²)	σ_h (cm ⁻²)	η (cm ⁻¹)
Acceptor	Ec-0.42	1×10 ⁻¹⁵	1×10 ⁻¹⁴	1.613
Acceptor	Ec-0.46	7×10 ⁻¹⁵	7×10 ⁻¹⁴	0.9
Donor	Ev+0.36	3.23×10 ⁻¹³	3.23×10 ⁻¹⁴	0.9

Nota Bene: Perugia 2006 p-type and Perugia 2016 are very similar

NIM A568, (2006) 51

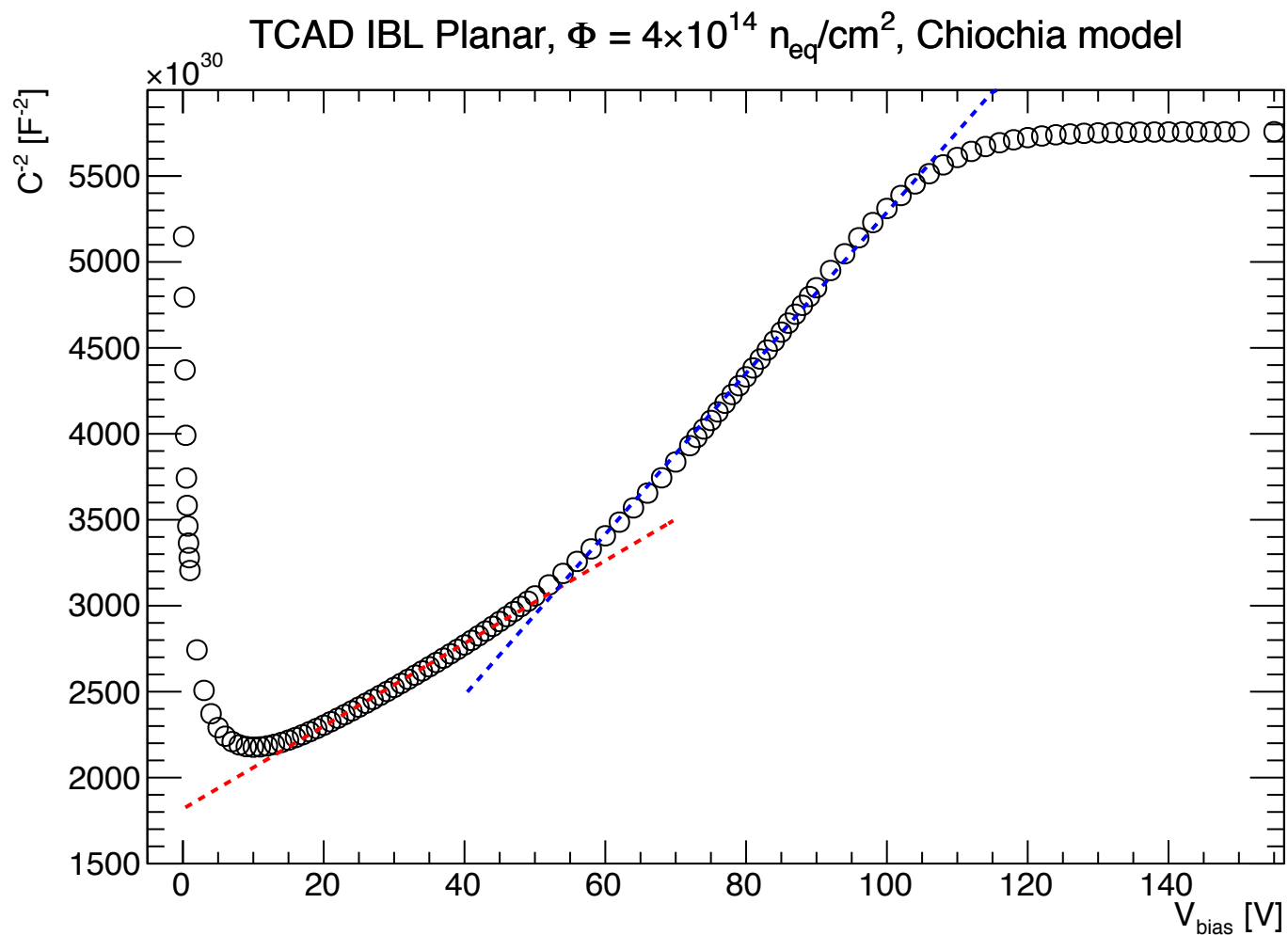
Chiochia 2006; E_A: Ec-0.525 eV; E_D: Ev+0.48 eV

Used for
ATLAS
digitizer

Table 1
Double trap model parameters extracted from the fit to the data

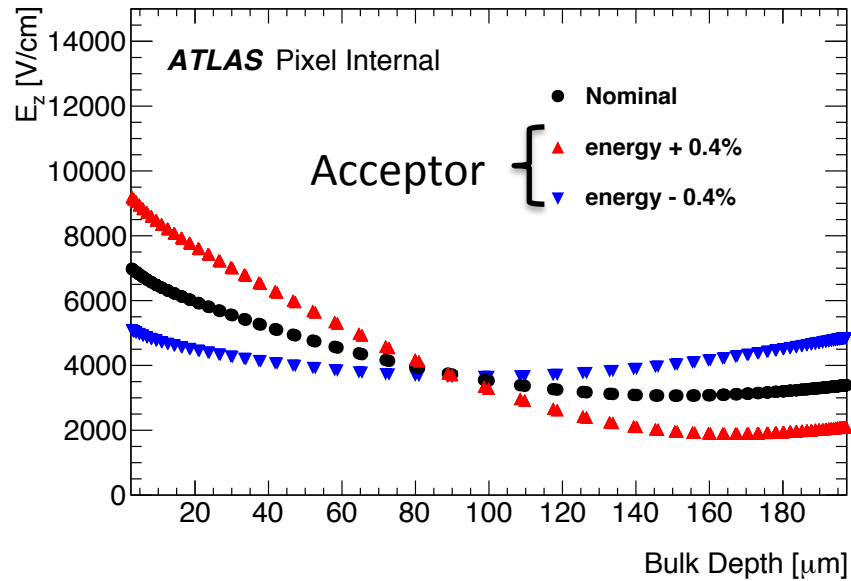
Φ (n _{eq} /cm ²) (×10 ¹⁴)	N _A (cm ⁻³) (×10 ¹⁵)	N _D (cm ⁻³) (×10 ¹⁵)	$\sigma_e^{A/D}$ (cm ²) (×10 ⁻¹⁵)	σ_h^A (cm ²) (×10 ⁻¹⁵)	(cm ²) σ_h^D (×10 ⁻¹⁵)
0.5	0.19	0.25	6.60	1.65	6.60
2	0.68	1.0	6.60	1.65	6.60
5.9	1.60	4.0	6.60	1.65	1.65

Simulated CV curve after irradiation

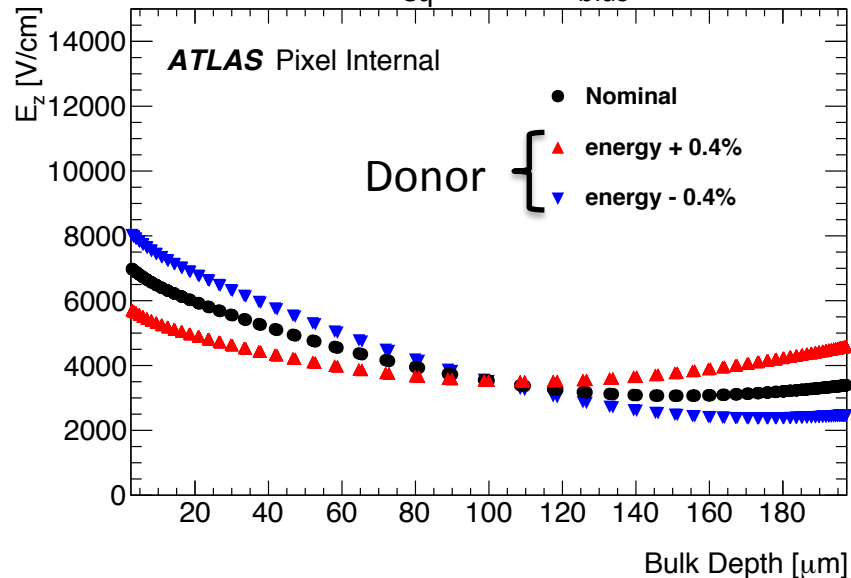


Systematic uncertainties from TCAD models

$\Phi = 1 \times 10^{14} \text{ n}_{\text{eq}}/\text{cm}^2$, $V_{\text{bias}} = 80 \text{ V}$

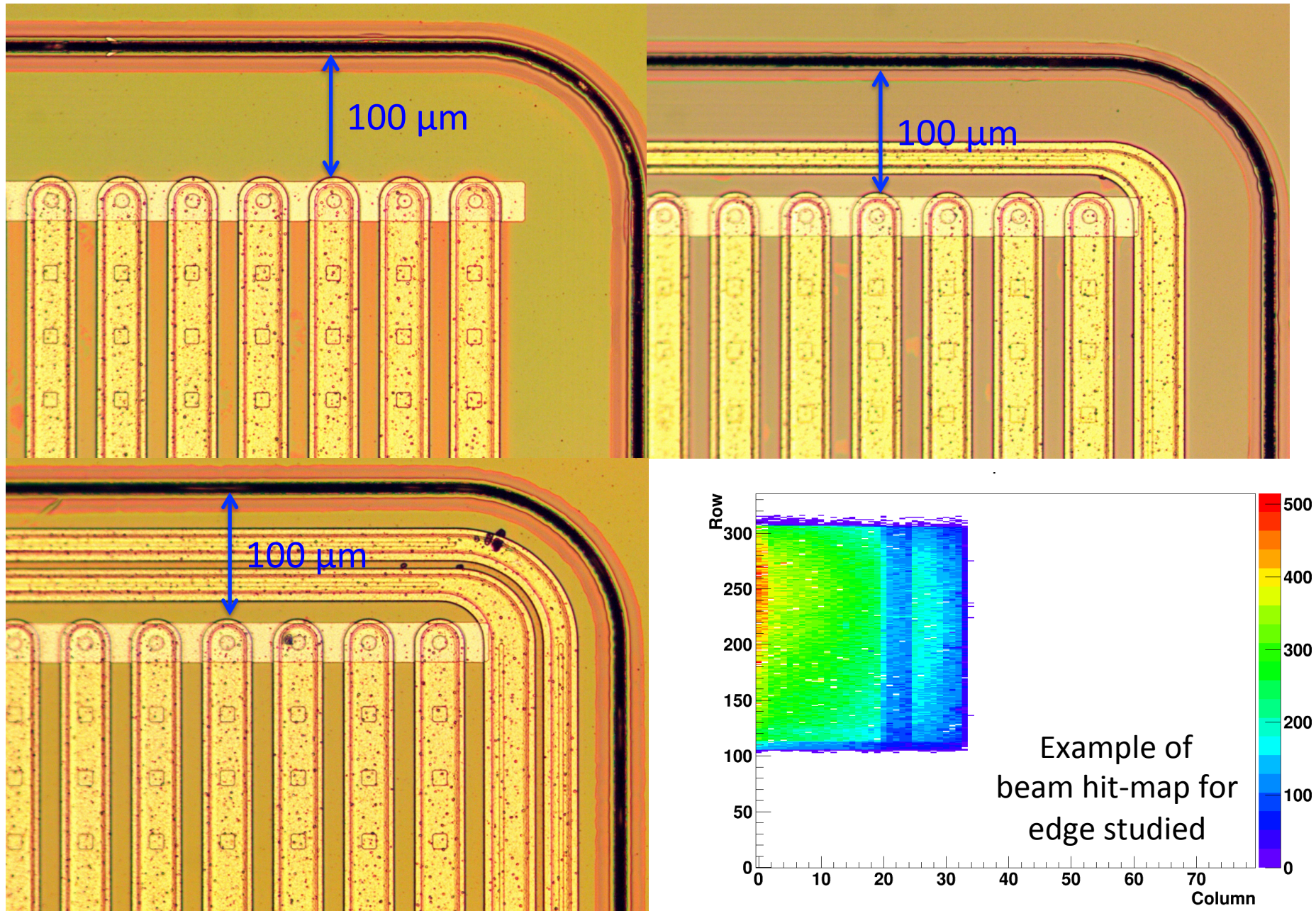


$\Phi = 1 \times 10^{14} \text{ n}_{\text{eq}}/\text{cm}^2$, $V_{\text{bias}} = 80 \text{ V}$

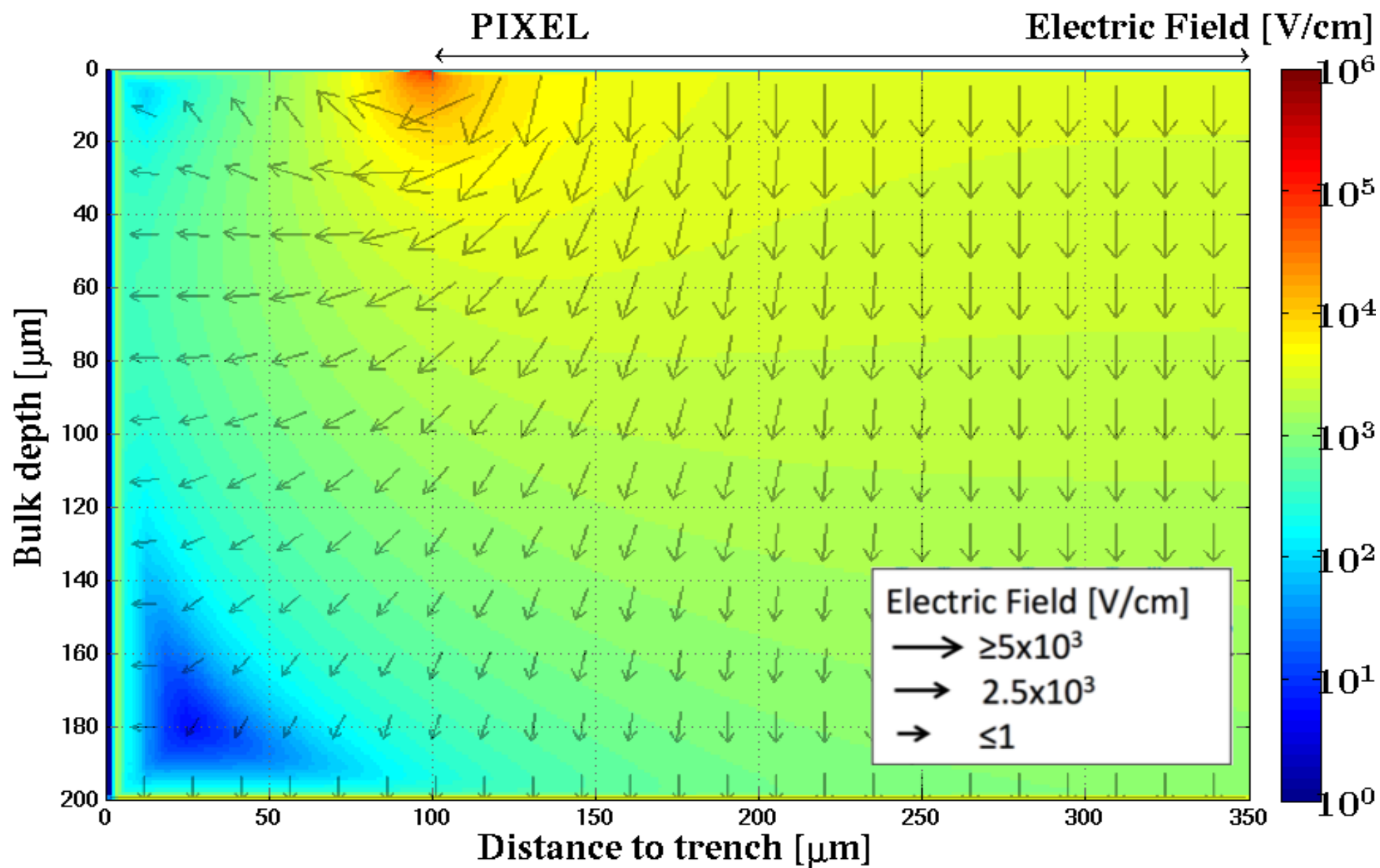


- As shown in the previous slide, TCAD radiation damage **models parameters** come with **no uncertainties**
 - Motivation: limited computing power/time, at least for early 2000s models
 - Authors provided no guidance at all
- We decided to **vary each trap parameter by a certain fraction of its value and see the effect on the electric field profile**
- Trap occupation probability P_t depends exponentially on trap energy E_t and linearly on the other parameters, so the following uncertainties were assigned:
 - E_t : +/- 0.4% ($\sim 1/10$ of $k_B T$)
 - Trap density N_t , cross sections $\sigma_{e,h}$: +/- 10%

PAE1 pixel production: edge studies



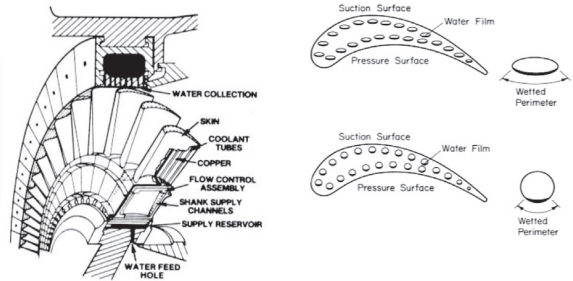
TCAD simulations – 0 GRs



μ -channels cooling applications

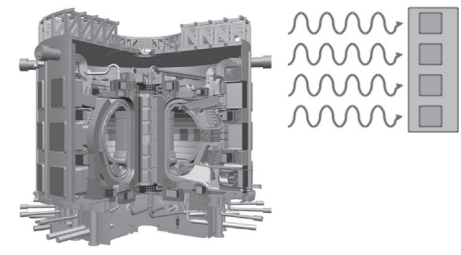
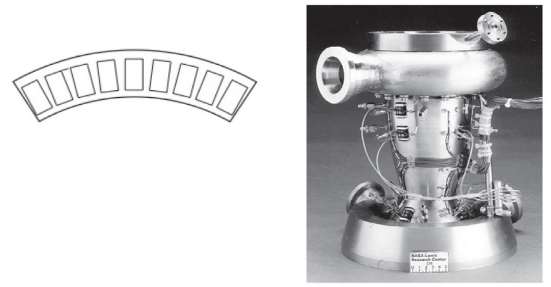
Sung-Min Kim, Issam Mudawar,
International Journal of Heat and
Mass Transfer 77 (2014) 74–97

Water cooling of turbine blades



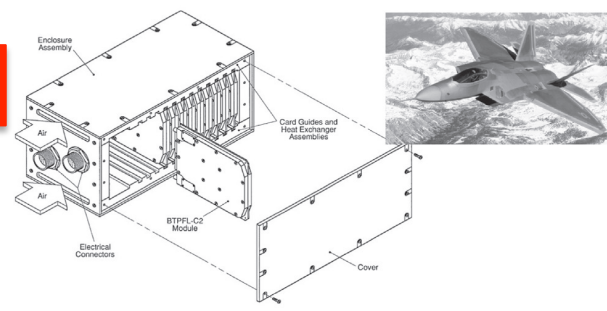
Computer data centres

Rocket engine nozzle cooling

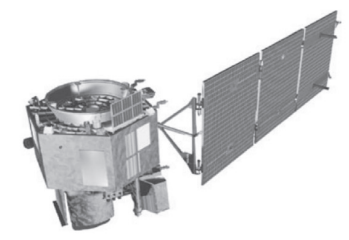


Fusion reactor blanket

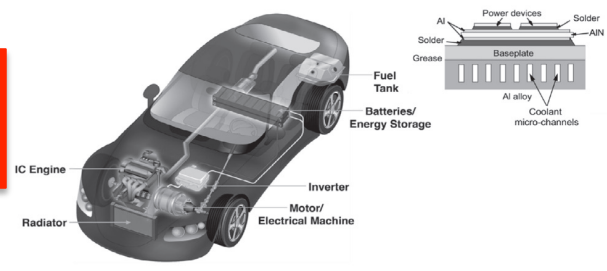
Avionics cooling



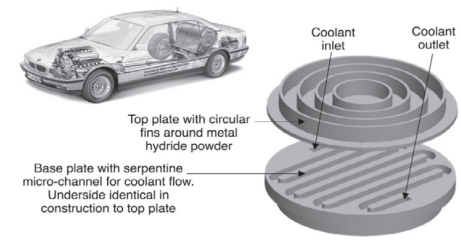
Cooling of satellite electronics
(e.g. HEP: AMS)



Hybrid vehicles data centres



Heat exchange for hydrogen storage



Motivations

Many modern devices are faced with two conflicting trends

- the need to dissipate increasing amounts of heat,
- and the quest for more compact and lightweight designs

Most present air cooling and single-phase liquid cooling solutions virtually obsolete

Paradigm shift from single-phase to two-phase cooling strategies to capitalize upon the coolant's sensible and latent heat rather than the sensible heat alone

- CO₂ boiling

Sung-Min Kim, Issam Mudawar,
International Journal of Heat and Mass
Transfer 77 (2014) 74–97

Motivations

Many modern devices are faced with two conflicting trends

- the need to dissipate increasing amounts of heat,
- and the quest for more compact and lightweight designs

Most present air cooling and single-phase liquid cooling solutions virtually obsolete

Paradigm shift from single-phase to two-phase cooling strategies to capitalize upon the coolant's sensible and latent heat rather than the sensible heat alone

- **CO₂ boiling**
- **into micro-channels!**

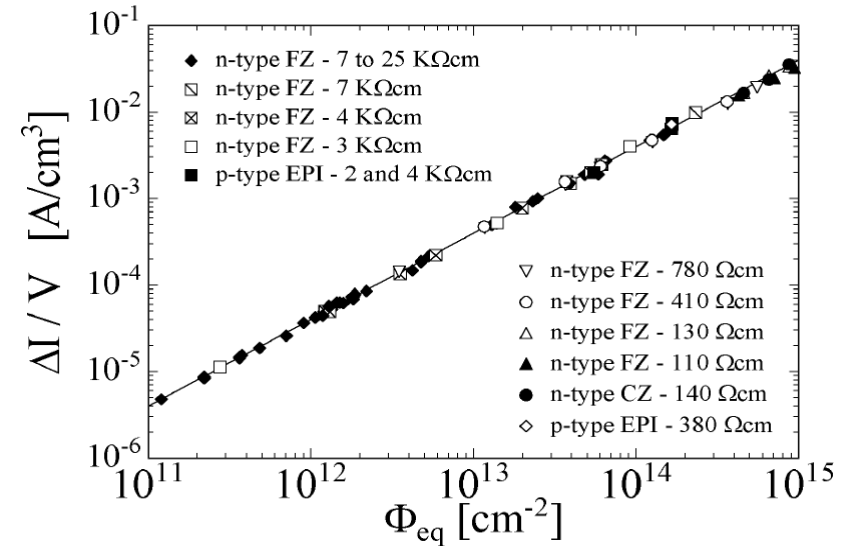
Sung-Min Kim, Issam Mudawar,
International Journal of Heat and Mass
Transfer 77 (2014) 74–97

New cooling system for ITk

- The leakage current increase is prop. to ϕ

$$\Delta I/V(\Phi=1e16/cm^2) \approx 0.4 \text{ A/cm}^3$$
$$16 \text{ mA if } V = 4\text{cm}^2 \times 100\mu\text{m}$$

$$\alpha = \frac{\Delta I}{\Phi \cdot V} \sim 4 \times 10^{-17} \text{ A/cm}$$



Efficient and powerful thermal management needed

HEP Experiments at Colliders and in Space

- **@Future Hadronic Colliders**
- To avoid thermal runaway **future sensors must be operated** well below 0 °C → **ideally: -20 °C**
- **Sensor+chip will dissipate \approx W/cm²**
- A very efficient cooling system is needed
- Important **constraint: very low material budget** (< 1% X₀ envisaged)
- **Space-Born experiments**
- Silicon detectors require:
- a high degree of **temperature homogeneity** across the apparatus
- a **cooling system** capable of **working for several years without** possibility of **intervention** during the space mission

**Promising solution:
micro-channel based cooling using CO₂**

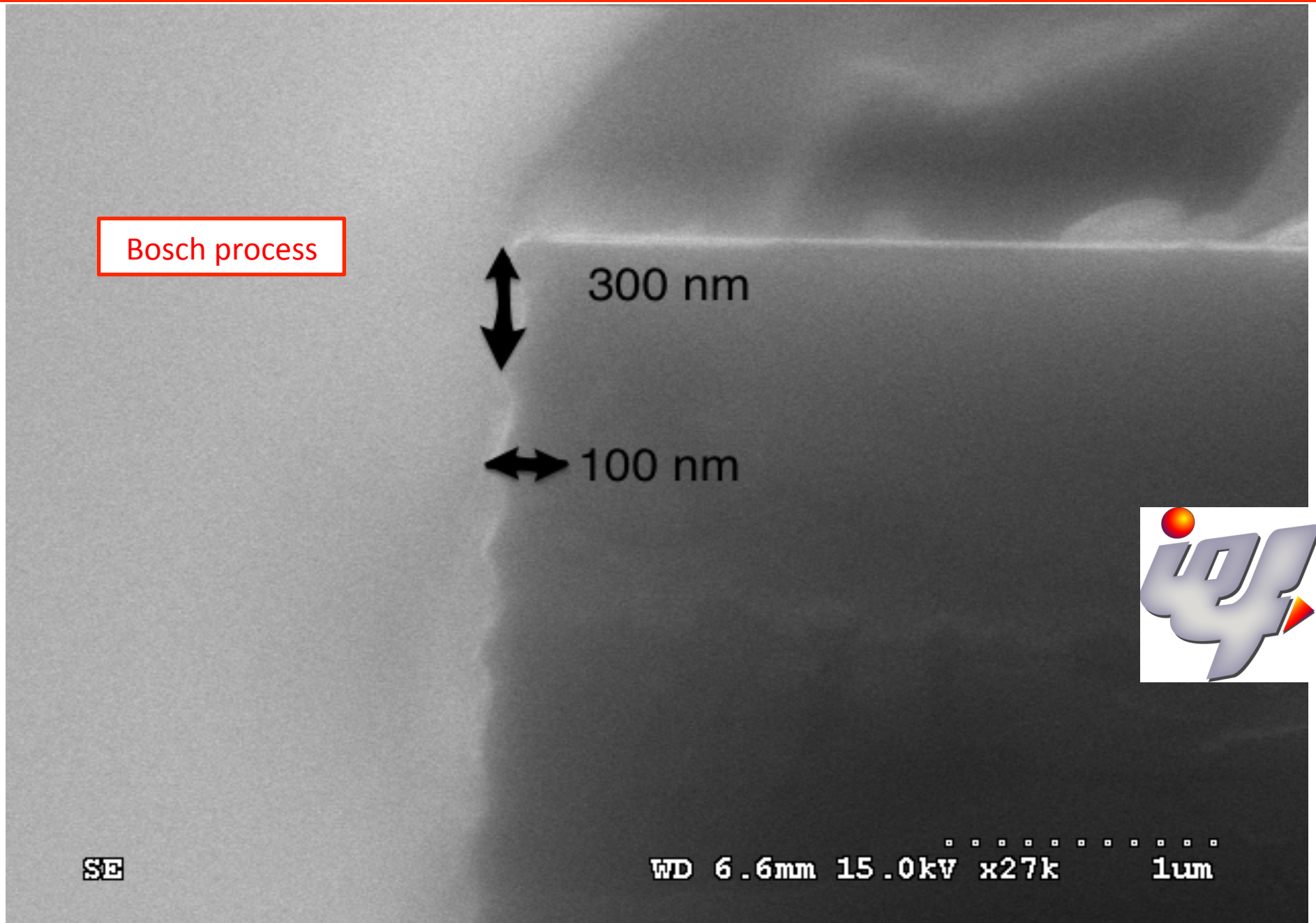
Evaporative CO₂ in silicon μ -channels

LHCb

Advantages of evaporative CO₂ microchannel cooling in silicon

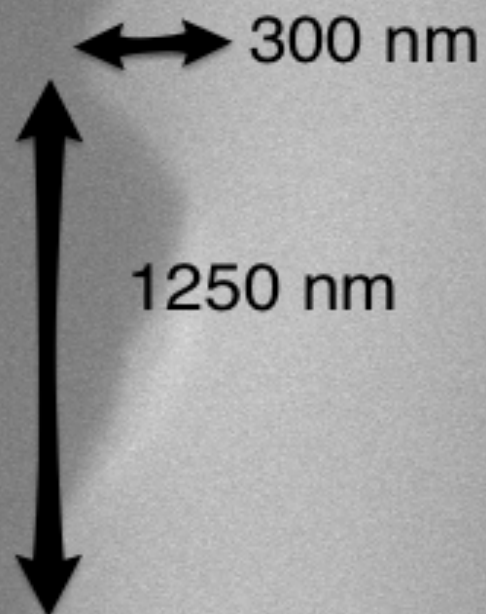
- Evaporative Cooling
 - Isothermal (low temperature gradient)
 - Easy to control by regulating the pressure
 - Very Stable: Temperature is quite insensitive to the variation of heat load
- CO₂
 - High latent heat
 - Low viscosity
 - Non-toxic and environment friendly
 - Chemical inert
 - Radiation hard
- Microchannels in Silicon
 - Cooling fluid is immediately underneath the heat source
 - Low mass – The cooling substrate is also the mechanical support
 - No mismatch of expansion coefficients

Scalloping



Scalloping

Boiling
influenced by
surface
roughness



SE

WD 8.7mm 15.0kV x32k 1um

Ceramic connectors (and microchannels)



Ceramic connector

Silicon micro-channels

